DISSERTATION

BEDLOAD TRANSPORT IN STEEP CHANNELS

TAKAHISA MIZUYAMA

Translated from the dissertation submitted in partial fulfilment of the requirements for the degree of doctor of agriculture to Kyoto University, Kyoto, Japan, January 1977

FOREWORD

This thesis elucidates the characteristics of bed load in mountain rivers, one of main objects of erosion control, and the associated phenomena of flow resistance and sediment flow, and it forms a basis for establishing reasonable erosion control plans.

Eighty percent of our country's surface area being mountainous, as a result of the population growth and vigor of the economy continues to extend the place of human activity over mountainous areas along with cities. Also, Japan is called a land of disasters, and there is much loss of life and property every year due to typhoons and concentrated torrential rains during rainy season.

Previously such disasters were mainly ones such as dikes of large rivers breaking, but floods from medium and small rivers, the crumbling of steeply sloped land, mud flows or extraordinary sediment flows in mountain rivers have become prominent. The SABO or erosion control is the prevention of such disasters due to sediment. Carrying out basic research so that erosion control plans and disaster prevention engineering works can be made in a reasonable manner is the role of erosion control engineering. Mentioned above are disasters directly related to sediment transport. There are various other phenomena due to sediment movement such as river bed lowering, rising, erosion of slopes, soil drift, sedimentation in reservoir dams, which after a certain period has elapsed become impediments to human activity. In order to understand the sediment transport phenomena, the object of this erosion control, and clarify the function of the structural materials involved in erosion control, knowledge concerning the amount and nature of sediment is necessary.

A distinction is made between the suspended load which is suspended and transported in the stream because of turbulence and the bed load which moves along in contact with the riverbed and whose grain size is greater than suspended load. For plains rivers suspended load is overwhelmingly greater quantitatively compared with bed transport. For mountain areas bed load becomes considerably larger. Further, one thing that becomes the object of erosion control for such problems as were mentioned earlier and river bed deformation is bed load gravel. Bed load research is one of the main divisions of erosion control engineering. Usually suspended load and bed load exists simultaneously and mutually interact, but in this thesis the influence of suspended load on bed load transport is disregarded.

Conventionally research on bed load transport has been developed important topics in sand hydraulics and considerable resutls were produced concerning river bed form, channel pattern, stream resistance, critical shear stress and bed load transport rate, etc. However if one forms to apply these results, derived largely for lower stream areas of plains rivers, to mountain rivers, there are many conditions and experimental limits such as relative water depth and gradient which do not match the condition of mountain rivers.

Thus, it is necessary to carry out fresh experiments under the limits and conditions for mountain rivers, and gather knowledge and information which can be applied to mountain rivers. Mountain rivers have the following special features, in contrast with plains rivers for which previous knowledge of bed load can be applied.

(1) Regarding the channel, at normal water levels the flow almost never fills the valley, and this is also true in times of flood.

(2) The grain size distribution of bed materials is extremely large. There are many cases where there are a large number of especially big rocks, and even in flood times the water depth is often of the order of the river bed gravels.

(3) River bed gradient is steep.

(4) The flow discharge has a wide fluctuation.

(5) In the upper stream areas there are many cases where the production of sand and gravel is in probabilistic ways or sudden outbursts and the sediement discharge and the flood discharge are often not in a one to one correspondence.

Mountain rivers have many special features such as the above compared with gently sloped plains rivers. Also, for mountain rivers the river bed in the vertical direction is reported to become stair-like, and this could influence the sediment transport, but that is not treated here. There have been studies 1), 2) investigating one part of these special features, but they are not yet sufficient. Thus, this thesis is based on these special feature, and using the previous research result on gentle sloped channel as a reference, treats bed load and related topics, clarifies the parameters involved in those phenomena, and examines the functional relationships both theoretically and experimentally.

Concrete procedures differ according to the application, but in a river where riverbed material and riverbed gradient are known, if one wants to know the sediemnt discharge for various flow discharges, first one must know the channel pattern and sediment transport form and find the water depth from the resistance law, finally finding the bed load transport rate.

This thesis has progressed keeping such procedures in mind. First, chaper one examines both channel pattern and sediment transport form for mountain streams. Channel pattern includes two-dimensional factors such as river bed form and plane surface aspects such as meandering. Sediment transport form invloves and flow and bed load transport. The scope of bed load transport, the object of this thesis, is made clear in the framework of the above distinctions. In addition, chapter one examines channel width and logitudinal vortices of the flow and sediment.

Chapter two examines experimentally and theoretically the nature of the flow resistance, which is basic when considering bed load, and flow velocity distirbution especially in steep channel. Further, the characteristics of mixed sand gravel river beds and their resistance are also investigated experimentally.

Chapter three examines the critical shear stress which determines the minimum required traction force for generating bed load phenomenon, which has engineering significance, it also makes clear the influence of grain size distribution, relative roughness, and gradient on the initiate condition for transporting mixed sand-gravel and evenly grained sand gravel.

Chapter four examines bed load transport rate for sand-gravel and evenly grained sand-gravel. Developing a new theory it introduces a new bed load equation, and shows its appropriateness by experiment. Further, with this formula it explains the experimental results in a steel slope.

Finally, it examines bed load phenomena which actually occurs in rivers.

Chapter five indicates the procedures and methods which apply the fundamental research presented previously to erosion control planning, especially to channel works planning. A summary of the above results forms the conclusion.

By this thesis, the special nature of bed load in mountain streams and characteristics of flows resistance associated with it become clear.

REFERENCES

1) Yuichi Iwagaki, and Yoshito Tsuchiya:
"Sediment Separation and Transport due to Rainwater", the Japanese Soceity of Civil Engineers (JSCE). Professional paper 51, pp. 34-40 1957.

2) Yoshito Tsuchiya:
"Some Ways of Hydraulic Consideration on the Study of Surface Erosion", JSCE. Professional paper 59, pp. 32-38, 1958.

CHAPTER 1 CHANNEL PATTERNS AND SEDIMENT TRANSPORT FORMS FOR MOUNTAIN RIVERS

Section 1: Introduction

If one intends to measure the water depth of a quantity of flow and the bed load transport rate, with both the riverbed gradient and the grain distribution of the riverbed material being given, he must know the channel pattern and the bedload transport form in advance to use a resistance law and a bedload equation appropriate to those patterns.

The channel pattern can, by scale, be divided roughly into two categories – the channel network of a river basin and the water way, and the channel pattern in the water way[1]). Since waterway position is usually taken up when discussing rivers technically, the chapter will deal primarily with the channel pattern within a water way. Furthermore, relating to the channel pattern, the discussion will be restricted to straight, uniform water way.

Since most of the rivers in flat areas of this country are protected by rigid banks and revetments, a stream runs, in times of flood, uniformly over the entire breadth of the channel constrained by those banks and revetments. It was unnecessary to discuss the channel pattern of existing rivers. Of course when planning new water ways, needless to say, for the safety of dikes, and the relative difficulty of maintaining a low water level, a knowledge of self-formed channel patterns. On the other hand, in mountain rivers, particularly in valleys where the entire area is a potential river path or a river with a fan, waterway width widens, water is not confined to it during flood and, the channel often meanders within the waterway. For this type of stream, if waterway width is too narrow, sediment begins to move, bed level rises and the water overflows. Also if bed slope is greater than a certain angle, it causes individual or collective transport of sediment, that is, mud flow. For these mountain rivers, as compared to those in flatter areas a knowledge of channel pattern and bedload form is vital, however, their classification and individaul characteristics have not yet been clarified.

In this chapter, channel pattern and sediment transport form in steep sloped waterways will be examined experimentally. In other words, the applicability of the 'regime theory', heretofor applied to easy grade and self-formed channel breadth will be discussed. We will examine what happens in the case of steep slope and large grained sediment and at the same time, discuss sediment transport peculiar to steep sloped channels.

Section 2: Experiments Regarding Channel Patterns and Sediment Transport Forms

The waterway used for the experiments was formed of steel 39 cm wide and 20 m long, and the gradient could be varied from 0° to 30° by way of a chain

block. In order to vary the width, two attachable waterways 15 cm and 29.5 cm could be fitted inside the large waterway. Materials for the experiments were, as noted in grain size distribution diagram (Fig. 1.1.) 4 types of natural gravel, one type being evenly grained and the other three having comparatively wide grain size distributions.

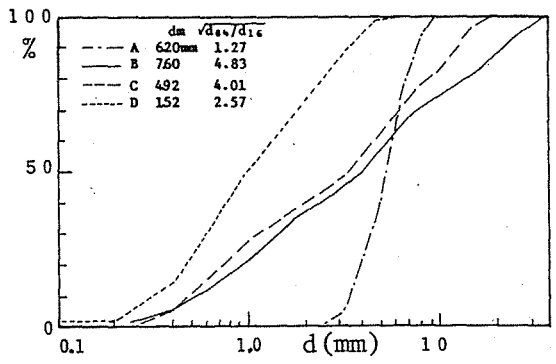

Fig. 1.1 Grain Size Distribution for Four Types of Sand used in the Experiments

The experiments were carried out in the following manner. Sand gravel stops were placed at upper and lower ends of the stream, and sand was spread at a thickness of D_0, and a prescribed volume of water was supplied from the upper end of the stream. The water supply time in most cases was set to 30 minutes, and in that time, appropriate measurements of channel breadth, water level, bed height, and sediment discharge were taken. Channel breadth was measured using a scale at a longitudinal spacing of 25 cm, water level was measured using a point gauge (a scale of 1/10 mm calibration) and an electronic point gauge which can detect if the device touches the bed surface was used to measure bed height. Bedload transport rate was measured at an appropriate time interval, and a sand collection box was placed at the end of the waterway. Information of how long it took until the flow becomes stable after the water is supplied is the most important point of the experiments to know whether the measured channel, under specified condition, was self formed.

Because the gradient in this experiment was an extreme 1/50 to 1/4, even in cases of a concentrated flow, the stabilization of flow required from 30 seconds to one minute. As for the measurement of range, no time trends were shown and a range related to equibrium is conceivable. Conditions of the experiment are listed in Table 1.1. First, using the 29.5 cm channel and materials A and C the test

Table 1.1 Conditions for Experiments

NO.	B_0	ℓ_0	D_0	i_0	material
1	29.5cm	9.8m	15cm	1/50~1/4	ABC
2	39.0	9.0	12	1/20~1/10	D
3	15.0	9.0	12	1/20~1/10	CD

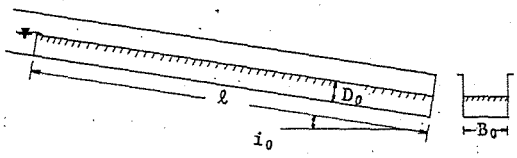

was carried out to obtain materials necessary for classification of channel and sediment transport forms.

Next, as a test for channel and sediment transport forms, an experiment was done concerning transversal distribution of sediment. When flow runs filling over a waterway, could the bedload be spread over uniformly in the transversal direction? According to the conventional observations, it had been reported that lines of bedload called longitudinal stripes were formed on the riverbed[2]. In the

observation by the author, when fine sand particles moved on a bed where there seemed to be non-moving sand particles, the longitudinal stripes are highly visible, but transport of sand particles whose grain size encompasses the whole range of grain size was not observed. It is conceivable that these stripes are formed by flow vortices. The present aside, it would be possible these will become a powerful key to the future study of the transversal channel pattern, and with this in mind, the experiments were conducted on a fixed bed.

To the 19.8 cm wide waterway, a steel waterway of 9 m length, uniform grained sand with an average grain diameter of 4.00 mm was fixed to the bed using varnish. From the upper end of such fixed bed, a mixture of gravel, with an average grain size of 2.48 mm, was supplied by a sand feeder. There were taken two waterway gradients of $\sin\theta = 0.0255$ and 0.05. Water depth was measured by a point gauge and the amount of flow by a triangular weir. The amount of sediment outflow was measured at the lower end of channel by a sand collection box, which is partitioned laterally into 2 cm blocks, to obtain the state of transversal distribution of sediment transport clearly. The number of longitudinal stripes of sediment transport was measured by observation.

In the next section, an examination of the results will be conducted.

Section 3: Channel Pattern

The experiment was carried out as described in Section 2, but the problem now is how to classify those results and what values should be chosen as parameters. Fig. 1.2 is domainial classification of channel pattern done by Leopold and Wolman[3], using natural rivers in the U.S.A. and India as samples.

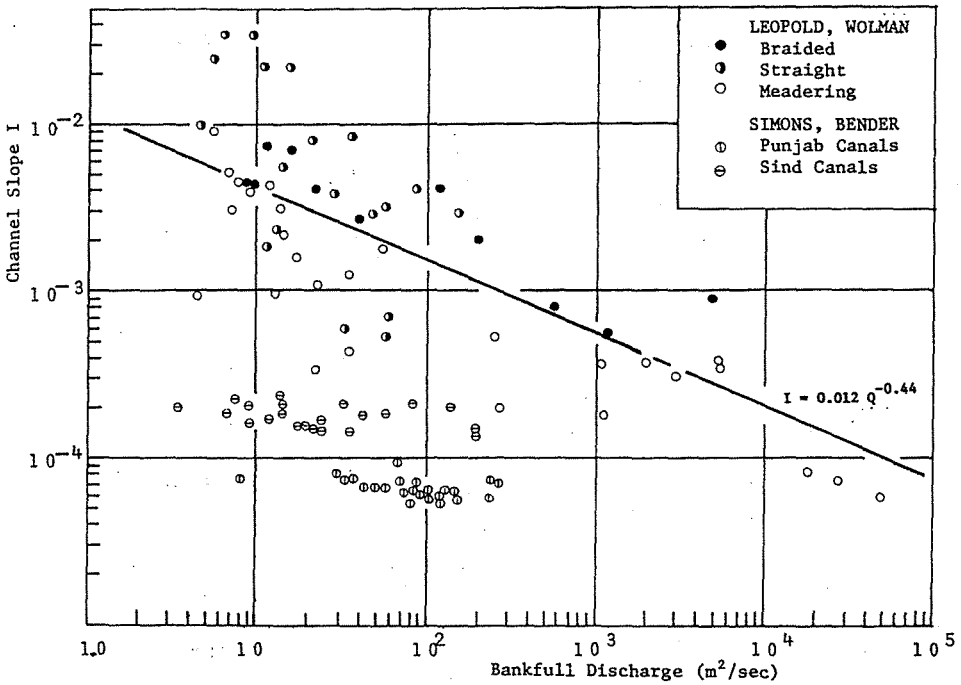

Fig. 1.2 The Domain Classification of Channel Pattern by Leopold/Wolman

Channel pattern is divided, with respect to channel slope and flow discharge, into 'Straight', 'Meandering' and 'Braided' types. Slope is plotted to as much as as 0.03, but results of the author's experiments showed a slope of greater than 0.1 in places off to the upper left of the graph in Fig. 1.2. Even here, the experimental results are expressed in terms of channel slope and flow discharge, and the classification is divided. Figs. 1.3a and b (materails A and C, respectively) indicate results by materials used.

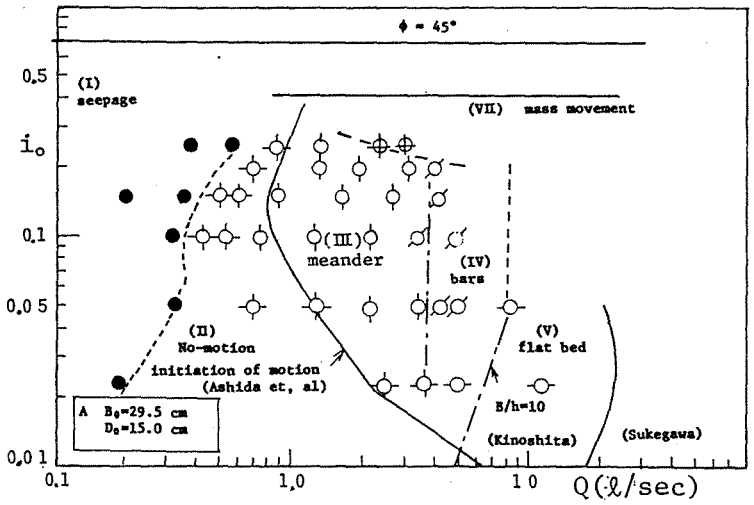

Fig. 1.3(a) Channel Pattern of Uniform Gravel

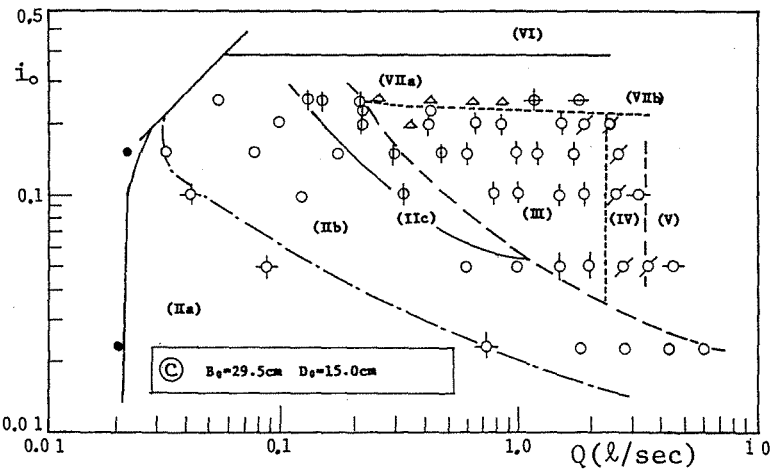

Fig. 1.3(b) Channel Pattern of Gravel Mixture

In the following paragraphs, characteristics of each classfied domain channel pattern, and parameters controlling their phenomena will be discussed.

Domain I: This domain had no occurrence of surface streaming. When a surface stream does occur, it is the case when bed gravel layer reaches the saturated seepage flow discharge. If the stream behaves according to the Darcy's Law, the seepage flow discharge in similar bed materials should increase proportionally to slope, the maximum run off, if seepage coefficient is K, will be $Q = Ki_0B_0D_0$ . . . (1.1). Here i_0 is bed slope, B_0 is channel width, D_0 is thickness of bed materials. A seepage coefficient of $K = Cd_{10}^2$ (cm/sec) . . . . . (1.2) is proposed by Hazen[4], here by d_{10} being 10% grain size on a grain size accumulation curve. For the sand used in the experiment, values of seepage coefficients and actual values are listed in Table 1.2, assuming C = 100.

Table 1.2 Seepage Coefficients of Materials used

MATERIAL	d_{10}	K(Hazen)	K(Observed)
A	3.5 mm	1 2.3 cm/sec	5.8 3 cm/sec
B	0.6 5	0.4 2	—
C	0.5 0	0.2 5	0.3 4
D	0.3 2	0.1 0	—

According to this, surveyed and theoretical values are in agreement with respect to order, by using the equation (1.1), we see that it is possible to deduce the limit of the occurence of a surface stream. However, if we try to calculate actual seepage in a canyon, estimating D_0 in the equation would be difficult, and there would also be problems of seepage through materials accumulated on bottom and side of the river bed.

Domain II: For this domain, there exists surface movement, but in this case it is not great enough to cause gravel movement. The upper limit of flow discharge is determined by the amount of flow corresponding to the ceasing critical tractive force. In Fig. 1.3(b) domain II is subdivided into IIa IIb IIc. In domain IIa, all particles of mixed gravel do not move. For domains IIb and IIc only large particles of gravel do not move. For IIb water covers the entire width of the waterway, and only fine particles move. This domain is completely armourcoated. The flow in IIc has more shear stress than IIb, and the domain forms as a braided channel. The braided channel of IIc is an intermediate phenomenon falling between the phenomenon of IIb and that of a meandering channel (III) its exact type being undefined. Division of each of the domain in II, defined by critical tractive force for the transport of uniform gravel and gravel mixture will be examined concretely in Chapter 3.

Domain III: Here a concentrated stream develops with the water supply, and a stream meanders in the waterway. The stream forming its own channel, in other words, self formed channel width (B) occurs in an area smaller than channel width (B_0).

Domain IV: Here water covers the entire width of the waterway, main flow meanders and bars are formed.

Domain V: When the flow volume is increased beyond that of IV, the bars are flashed, and bed form becomes two dimensional. This is in general the domain where various bed patterns are formed, but this domain was a flat bed in our experiment taken at that time.

DomainVI: This is the domain where a slant rupture occurs. Its maximum slope including a rupture, in the case of non-cohesive materials accords with the static frictional angle of river bed gravels, and it was 45° in our experiment. Furthermore the minimum slope is given by a stable limit in case where saturated seepage water appears in parallel with an endless slope. For cohesionless materials, this slope θ is derived from the following equation.

$$\frac{C_*(\sigma/\rho-1)}{C_*(\sigma/\rho-1)+1}\tan\varphi < \tan\theta \qquad \cdots\cdots\cdots (1.3)$$

where σ is the density of soil particles, ρ is water density, ψ is angle of internal friction in soil, and C_* mass concentration of river bed materials. In this experiment, if $\psi = 45°$, $\sigma/\rho = 2.66$, $C_* = 0.6$, θ will equal 26°. If $\psi = 35°$ and other factors remain constant, θ will be approximately 19°. If the slope of the river bed is made steeper than the given slope, before the start of a surface flow the movement of sediment occurs as underground water level rises.

Domain VII: Where there is a collective sediment transport with surface flow being present occurs — the so-called domain of mud flow. The lower limit for this domain is called the limit of initiating a mud flow.

For gravel mixture this domain must be further divided into VII_a and VII_b. VII_b is a domain where an undurated mud flow takes place, VII_a is a domain where bed is formed in waving longitudinally. VII_a is seen more often than VII_b in case of small flow, and if minimum gradient is slightly smaller than VII_b. This phenomenon is referred to as dunes in a steep sloped channel and will be further discussed in Chapter 6.

Channel pattern is classified in the above way, according to the results of the experiment. Because materials A and C are of the same average grain size, using outflow from saturated flow, if diagrams (a) and (b) of Fig. 1.3 are expressed together in one diagram, taking a flow discharge obtained by subtracting the seepage flow discharge from the total flow discharge the diagram is given as Fig. 1.4, where both domains prove to be in a good agreement. The case of $B = B_0$ is discussed in chapters following Chapter 2 in this thesis, in which domains II and V correspond to this domain classification.

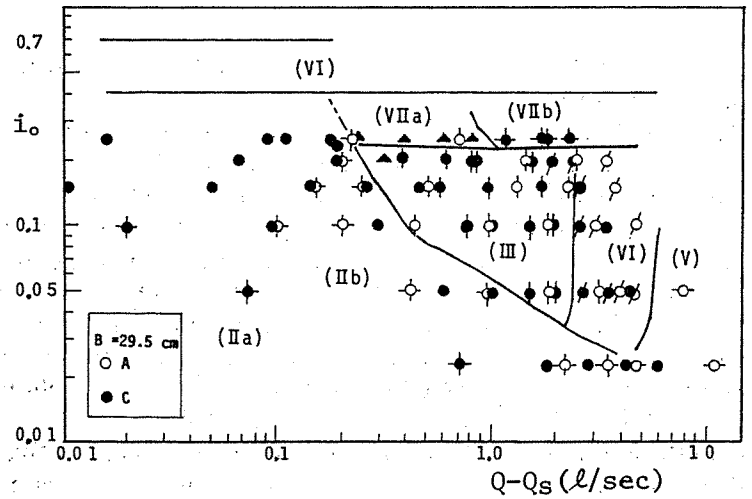

Fig. 1.4 Channel Patterns

Section 4: Channel Breadth and Meander Wavelengths

(1) Channel breadth

For division of channel pattern, whether or not the channel will meander or not in a water way of limited width is determined by the difference of breadth between self-formed waterway and channel.

Here, materials are changed and the relationship between channel breadth and flow discharge are shown in Fig. 1.5. The dispersion is large, however, it appears that the dominant factor is flow discharge, rather than bed slope and materials, relative to channel breadth. For channel breadth and flow discharge in this type of regime, heretofor, the proportion of width (B) to flow discharge (Q) has often been indicated to the 1/2 power. This theory has been tested by Lane[5], Henderson[6], Simons and Albertson[7] and Blench[8], however, all ended unsuccessfully. Furthermore, Leopold[9], introducing the cencept of entropy of the problem,

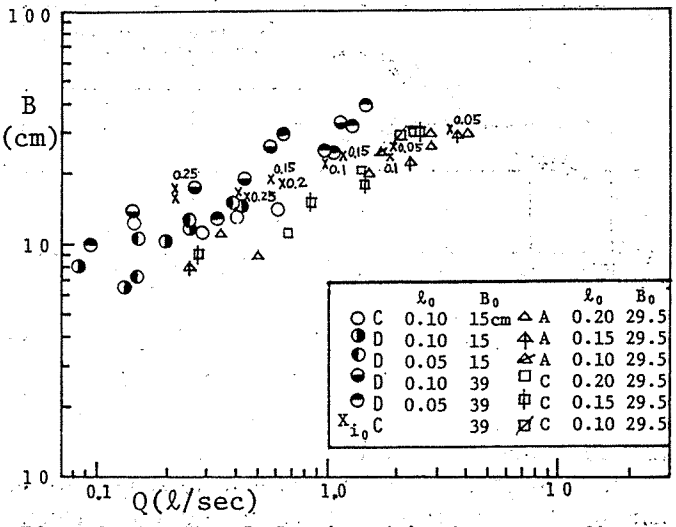

Fig. 1.5 The Relationship between Channel Breadth and Flow Discharge

explained it as $B \propto Q^{1/2}$, but the analogy of thermodynamic entropy to that of a stream in this case is invalid.

In relation to 'Regime theory' various reference works[10], author's experiments, etc.[11], using as wide a range as possible of slopes, flow discharge, and materials have been used as supplents. Heretofor, as reflected in this text, the regime theory as documented uses easy sloped rivers. Whether or not this is applicable in the case of a steep-sloped river of relatively large grain density is examined in Fig. 1.6. According to this, the channel breadth is proportional to 1/2 power of flow discharge regardless of channel slope, grain size of bed materials, and cohesion of bed materials, and the proportional constant is seen to always be fixed. If expressed with an equation in unit of m-sec, the following is given.

$$B = 3.5 \sim 7.0\, Q^{1/2} \quad \ldots\ldots\ldots\ldots\ldots\ldots (1.4)$$

When the breadth in relation to flow discharge is readily found in this manner, the flow discharge of a completed meandering channel in a given water way can be determined.

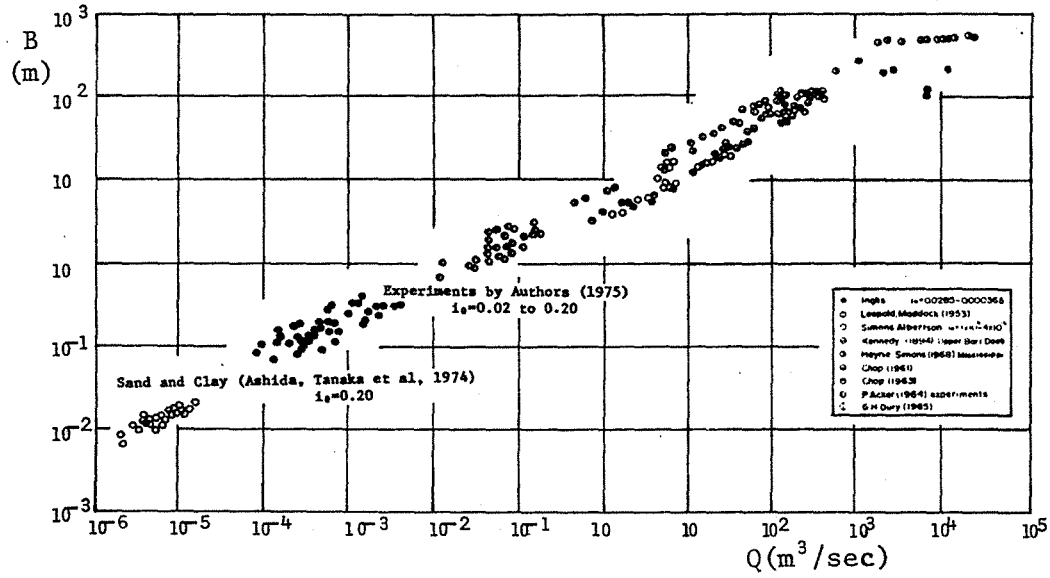

Fig. 1.6 The Realtionship between Channel Breadth and Flow Discharge

(2) Meander wavelength

In relation to meander, we will now take up on of its special features, wavelength L_B. According to the regime theory, wavelength is also proportional to the 0.46 ~ 0.62 power of volume, the relationship $L_B = 10 \sim 11B$[12), 13)] shown in Fig. 1.7.

From examination of the original meander Anderson[14] proposes

$$\frac{L_B}{\sqrt{A}} = 72\ F_r^{1/2} \quad \cdots (1.5)$$

F_r = 0.04 to 1.2 conforming to values found in this experiment. Here, A is the cross section of the flow, F_r is Froude's number ($U/\sqrt{gh}$, U = average water speed, g = gravitational acceleration, h = water depth). Assuming A = Bh, we get

$$\frac{L_B}{B} = 72\left(\frac{h}{B}Fr\right)^{1/2} \quad \cdots (1.6)$$

The results obtained in this experiment, L_B/B is shown in relation to $(h/B)F_r$ in Fig. 1.8, where the dispersion is large, but more than in formula 1.6, the trend of $L_B \doteqdot 10B$ is indicated. This relationship has been shown even for water flowing on ice, and along with the previous findings on channel width is extremely interesting.

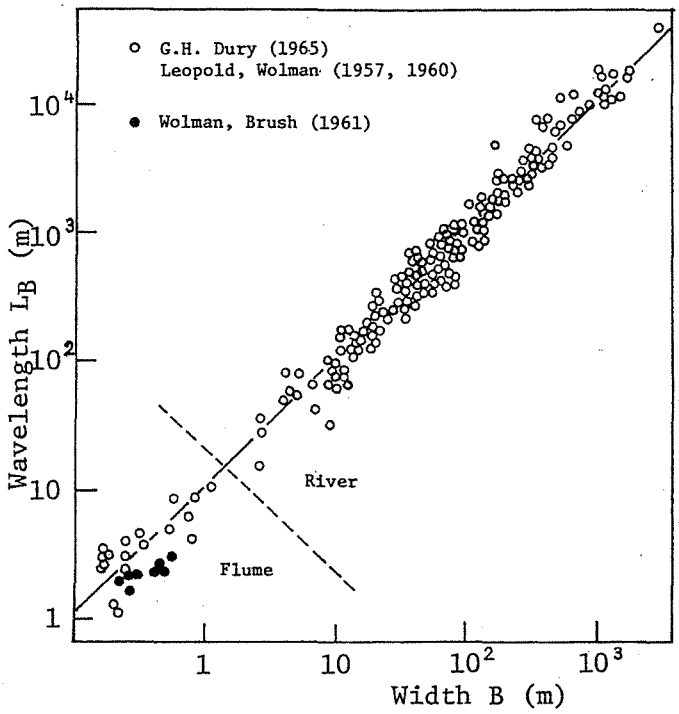

Fig. 1.7 The Relationship between Meandering Wavelength and Channel Width

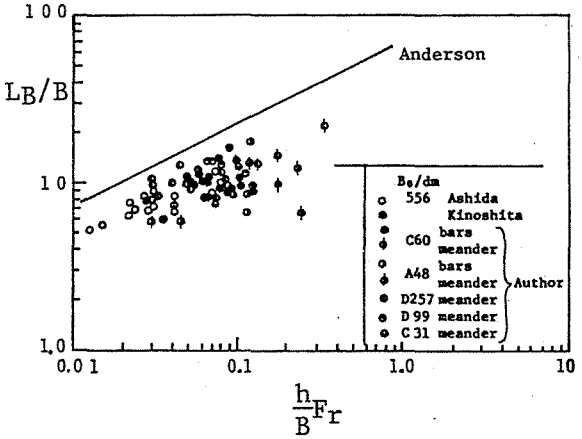

Fig. 1.8 Meandering Wavelength

Section 5: Bed Forms

(1) Small scale bed forms

For a movable bed, according to hydraulic conditions, and special properties of bed gravels, various bed forms are generated and influence is dominantly exerted on resistance coefficient, sediment transport rate, and channel fluctua-

tion in stream why do bed waves occur and what forms do they take, furthermore, what change takes place along with hydraulic quantity? Although there are many interesting questions, the discussion here will be what types there are and under what conditions they occur.

First, the types of bed form, according to the Sectional Meeting for Study of Bed Form in Hydraulic Committee, Japanese Society of Civil Engineers are ripples, dunes, anti-dunes, flat bed, and transition bed. For medium size rivers, there are also bars[16].

Based on much experimental data and semi-theoretical examination, study of so called domain classification as to what bed forms appear in what conditions has been developed. For example, in Fig. 1.9, partitioned diagrams were obtained by Garde and Raju[17], and also by Ashida and Michiue[18].

As is apparent from the diagram, almost no information is provided for the relative water depth of $R/d = 1$ to 10, Froude number of $Fr > 1$, and for bed gradient of $0.2 > I > 0.01$. In the work of Ashida and Michiue, from the stand point of estimating resistance, bed form can be thought of as being divided into Lower and Upper regimes. As reference for analytical results of the theory of bed wave stabilization, they consider $Fr \geq 0.8$ for the upper regime. Following this line of thought, the area of this research falls in the range of upper regime. In this experiment and others referred to, there was formation of Bars, but dunes and anti-dunes were not seen, and bed pattern was of flat-bed type.

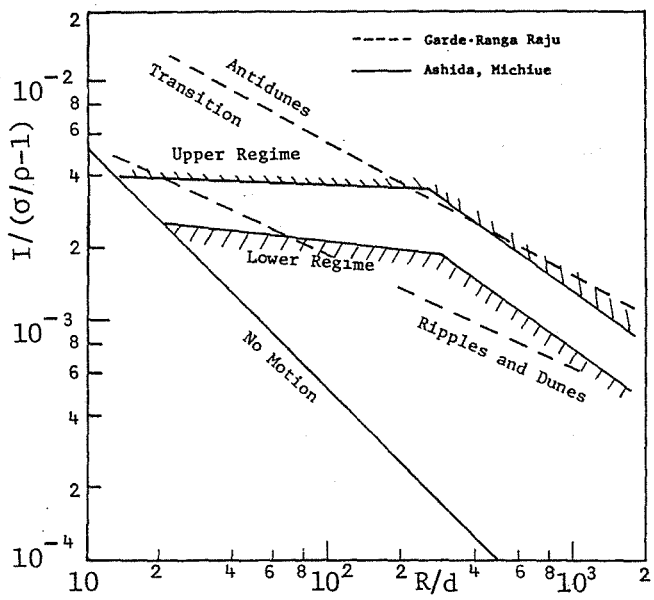

Fig. 1.9 Classification of Bed Forms into Domains

(2) Gravel bars

Gravel bars is a type of aforementioned bars, which is known as alternating bars. The alternating bars is seen to meander in the thalweg of the stream, and a single arrayed bars digs deep on the sides, and under certain conditions there is formation of multi-arrayed bars. For more concerning this see Kinoshita[19] and others. Although the experiment has been repeated by many others, under Kinoshita's conditions of bars formation, water way width was more than 10 times that of depth ($B/h > 10$) in certain instances.

According to Ikeda's method[20], the bed forms are divided into 4 tupes – type 1; multi-arrayed bars, type 2; alternating bars having a clear front edge, type 3; alternating bars having an unclear front edge, and type 4; the bed form where no basrs is formed.

He also categorizes the relative frictional velocity to the critical frictional velocity as U_*/U_{*c}, and non-dimensional quantity, iB/h consisting of bed gradient (i), waterway breadth (B), and water depth (h). According to the classification, the domain in which no bars is formed can be represented with eq. (1.7).

$$U_*/U_{*c} > 10(i \cdot B/h)^{1/3} \qquad \cdots\cdots (1.7)$$

Ikeda called this equation, iB/h, a river channel shape indicating number. Kuroki, et al[21], also reported similar results.

Sukegawa introduces a formation limit for bars that bars is formed when there is a small tractive force and there is a shallow stream, and he provided for the following equation (See Fig. 1.10).

$$R/B \geqq 5\left(\frac{U_* c^2}{g B}\right)^{2/3} i^{-1/3} \qquad \cdots\cdots (1.8)$$

Fig. 1.3(a) shows the formation limit by Sukegawa and that by Kinoshita. The Sukegawa's method is ambiguous for determining whether bars has been formed, but its experimental result agrees well with that of Kuroki.

Although physical meaning of parameters that dominate the cause of bars formation and the phenomena is not made clear, it proves that the domain of bars formation can be deduced from the conventional studies.

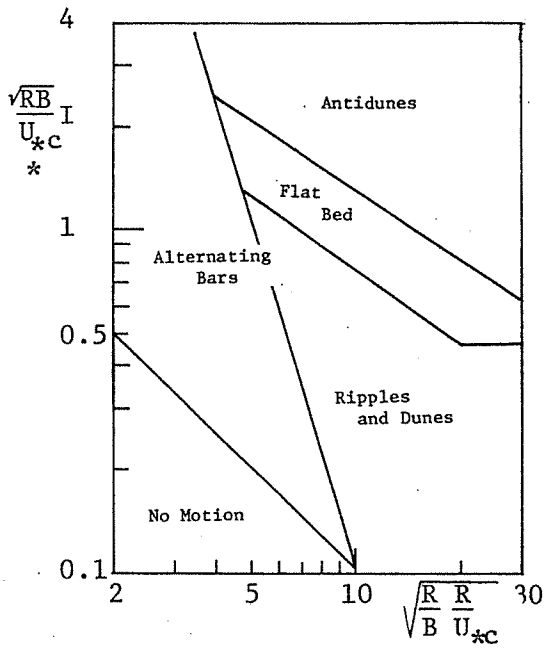

Fig. 1.10 Formation Domain for Bars by Sukegawa

Section 6 Forms of Sediment Transport and Sediment Discharge

(1) Bedload

In this section, sediment tranposrt form will be examined. The sidiment tranposrt form is classified as follows.

- Individual transport
  - wash load
  - bed material load
    - suspended load
    - bed load
- Collective transport (mass movement)

The individual sediment transport refers to a type of sediment transport through which sand gravel is transported individually piece by piece, while the collective sediment transport is defined as another type of sediment transport through which sediment is transported as a mass and which is so called mud flow. However, according to the recent study on mud flow there are many unknown phenomena which are difficult how it should be classified. Thus, such qualitative classification has become inadequate. Of the types of individual sediment transport the wash load consists of finely grained sand particles that do not exist in riverbed but are considered to be discharged from exposed mountains side slopes or, earth grounds left collapsed, or from roads. Sand gravel that exists as bed materials are transported in either suspended load or bedload mode. The suspended load is suspended by turbulence and has a concentration in the depth direction in proportion to grain size. On the other hand, the bedload consists of particles that in many cases move while touching with riverbed and its motion is controlled dominantly by the flow velocity in the neighborhood of the bottom of the river. The distinction between suspended load and bedload is determined by the limit of suspension which is further determined by the condition that $\sqrt{\overline{v'^2}}$, the vertical strength of the turbulent flow in the neighborhood of riverbed, is equal to W_O, the settling velocity. As $\sqrt{\overline{v'^2}}$ is approximately 0.93 times the frictional velocity U_*, $U_*/W_O = 0.8 - 1.0$ is used practically. Asada[23] examined Bogardi's[24] empirical equation, $U_O^2/gd_C = 360$ (U_O: Average flow velocity, d_C: Critical grain diameter for suspension), and concluded that the above equation seems no exaggeration at the present time when there is not provided adequate information. Although in some cases the presence of suspended load exerts a large influence on bedload, discussion will be continued ignoring this interaction in this thesis.

Fig. 1.11 shows values of the Darcy-Weisbach's resistance coefficient $f(=8U_*^2/U_O)$ obtained by this research, using τ_{*m} $(= \delta U_*^2/(\sigma/\rho-1)\, gd_m$, σ/ρ: Specific weight of a particle, and d_m: Average grain diameter) as parameters, vs the relative roughness dm/R (R: radius depth, which is roughly equal to the flow depth h if the channel breadth is sufficiently larger than the water depth).

The figure shows the distinction of resistance coefficient between streams with no sediment transport lower than incipient motion, with bars, with meandering, and the flat bed without meandering and bars. They are about the same except that the resistance coefficient of a meandering flow is slightly larger. Also, Fig. 1.12 shows bedload transport rate by channel pattern and by bed form. According to the figure, the bedload transport rate is small for a meandering flow and is about the same for other cases. According to the Daido's[25] experiment, the sediment transport rate for mud flow is as great as that for meandering flow. Although according to the Kinoshita's experiment, the bedload transport rate at the time of bar formation fluctuates within a range of 0.5 to 1.5 times the average value. However, the average value is about the same as the conventional experimental values of bedload transport rate. Kuroki[21], et al, also reported that the ratio of the effective shear stress at the time of bar formation to the total shear stress, τ_{*e}/τ_{*}, is around 0.8. The result of the experiment for this thesis also has the tendency similar to the conventional studies. Furthermore, the bedload equation[18] by Ashida and

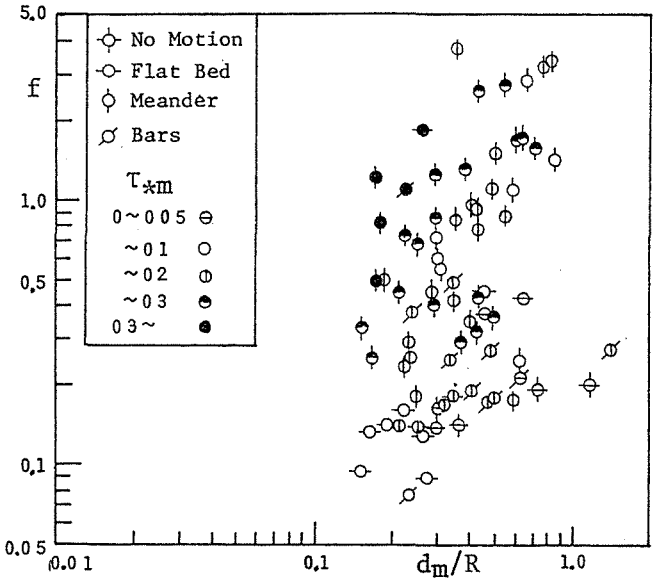

Fig. 1.11 Resistance Coefficient

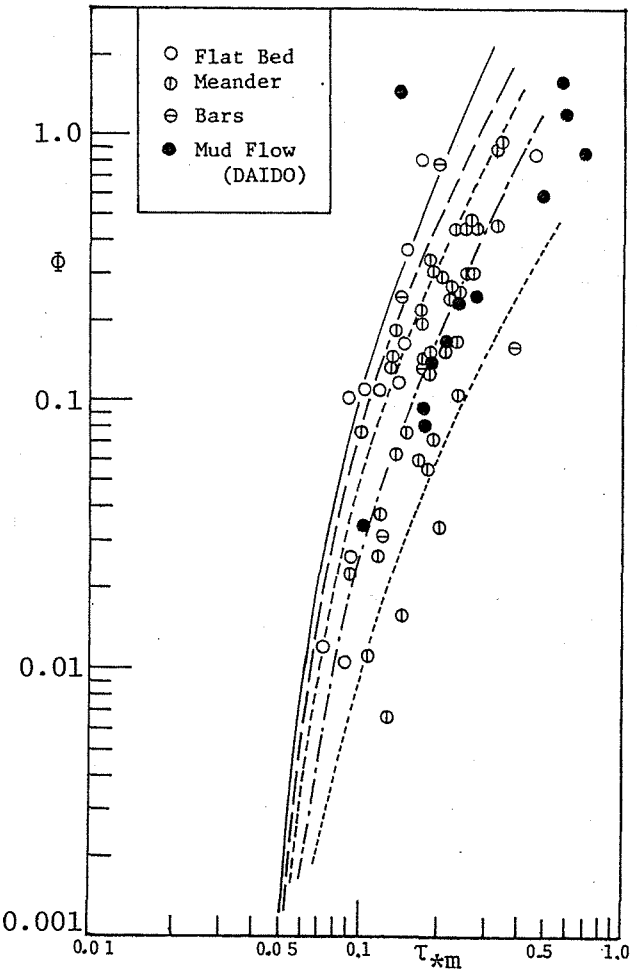

Fig. 1.12 Sediment Transport Rate

Michiue is shown in Fig. 1.12 for reference.

Next, we will discuss the experimental results of transversal distribution of bedload transport rate. First, the results of measuring the velocity distribution along the center line of waterway in both cases of the presence and the absence of bedload are shown in Fig. 1.13, in which there can be seen almost no difference between both cases. As a result of observation, in case bedload is present, there appeared some parts of riverbed with bedload and other parts without bedload, where there was bedload it was observed as longitudinal stripes. Those stripes more or less fluctuated in the transversal direction, but they were relatively made stable and neither separation nor confluence of those stripes were seen. Those longitudinal stripes appear to be controlled by a longitudinal vortex of flow, but the structure of this vortex is unclear. In order to see if a vortex appears where those longitudinal stripes encounter a second flow more upward or downward, sand particles were dropped from the water surface so as to be placed between stripes. The sand particles were then taken into the left and right

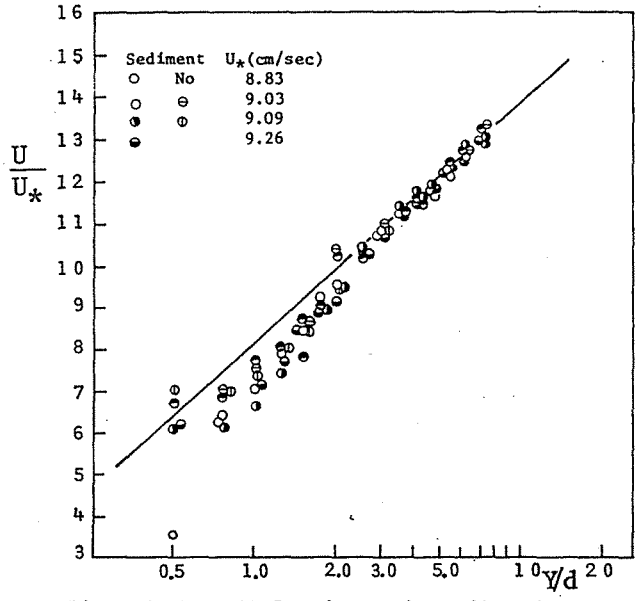

Fig. 1.13 Velocity Distribution of Flow with Sediment and without Sediment

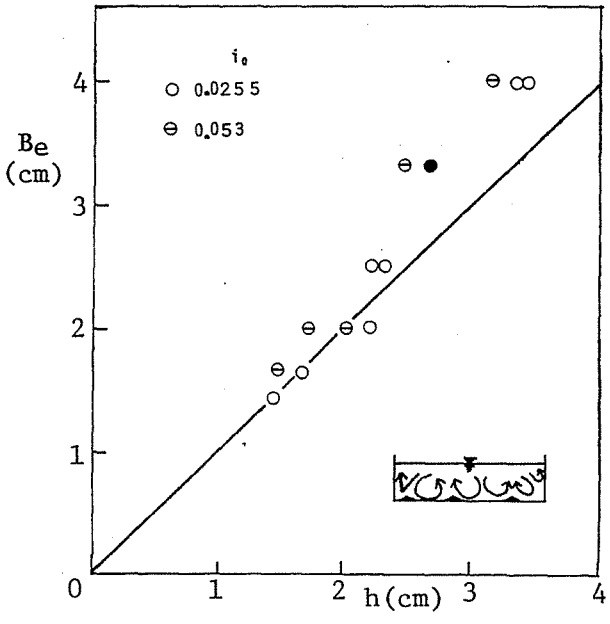

Fig. 1.14 The Relationship between Vortex Width and Flow Depth

adjacent stripes while being tracted in the left and right directions. This experiment proves that the flow direction is upward at longitudinal stripes. Thus, it results in the following relationship between the number of longitudinal stripes N and the number of longitudinal votices Ne.

$$N_e = (N-1) \times 2 \quad .. (1.9)$$

Fig. 1.14 shows the relationship between the average width of vortices (Be) and the water depth, and it can be found from this that the average width of vortices is about the same as the water depth. Next, Fig. 1.15 shows sample measurements of transversal velocity distribution. This is for a case without bedload, and alternating fast and slow current velocity can be seen near the bottom of channel. When there is sand supply in this type of stream, longitudinal stripes will appear in the higher velocity areas. If stream is divided widthwise by 2 cm, distribution of bedload transport rate appears as in Fig. 1.16.

Because the spacing between sand collecting boxes does not match with longitudinal stripes, the correct distribution may not be obtained. However, the figure shows the overall transversal distribution of sediment transport rate. Longitudinal stripes as can be seen in this way appeared when *(Continued)*

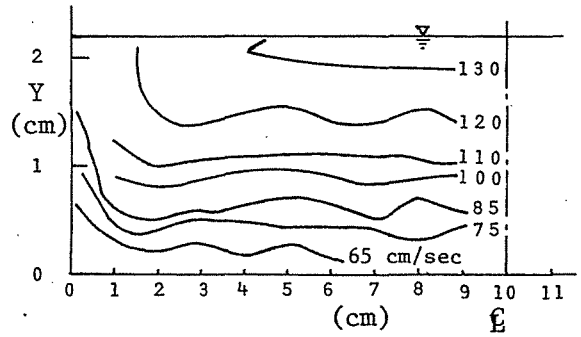

Fig. 1.15 An Example of Velocity Distribution Measurement

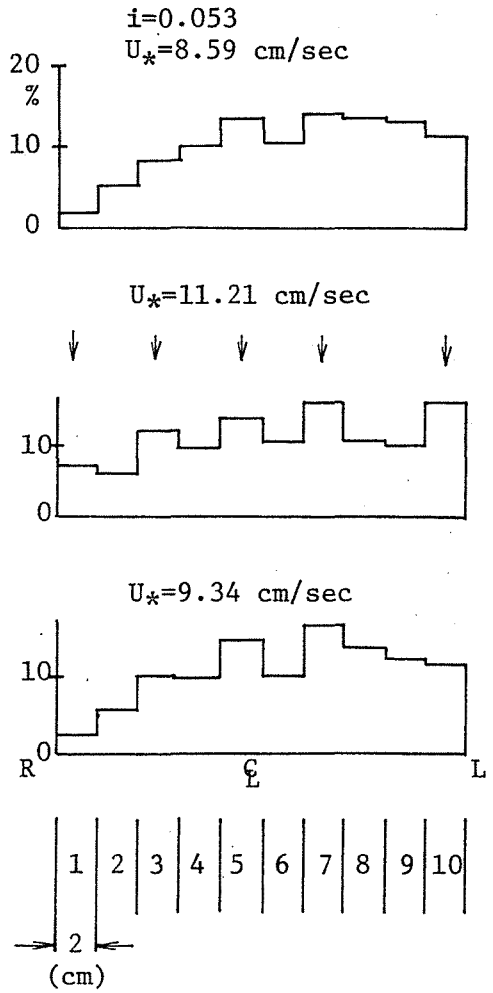

1.16 Distribution of Sediment Transport Rate

armorcoat was formed but could not be seen in cases of a gravel movement all over grain sizes. After all, it was not possible to make sure what influence the formation of longitudinal stripes in a general moving bed exerts on the bedload transport rate, but their existance and some of their features were discussed.

(2) Dunes on a steeply sloped flume

Looking at domain VIIa shown in Fig. 1.3(b) there was seen the phenomenon that appears to be a discontinuous dune sliding type debris flow by the Radio's[26] classification. In this phenomenon, gravel movement immediately after the water supply generates locally some areas with rough grain size distribution and other areas with fine grain size distribution, and where there is a rough grain distribution the surface flow is reduced and sand gravel is deposited and the sediment transported from upper stream areas is further deposited there to form a hill (see Fig. 1.17).

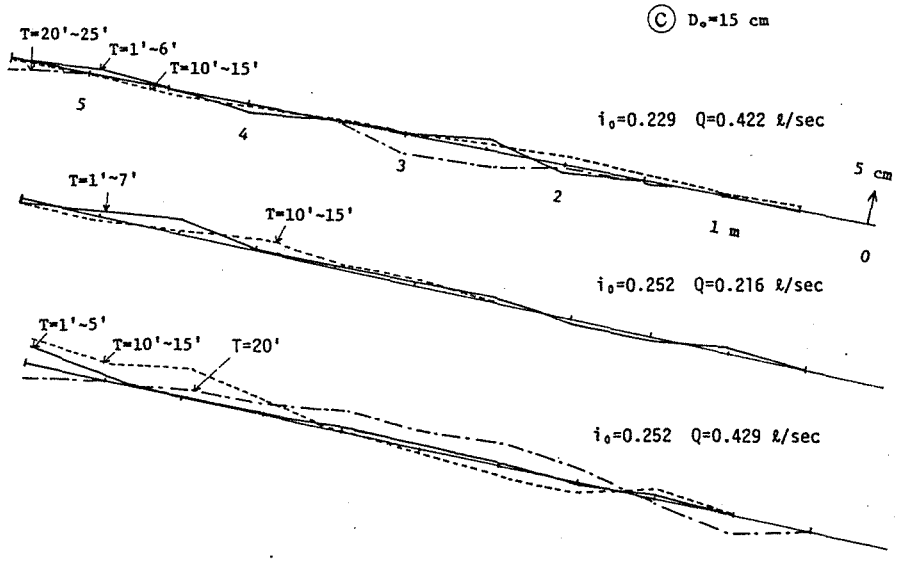

Fig. 1.17 Movement of Dunes in a Steep Flume

The portion downstream from the crest of this dune takes a gradient of 18 to 21° and the sediment thee is extremely coarse and there is no surface flow. As a dune develops to some extent, the piping occurs continually and the dune is once levelled and redevelops again. Such phenomenon is repeated to form a dune. In addition the gradient of the portion upstream from the crest of the dune 9 to 13°, and the stream meanders. This phenomenon can be considered to take an intermediate sediment transport mode between the individual sediment transport and where h_o is the depth of surface flow immediately preceding the occurrence of mud flow and d, the representative grain diameter. Although the limit of the occurrence of mud flow is determined by the above equation, the question rises what is the mechanism of the motion? In general, both a muddy flow that may be

the collective sediment transport since the individual sediment transport and the collective sediment transport since the individual and the collective sediment transport phenomena appear alternately. This intermediate sediment transport phenomenon is peculiar to mixed sand gravel, and it appears that as the range of grain size is wider the dune is higher. In addition, it is learned that this kind of phenomenon can be seen at mountain rivers in New Zealand.

(3) Debris flow and mud flow

As the slope gets steep (In this experiment, $i_0 \geqq 0.25$, $\theta \geqq 14°$), sand gravel moves in a laminar state rather than piece by piece, and also moves as a collection while being piled up. This kind of phenomena is called debris and mud flow and it has been studied extensively in recent years as it has a threat of causing many disasters. Condition that bed gravel is sheared deeper than one grain diameter, according to Takahashi[27], is given by the following equation (1.10).

$$\frac{C_*(\sigma/\rho-1)}{C_*(\sigma/\rho-1)+1+\frac{h_0}{d}}\tan\phi \leqq \tan\theta \qquad \cdots\cdots\cdots (1.10)$$

regarded as Bingham flow and a flow that is preferable to be handled as Dilatant flow to which the impact effect of particles is dominant are categorized in debris mud flows. A flow which causes bed deposit to move may be considered as Dilatant flow which is composed of sand gravel particles varying in size from boulders to fine grained sand. The appropriateness of handling the above flow as Dilatant flow was confirmed by Takahashi[27], et al., through their experiments using uniformly grained gravel, according to which the velocity distribution of particles lies on a straight line with an inclination of 3/2 in a full lograrithmic chart.

On the other hand, according to the author's experiment dealing with the mixed sand gravel transport through which the transport rates of particles were obtained by taking side pictures, it was observed that the bottom layer of the mud flow tends to have a Diratant flow at a gradient greater than 0.15 and particles in the uppermost part move more freely as shown in Fig. 1.18, and the individual sediment transport and the collective sediment transport can be considered a continuous phenomenon. Materials used in the experiment as shown in Fig. 1.18 are mixed gravel composed of grains with the minimum grain diameter of 0.42 mm, the maximum grain diameter of 24.5 mm, and with the average grain diameter of 5.67 mm.

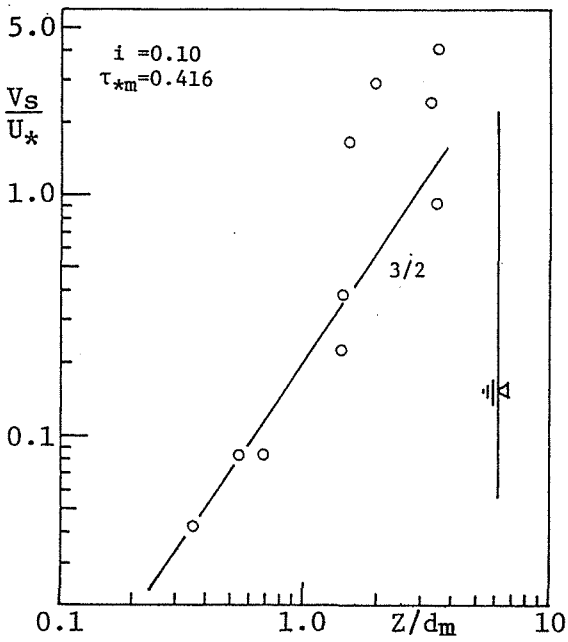

Fig. 1.18 Velocity Distribution of Movable Sand Gravel

Section 7: Conclusion

Channel pattern and sediment pattern have been discussed. First, experimentally channel and sediment pattern were classified in a plane diagram by slope and run off. Their characteristics have been clarified and at the same time a method of partitioning pattern domains was provided. Through these, the following things have become clear.

It has been widely recognized that self-formed channel breadths can be treated by the relationship of $B \propto Q^{1/2}$. It further proves that this relationship can apply to a self-formed channel with a steep slope up to 0.2 and without regard to cohesiveness of bed materials, and cam be provided with formula $B = 3.5$ to $7.0\ Q^{1/2}$ (in unit of m/sec). Also meandering wavelengths are approximately 10 times the channel breadth. Pertaining to bed pattern, bars was observed distinctly in this experiment and no bed waves such as dunes and anti-dunes were not formed.

Pertaining to sediment discharge, it was less in a meandering channel, and in flat beds and bars it was about the same. The sediment discharge for mud flow is about the same as that for a meandering channel. For bedload, on a fixed bed or on a bed where non-moving particles are present, stripes are formed. This was confirmed experimentally, and deduction of longitudinal scale indicated that water depth is similar. Also, regardless of whether there is bed load distribution, the current velocity does not change significantly.

Finally, for debris flows and dunes that have a sediment transport pattern in a steep sloped flume, its limit of occurrence and characteristics were made clear.

Above all, given bed slope, properties of bed materials, and flow discharge, it can be deduced what types of channel and sediment transport patterns will be determined. Moreover, the range of bedload to be discussed later, in Chapter 2, and in the following chapters belongs to domains II and V classified in this chapter.

REFERENCES

1) Yoshio Muramoto:
"Channel Patterns", Hydraulic Engineering Series 76-A-8, July 1976 pp. 1-27
2) Yoshio Muramoto, Yoshiaki Kawata, and Akihiko Nunomura:
"Sediment Transport on Gravel Bed", JSCE's Kansai Chapter, Annual lecture summary II-42-1~2, May 1976.
3) Leopold, L.B. and M.G. Wolman:
"River Channel Patterns; Braided, Meandering, and Straight", USGS. Professional paper, 282-B, 1957.
4) Edited by JSCE:
"A Collection of Hydraulic Formulas", Gihodo Co., p. 366
5) Lane, E.W.:
"Design of Stable Channels". Trans. ASGE. vol. 120, 1955, pp. 1234-1279.
6) Henderson, F.M.:
"Stability of Alluvial Channels", Proc. ASCE. vol. 87, HY6, 1961, paper 2984.
7) Simons, D.B. and M.L. Albertson:
"Uniform Water Conveyance Channels in Alluvial Material", Proc. ASCE. vol. 86, HY5, 1960, p.33.
8) Blench, T.:
"Regime Theory for Self-formed Sediment Bearing Channels", Proc. ASCE. vol. 77, separate no. 70, May 1951, pp. 1-18.
9) Leopold, L.B. and W.B. Langbein:
"The Concept of Entropy in Landscape Evolution", USGS. Professional paper 500-A, 1962, pp. 11-14.
10) Ackers, P:
"Experiments on Small Streams in Alluvium", Proc. ASCE. July 1964.
Haynie, R.M. and D.B. Simons:
"Design of Stable Channels in Alluvial Materials", Proc. ASCE. Nov. 1968, pp. 1399-1420.
Canal and Headworks Observation Programme of West Pakistan, 1961.
Kennedy, R.G.:
"The Prevention of Silting in Irrigation, Min. Proc. Instn. Giv. Engrs, vol. 119, 1894.
11) Kazuo Ashida, Kenji Tanaka, and Shin Tsuboka:
"The Process of forming a channel on a Bared Slope", JSCE's Kansai Chapter, Summary II-23-1~2.
12) Shigemi Takayama:
"River Morphology", Kyoritsu Shuppan Co., 1974
13) Dury, G.H.:
"Discharge Prediction, Present and Former, from Channel Dimensions, Jour. of Hydrology, 30, 1976, pp. 219-245.
14) Anderson, A.G.:
"On the Development of Stream Meanders", Proc. IAHR. vol. 1, No. 1, 1976, pp. 370-378.
15) Zeller, A.G.:
"Meadering Channels in Switzerland, 1967, pp. 174-186.
16) Edited by the Sub-Committee for Flow Resistance on a Movable Bed and Bed Transport forms in Hydraulic Committee of JSGE:
"Bed Transparent Forms and Roughness of Bed Material in a Flow on a Movable Bed", Professional paper 210, 1973.
17) Garde, R.J. and K.G. Ranga Raju:
"Regime Criteria for Alluvial Stream", Proc. ASCE. vol. 89, HY6, 1963, pp. 77-100.

18) Kazuo Ashida, and Masanori Michiue:
"A Fundamental Study of Resistance of a Flow on a Movable Bed and Bed Load Transport Rate", JSCE, Professional paper 206, Oct. 1972, pp. 59-60.
19) Ryosaku Kinoshita:
"Bed Transformation Survey in the Ishikari River", The Natural Resources Bureau of the Science and Technology Agency, Professional Material 36, 1961, Japan.
20) Hiroshi Ikeda:
"Bars in an Experimental Flume and their Formation Conditions", the Geological Review 46-7, 1973, pp. 435-451.
21) Mikio Kuroki, Chikara Kishi, and Tadaoki Itakura:
"Hydraulic Characteristics of Alternating Bars, Bed Forms and Flow Resistance in Alluvial Stream", from general studies supported under the budget for science studies in fiscal year from 1973 to 1974, pp. 80-88, Japan.
22) Hiroshi Sukegawa:
"Conditions for Forming Bars in a Straight Channel", the 26th JSCE annual summary of lecture II-69, 1971, pp. 189-190.
23) Hiroshi Asada:
"Some Ways of Technical Consideration on Sediment Transport in Mountain Rivers", the SHIN SABO 89, Nov. 1973, pp. 4-13.
24) Bogardi, J.L.:
"European Concept of Sediment Transportaion", Proc. ASCE. HY1, 1965.
25) Atsuyuki Daido:
"The Threshold of Initiating Mass Movement of Sediment", the 17th Hydraulic Lecture Meeting, Professional lecture, 1973, pp. 85-90.
26) Atsuyuki Daido:
"A Fundamental Study on Debris Flow", Doctor thesis, 1970.
27) Tamotsu Takahashi, Masashi Terada, and Shiro Hamada:
"The Influence of a Highly Concentrated Flow on the Occurence of Debris Flow", JSCE's Kansai Chapter, Summary of prefoessional paper, May 1976.

CHAPTER 2 RESISTANCE LAW FOR A TORRENTIAL STREAM

Section 1: Outline

There is a close relationship between riverbed configuration, resistance law, and sediment discharge in a movable riverbed. Thus, before studying bed load, it is necessary first to clarify flow velocity distribution, and the resistance law. The resistance of a has long been the subject of research. However, for a turbulent flow it is necessary to determine numerical values experimentally, and there has not yet been discovered a universal law applicable to any stream. Mountain streams, the object of this research, have in general rough turbulent flows with a large relative roughness; Previous research mainly concerns plains rivers, and their having a greater relative water depth, the information materials for the case of large relative roughness are extremely scarce. Thus, this Chapter examines resistance coefficient and flow velocity distribution for rough turbulent flows with a large relative roughness for a flat riverbed, and touches on the special nature of mixed sand-gravel beds. Further, for a deep stream in steeply sloped shallow water, there is a tendency to think a train of roll waves would be marked, but that is for the case of a comparatively smooth. Surface of a fixed riverbed, and for streams with a large relative roughness as in this research it was not observed.

Section 2: Velocity Distribution

For turbulent flow velocity distribution there is a logarithmic law known as Prandtl-Von Kármán's universal velocity distribution. For a prefect rough surface $U_* k_S/\nu > 60 \sim 100$, it is:

$$\frac{U}{U_*} = Ar + \frac{1}{\kappa} \ln \frac{y}{ks} = 8.5 + 5.75 \log \frac{y}{ks} \qquad \cdots\cdots\cdots (2.1)$$

where U_* : friction velocity $= \sqrt{\tau_O/\rho}$ $(= \sqrt{ghi})$, (τ_O: shearing force at the water channel bed surface, ρ: density of water, g: gravitational constant, h: water height, i: water surface slope),

κ : Kármán's constant (= 0.4),

y : Height from the bottom surface

U : Flow velocity at height y above the bottom surface,

k_S : Relative roughness,

ν : Kinematic viscosity of water,

Ar : A constant.

However, it is doubtful whether equation 2.1 is applicable in the region of a riverbed with a considerable roughness height. Fig. 2.1 presents the flow velocity distribution, measured with a Petot tube and an inclined magometer, above a fixed riverbed on which natural gravel of d = 12.0 mm is attached. According to that, the velocity distribution has a point of change in slope around y = 0.8d, and the flow velocity near the riverbed tends to be uniformalized to depart from Prandtl's logarithmic law.

The velocity distribution in Fig. 2.1 permits us to regard the upper and lower layers of flow as having respectively respectively different logarithmic distributions. Thus, for the lower layer below the change point in slope it is expressed as

$$\frac{U}{U_*} = A + \phi \ln \frac{y}{\delta} \qquad \cdots (2.2)$$

and for the upper layer as

$$\frac{U}{U_*} = A + \frac{1}{\kappa} \ln \frac{y}{\delta} \qquad \cdots (2.3)$$

From Fig. 2.1 the constants are K = 0.4, δ = 0.8d, ϕ = 0.87

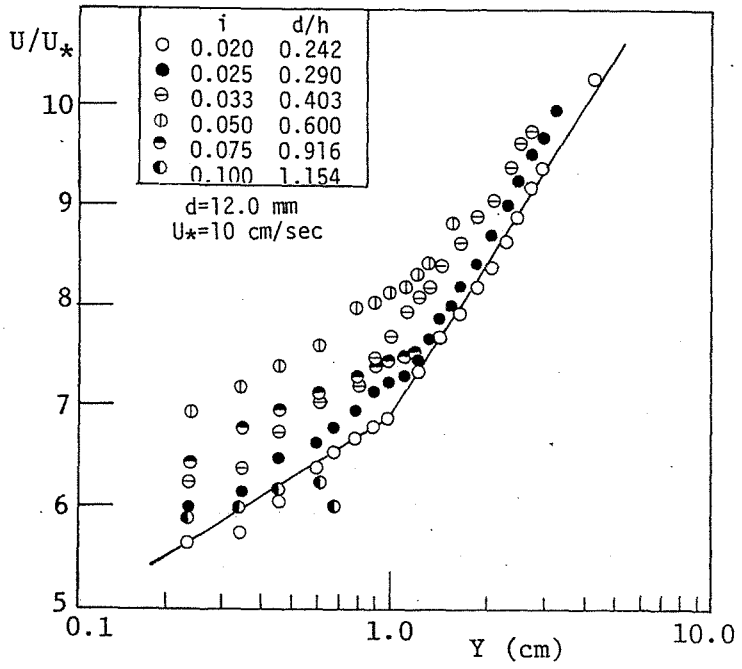

Fig. 2.1 The Result of Velocity Distribution Measurement

$A = U\delta/U_*$($U\delta$; Velocity at the position of $y = \delta$), according to Fig. 2.1 seems to change in a complicated way according to relative roughness. However, the pattern of velocity distribution in the neighborhood of the bottom surface changes with the placement of the origin of the coordinate system. Fixing the origin for the water height h is difficult and researchers have used various methods. Tsuchiya[2] for a fixed riverbed of mixed gravel finds a relationship between $\sqrt{d_{84}/d_{16}}$ and the position of origin of the coordinate system so that the value of friction velocity is equal to a value which can be found by applying the logarithmic law to the flow velocity distribution and friction velocity found from the water surface slope and water depth. Here, d_{84}, d_{16} indicate, respectively, 84% and 16% of the grain size in the grain size accumulation curve. According to the Tsuchiya's method the origin is located at the value 0.25d below the crest of a particle for uniform grain size. Also, Einstein and Elsamni[3] say it is appropriate to fix the origin coordinate at a value 0.2d below the crest of a particle because the slope of the velocity distribution is in conformity with the logarithmic law. Cheng and Clyde[4] investigated the applicability of Manning's formula and Chézy's formula with respect to uniform spherical roughness, and fix the origin at a value 0.15d below the crest of a varticle. The author considers the riverbed to be the height where 25% of the riverbed surface is exposed, a higher value, because the experimental results concerning initiation limit of gravel related in Chapter 3 can be arranged well regardless of grain size. A suitable height for uniform spherical grains is about 0.15d below the crest. This result places the origin above the result of Tsuchiya et al. who apply the logarithmic law to the velocity distribution. Fig. 2.1 illustrates the velocity distribution using these riverbed origins. The results indicate a tendency of uniformalization for the velocity distribution to depart from Prandlt's logarithmic law near the riverbed. Further, for the case where the riverbed origin is 0.25d below the crest of a gravel varticle the velocity distribution of Fig. 2.1 is as shown in Fig. 2.2. From this one can see that the velocity distribution pattern changes in a number of ways according to the placement of the origin, and that the uniformly changing trend of stream velocity near the bottom surface is the essential problem. There are two or three studies which have examined his tendency.

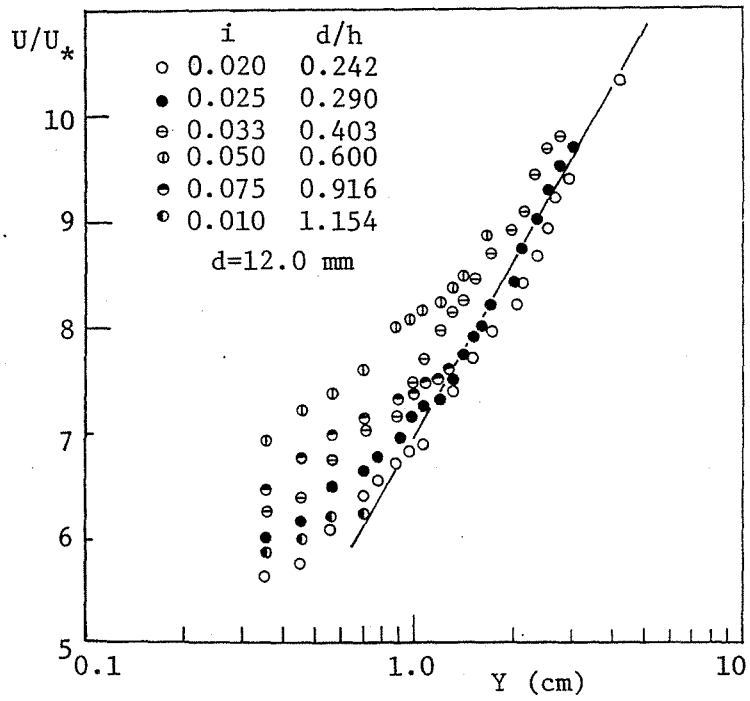

Fig. 2.2 Velocity Distribution of Flow in case the Standard Surface of Bed is taken below the Crest of Gravel

Christensen[5] studied the velocity distribution near a rough surface and explains it by taking the mixing length ℓ as

$$l = \frac{\nu}{U_*} + \beta d + \kappa y \qquad \cdots\cdots (2.4)$$

where κ is Kármán's constant,
β is a coefficient.
For a turbulent flow near a perfect rough surface $\nu/U_* \ll 1$, the formula is

$$l = \beta d + \kappa y \qquad \cdots\cdots (2.5)$$

O'Loughlin and Annambhotla[6] use this formula for the coefficient of kinematic eddy viscosity:

$$\epsilon = \epsilon \log + \epsilon w \qquad \cdots\cdots (2.6)$$

where ϵ_{log} is the kinematic eddy viscosity for logarithmic law ϵ_w is an additional kinematic eddy viscosity near the wall ϵ_w is taken to be a fixed value up to 2 times the height of the rough elements above the bed, and is taken to be zero above that. Iwagaki[7] too explains the uniform change of flow velocity as it occurs near the riverbed, taking the mixing length to be

$$l = l_o + \kappa y \qquad \cdots\cdots (2.7)$$

where ℓ_o is the additional mixing length near the riverbed. These above are hypotheses put forward to explain the velocity distribution, but all consider additional mixing due to rough elements. Further, such uniform change of flow velocity in the environs of the riverbed is observed also in cases where there is bed load[8] or suspended load[9], and is explained by activization of mixing by both large rough elements or bedload and suspended particles.

Yamaoka[10] measured the flow velocity distribution in the neighboring region of a rectangular roughness element, and explains the flow velocity near the rough surface by the theory of wake.

According to this explanation, as shown in Fig. 2.3,

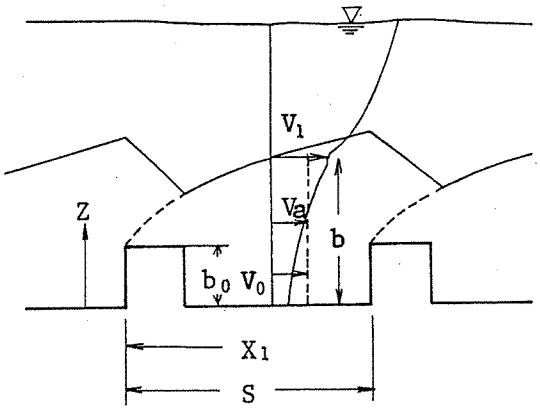

Fig. 2.3 Explanation of Velocity Distribution by Wake

One can find a section which deviates from the logarithmic law, where the so-called roughness wake layer is generated near the riverbed due to the existence of rectangular roughness elements. The flow velocity distribution within the roughness wake layer is explained as the velocity distribution of the wake caused by single rectangular bodies, and there are waves in the stream direction for the thickness of the boundary layer b. When it becomes largest in the case of an interference stream:

$$b = 1.781\sqrt{C_2 C_D b_0 X_1} \qquad \cdots\cdots\cdots (2.8)$$

where C_D is a drag coefficient, C_2 a constant determined by the flow velocity distribution, and b_0 the roughness height. If one extends this over a riverbed surface with a grain diameter of a spaced λ'd, the thickness of the maximum thickness of wake layer b_{max} is proportional to $\lambda'^{1/2}$ d. For natural riverbeds the relationship between the representative grain diameter d and the grain spacing λ'd is analogous, and since one can consider λ' a fixed value, b_{max} is proportional to grain diameter. Further, the mixing distance ℓ, within the roughness surface wake layer is also proportional to $\lambda'^{1/2}$ d, and is constant in the direction of measuring water depth. This supports the average agreement of Christensen mentioned before and the hypothesis of Iwagaki. More correctly, for the ratio b/b_0 of the thickness of the roughness wake layer b to the roughness height b_0, a tendency to change can be seen due to slope, not only to roughness spacing. According to these experiments the ratio b/b_0 has a dispersion around 1.6—3.0, which if one considers the treatment of the bed surface is almost identical with $\delta = 0.8d$ mentioned before. Here δ is the turning point of the flow velocity distribution. As for other explanations of the uniform change of flow velocity near the riverbed there is the water permeability of the riverbed materials.

However, Zagni and Smith[11] found the resistance coefficient increased for the case of rough uniform gravel compared with an impermeable riverbed, but for mixed sand permeability need not be considered.

That report was on resistance coefficient and not an argument concerning change near the bed of flow velocity distribution, but it seems in general that permeability does not exert much influence.

Thus, having compared previous research, the uniform change of flow velocity near the bed with rough turbulent flow is a general phenomenon, and since it seems quite valid to take 0.8d as the height of the turning point of the slope, it is used here (equations 2.2 and 2.3) to predict the flow velocity near the riverbed. Integrating equations 2.2 and 2.3 to find the average cross sectional flow velocity Uo, as a two-dimensional stream, for $h \geqq \delta$, we have

$$\frac{U_0}{U_*} = \frac{U_\delta}{U_*} + \frac{1}{\kappa} \ln \frac{h}{\delta} - \frac{h-\delta}{h} \frac{1}{\kappa} - \frac{\delta}{h} \phi \qquad \cdots\cdots (2.9)$$

for $h < \delta$,

$$\frac{U_0}{U_*} = \frac{U_\delta}{U_*} + \phi \left(\ln \frac{h}{\delta} - 1 \right) \qquad \cdots\cdots (2.10)$$

In formulas 2.2 and 2.3, in order to determine A (U_d/U_*) it is necessary to know the value of U_0/U_*, namely the resistance coefficient.

Section 3: Coefficient of Resistance

(1) Coefficient of resistance for a rigid bed

As explained in the Section 1: Outline, there are many studies on resistance coefficient for a fixed bed when the relative roughness is not large. Studies on flow resistance for a large relative roughness mostly concern artificial roughness called spherical roughness or frame-type roughness[12), 13).

For example in Moody's diagram[14) experimental values are indicated up to the value d/h = 0.2 for the conduit.

Mirajgaoker[15), from dimension analysis and experiments using natural stones (large cobble stones), reports that the resistance coefficient increases not only according to the relative roughness but also according to the Froude number Fr ($= U_O/\sqrt{gh}$).

Also, Iwagaki[7), concerning the Ar of equation 2.1, has found an experimental formula from research on thin layer streams.

$$\left.\begin{aligned} &Fr \leqq 0.89 \text{ では, } Ar = 10, \\ &Fr \geqq 0.89 \text{ では, } Ar = 9.7 - 5.75 \log Fr + 1.2 (\log Fr)^2 \end{aligned}\right\} \cdots (2.11)$$

Also, Honma[16), in case when the resistance coefficient is for a torrential flow, investigated experimently that it is not only a function of Reynolds Number. Re ($= U_O h/\gamma$) but also a function of Froude Number. Since the value of d/h < 0.2 in Moody's diagram is insufficient, for mountain rivers, experiments carried out for values of d/h greater than 0.2 using an experiment for artificial roughness in order to investigate appropriate values of the resistance coefficient.

(a) Outline of the experiments

In the experiments the downstream 2 m end of a 15 m long and 36.5 cm wide flume (steel with one side glass, whose slope can be varried freely from 0° to 20°) was used.

Two types of glass beads of diameters 24.5 mm and 12.6 mm respectively were used as roughness elements.

These were spread out in a single layer densely in an aluminum box of width 36.5 cm, length 1.96 m as shown in Fig. 2.4.

The box was inserted in the channel, and with a slope of 0.02 to 0.17, the flow depth was observed while changing the flow discharge.

Further, the flow depth was measured with a point gauge, and the flow discharge by a triangular weir.

(b) Experimental results and observations

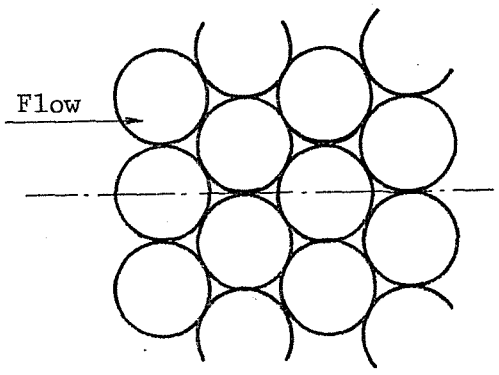

$Nd^2=1.155$

Fig. 2.4 An Array of Roughness Elements

Chézy's c and Manning's n are well known as coefficients of flow resistance, but here Darcy Weisbach's coefficient of frictional resistance $f \fallingdotseq 8U_*^2/U_O^2$ in used.

The resistance coefficient of friction f due to close packed sand particles can be considered a function of a coefficient dependent on friction velocity U_*, gravitational constant g, grain diameter d, water depth h, water viscosity co-efficient μ, and the water density ρ, and using dimension analysis the value of f can be expressed as:

$$f=\Phi_1\left(\frac{U_* d}{\nu}, \frac{U_*^2}{gd}, \frac{d}{h}\right) \quad \cdots (2.12)$$

The first term on the right side is called the Reynolds Number Re_* and can be considered to exert no great influence on a perfect rough surface turbulent flow.

If we add to the prameter the density N of the roughness, Nd^2 is added to the right side of function 2.12.

This is the same as White's[17] packing coefficient, and for the arrangement shown in Fig. 2.4 $Nd^2 = 1.155$ we see from function 2.12 that for in the case where the arrangement of roughness elements is fixed, it is best to arrange the relative roughness d/h and U_*^2/gd the parameters.

Fig. 2.5 indicates the change of the resistance co-efficient due to relative roughness from experimental results.

The lines determined by eye show the overall trend.

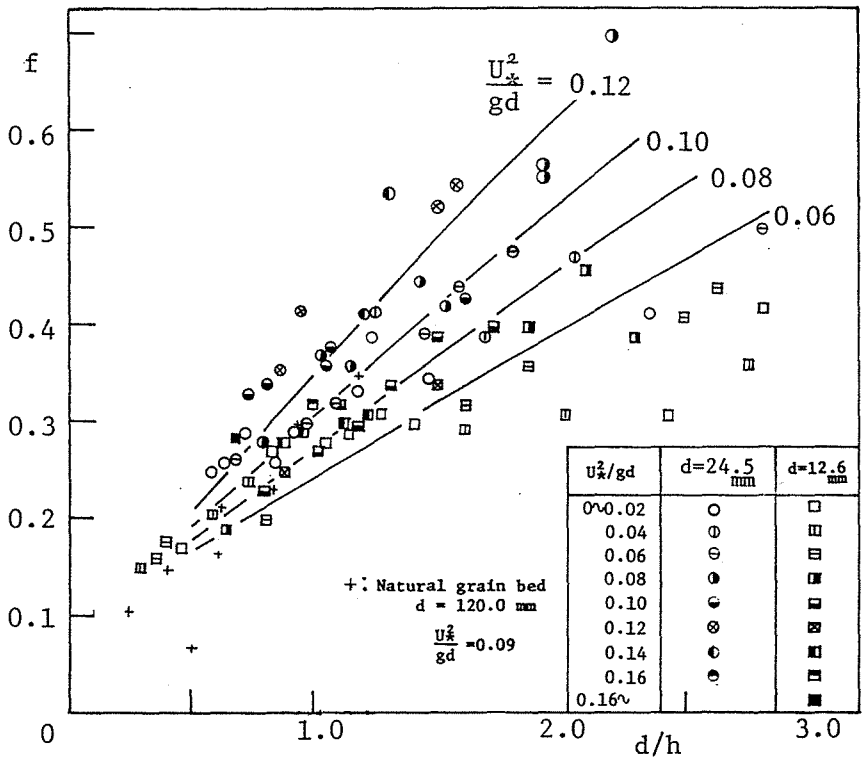

Fig. 2.5 Experimental Results of Resistance Coefficients

From this we see that as the relative roughness increases the resistance coefficient f increases sharply, and that the larger the value of U_*^2/gd the larger the value of f becomes.

In Fig. 2.5, a diffence in resistance can be seen for the two different diameters, but it is not a significant difference, the reason being that a considerable error is included in the depth measurements since the absolute water depth is small.

Further, taking the theoretical riverbed surface to be 0.15d below the crest of a particle, the influence of the sidewall is corrected for using Einstern's method[18].

When the width is large with respect to the water depth there is practically equivalent to Rb.

Here Rb is the hydrantic radius with respect to the riverbed.

The relationship between Froude Number and U_*^2/gd is:

$$Fr^2 = \frac{U_0}{gh} = \frac{U_*^2}{gd} \frac{U_0^2}{U_*^2} \frac{d}{h} = \frac{U_*^2}{gd} \cdot \frac{8}{f} \cdot \frac{d}{h} \qquad \cdots\cdots (2.13)$$

and if three of the variable F_r, U_*^2/gd, f, d/h are found the fourth is uniquely determined. The reason for using U_*^2/gd as the parameter instead of Froude's Number is that given the water depth and slope the flow velocity can be immediately caluculated.

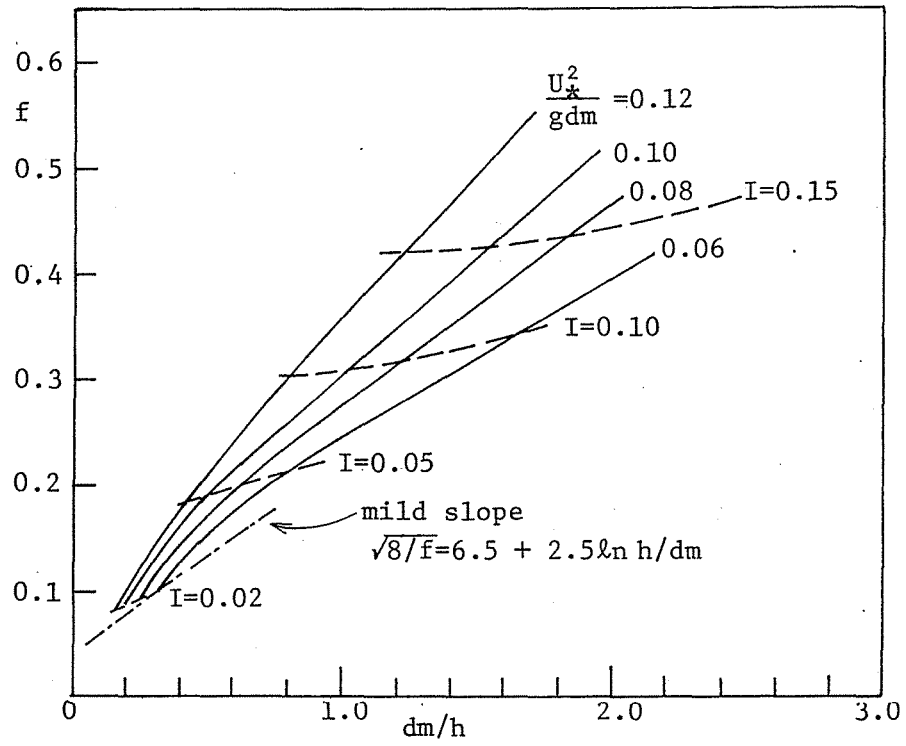

Fig. 2.6 Change in Resistance Coefficient dependent on Slope and Relative Roughness

Fig. 2.6 indicates the coefficient of dray as a function of slope. Finding the f from Iwagaki's equation (2.11), we get

$$\left.\begin{aligned} &Fr \leqq 0.89, \\ &f = 8/\left(7.5 + 5.75 \log\frac{R}{d}\right)^2 \\ &Fr \geqq 0.89, \\ &f = 8/\left\{7.2 - 5.75 \log Fr + 1.2 (\log Fr)^2 + 5.75 \log\frac{R}{d}\right\}^2 \end{aligned}\right\} \cdots\cdots (2.14)$$

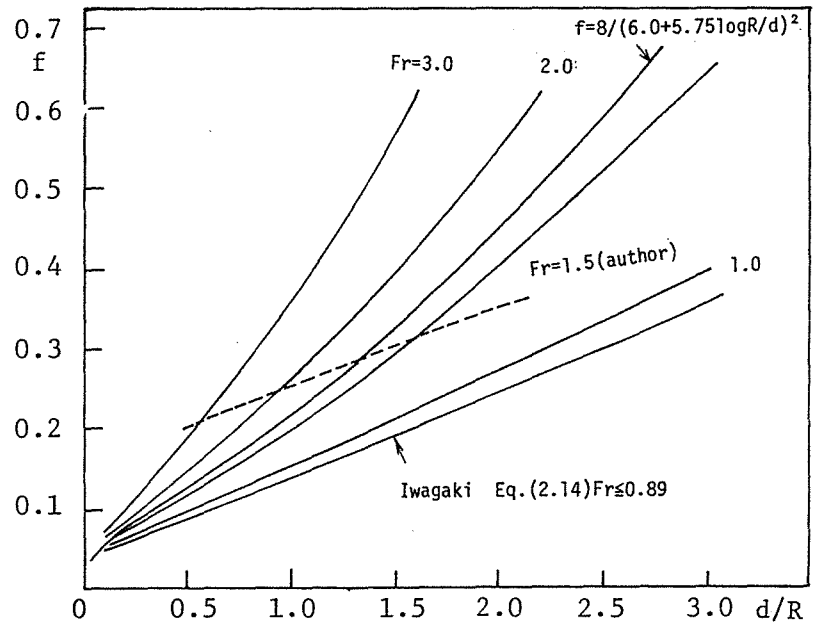

Fig. 2.7 Comparison of Various Resistance Coefficients with the Empirical Equation by Iwagaki

There are a number of differences with the experimental results of Fig. 2.5, what is the cause of such increase in resistance?

First, one can consider the loss of energy due to a vortex behind the riverbed gravel. Then, using an abrupt drop model one explains the characteristics of the variation in resistance coefficient due to U_*^2/gd and d/h.

(c) Explanation using a step-down model

Consider a riverbed lined with spheres as in Fig. 2.4. In Fig. 2.8, let λd be the length of the boundary of the vortex caused by wake. Deriving an equation of momentum for the range between the cross-section I at the crest of a particle and the cross-section II at the reattach point, ignoring friction, we get

$$\frac{\rho g(h_1+\beta d)^2}{2}-\frac{\rho h_2^2}{2}=$$

$$\rho\eta_2 v_2^2 h_2 - \rho\eta_1 v_1^2 h_1 \quad \cdots\cdots (2.15)$$

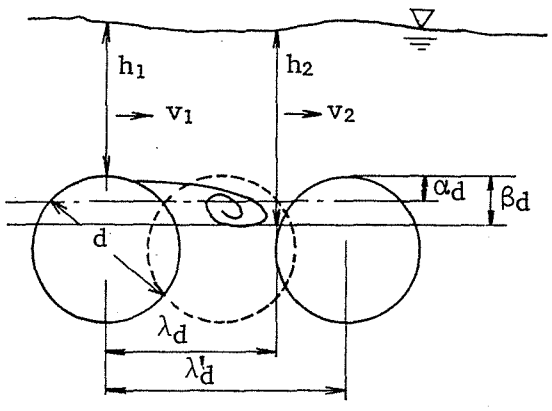

Fig. 2.8 Explanation of a Stepped-Down Model

where, η_1 and η_2 are correction coefficients for the momentum at cross-sections I to II, and the other sumbols are indicated in Fig. 2.8.

The equation of continuity is

$$h_1 v_1 = h_2 v_2 = hv \qquad \cdots\cdots (2.16)$$

where h is average depth, v is average velocity.

The equation of energy is

$$\beta d + h_1 + \frac{v_1^2}{2g} - \left(h_2 + \frac{v_2^2}{2g}\right) = hl \qquad \cdots\cdots (2.17)$$

The loss of water head is written

$$hl = i_0 \lambda d = \left(\frac{U_*^2}{gh}\right) \lambda d \qquad \cdots\cdots (2.18)$$

where i_0 is the water channel slope. Taking

$$\frac{v}{U_*} = A\acute{r} \qquad \cdots\cdots (2.19)$$

$$h = h_1 + ad \qquad \cdots\cdots (2.20)$$

$$\eta_1 = \eta_2 = 1, \quad a = \beta \qquad \cdots\cdots (2.21)$$

From equation 2.20

$$\frac{h_1}{h} = 1 - a\frac{d}{h} \qquad \cdots\cdots (2.22)$$

Then from equation 2.22

$$\frac{h_1}{h_2} = \frac{h_1}{h} \cdot \frac{h}{h_2} = \left(1 - a\frac{d}{h}\right)\frac{h}{h_2} \qquad \cdots\cdots (2.23)$$

From equation 2.16 and 2.19,

$$v_2 = \frac{h}{h_2} v = \frac{h}{h_2} U_* A_r' \qquad \cdots\cdots (2.24)$$

$$v_1 = \frac{h}{h_1} U_* A_r' \qquad \cdots\cdots (2.25)$$

From equations 2.15, 2.24, and 2.25

$$\frac{g h^2}{2} - \frac{g h_2^2}{2} = \left(\frac{h}{h_2}\right)^2 A_r'^2 U_*^2 h_2 - \frac{h}{1-a\frac{d}{h}} U_*^2 A_r'^2$$

Cancelling $gh^2/2$ on both sides of the above equation the following relation results:

$$1 - \left(\frac{h_2}{h}\right)^2 = \frac{2 A_r' U_*^2}{g d} \cdot \frac{d}{h} \cdot \left(\frac{h}{h_2} - \frac{1}{1-a\frac{d}{h}}\right) \qquad \cdots\cdots (2.26)$$

From equation 2.17, the following relation results:

$$h + \frac{1}{2g}\left(\frac{h}{h_1}\right)^2 U_*^2 A_r'^2 - \left[h_2 + \frac{1}{2g}\left(\frac{h}{h_2}\right)^2 U_*^2 A_r'^2\right] = \frac{U_*^2}{g h} \lambda d$$

Cancelling h on both sides of the above equation, the following relation results:

$$1 - \frac{h_2}{h} - \frac{U_*^2}{g d} \lambda \left(\frac{d}{h}\right)^2 = \frac{1}{2} \frac{U_*^2}{g d} \frac{d}{h} A_r'^2 \left[\left(\frac{h}{h_2}\right)^2 - \frac{1}{\left(1-a\frac{d}{h}\right)^2}\right] \qquad \cdots (2.27)$$

or, rearranged into:

$$\frac{U_*^2}{g d} \frac{d}{h} A_r'^2 = \frac{2\left[1 - \frac{h_2}{h} - \frac{U_*^2}{g d} \lambda \left(\frac{d}{h}\right)^2\right]}{\left(\frac{h}{h_2}\right)^2 - \frac{1}{\left(1-a\frac{d}{h}\right)^2}} \qquad \cdots\cdots\cdots\cdots (2.28)$$

Substituting eq. 2.28 in eq. 2.26 and rearranging it, the following relation results

$$\left(\frac{h_2}{h}\right)^3 - 3\left(1-a\frac{d}{h}\right)\left(\frac{h_2}{h}\right)^2 + \left\{4\left(1-a\frac{d}{h}\right)\left(1-\frac{U_*^2}{gd}\lambda\left(\frac{d}{h}\right)^2\right)-1\right\}\frac{h_2}{h}$$

$$- \left(1-a\frac{d}{h}\right) = 0 \qquad \cdots\cdots\cdots (2.29)$$

In eq. 2.29 let $h^2/h = x$, $1 - a\,d/h = A$, $1 - U_*^2/gd\,\lambda\,(d/h)^2 = B$, the following results:

$$X^3 - 3AX^2 + (4AB-1)X + A = 0 \qquad \cdots\cdots (2.30)$$

Because this is a trinominal equation with respect to X, it can be solved using the Cardan's method. When obtaining the solution with a real number, the following relation results from eq. 2.28

$$A_r'^2 = \frac{2(B-X)}{\frac{U_*^2}{gd}\cdot\frac{d}{h}\left(\frac{1}{X^2}-\frac{1}{A^2}\right)} \qquad \cdots\cdots\cdots\cdots (2.31)$$

and the coefficient of resistance becomes

$$f = \frac{8}{A_r'^2} \qquad \cdots\cdots\cdots\cdots (2.32)$$

From the above, the resistance coefficient can be calculated for an arbitrary combination of U_*^2/gd and d/h, provided the coefficients a and λ are determined. Considering this two-dimensionally in such arrangement as in Fig. 2.8, if we take a = 0.15, λ becomes 1.375. Let's observe a vortex behind spherical grain particles laid most densely on the riverbed. Glass beads of 24.5 mm in diameter were spread over 4.5 m in width within the water channel, and through the glass wall, the flow in the periphery of the spheres was observed from the side. To make the observation clear a solution of pearl clay added by potassium manganate is put into the flow. Clear observation of the domain of he vortex in the wake by experiment was difficult due to the dispersion of dyestuffs, but a peel-off point could be observed well. According to those observations the peel-off could be seen near the crest of a particle, and it resembled photographs of a flow in the vicinity of cylinders by Prandtl, or those of spheres in a uniform flow by Wieselsberger. Further, the vortex behind the roughness elements reached as far as the particle behind, which proved the appropriateness of the model of Fig. 2.8 to the phenomena.

According to calculations using the stepped model, as in Fig. 2.9, for the case $\lambda = 1.50$, $a = 0.10$ there is good agreement with the experimental values, and it seems the three dimensional influence is exerted to some extent.

Thus, using the step-down model as above, the change of the resistance coefficient f by U_*^2/gd and d/h can be explained.

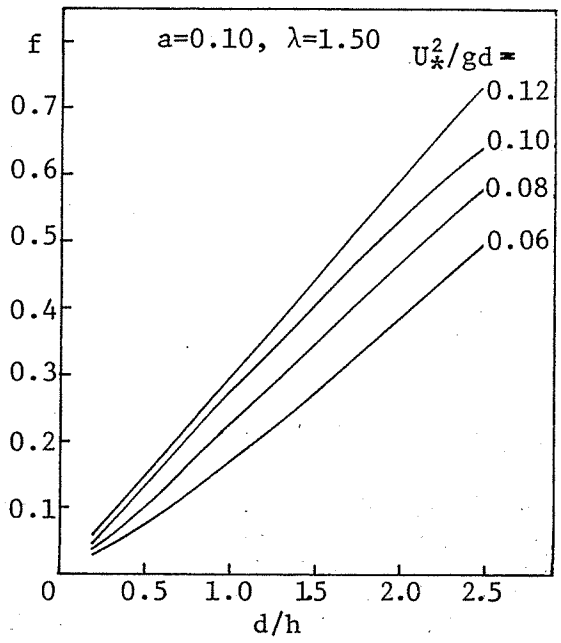

Fig. 2.9 Calculated Results of Resistance Coefficient

(2) The stream resistance law for a movable bed

The previous section concerned the resistance law for a flow on a fixed bed. Here, the case of a movable bed. The average cross-sectional velocity U_0 for a movable bed is assumed to be determined by μ, g, d, R, I, σ, ρ. Replacing the energy gradient I by $U_* = \sqrt{gRI}$, and the gravitation constant g by the weight of gravel in the water $(\sigma - \rho)g$, U_0/U_* can be written, using dimension analysis, as

$$\frac{U_0}{U_*} = \Phi_2 \left(\frac{U_* d}{\nu}, \frac{U_*^2}{(\sigma/\rho - 1)gd}, \frac{R}{d}, \frac{\sigma}{\rho} \right) \qquad \cdots\cdot (2.33)$$

where R is the hydraulic radius. In the case where river bed waves are formed, the height of the waves, not R/d, is important. The hydraulics Committee of the Japanese Society of Civil Engineers[21] processed a large number of materials on experiments concerning resistance of a movable bed. However, as explained in Chapter 1, this research assumes that the river bed patterns are for the most part flat river beds, and in the region of a perfect rough surface turbulent flow. The influence of Reynolds Number for the sand particle is not marked. Further, since the object of this research was natural river beds, the ratio σ/ρ is practically constant at about 2.5 to 2.65. Finally, for a flat movable bed resistance coefficient the parameters become the tractive force τ_* $(= U_*^2/(\sigma/\rho - 1)gd)$ and R/d. According to Kishi[22] the experimental resutls of resistance coefficient for flat beds is close to

$$\frac{U_0}{U_*} = 6.0 + 5.75 \log \frac{h}{d} \qquad \cdots\cdots\cdots\cdots (2.34)$$

Ashida and Michigami[23] for a flat movable bed propose the following, considering that the jump height of a sand influences the roughness.

$$\frac{U_0}{U_*} = 6.0 + 5.75 \log \frac{h}{d(1+2\tau_*)} \qquad \cdots\cdots\cdots\cdots (2.35)$$

In order to obtain values for the roughness coefficient for the case of large relative roughness, the author carried out experiments on a movable bed. The sand utilized in the experiments was uniform sand gravel with average diameter of 5.51 mm and mixed sand gravel with average diameter of 6.4 mm. Fig. 2.10 shows resistance coefficient as a function of d/Rb and τ_*. For the resistance coefficient on a movable bed, experiments were carried out under conditions of both U_*^2/gd and the relative water depth being large compared with the previous experiments for fixed bed. As is clear from the figure, the resistance coefficient seems to vary continuously from the trend of the fixed bed experiments. Ashida and Michiue[23] find good agreement when comparing the experimental data for $R/d \geq 10$ with equation 2.35 for the upper regime. However, as shown in Fig. 2.10 for $d/R > 0.1$ the experimental values are considerably larger than those of equation 2.35.

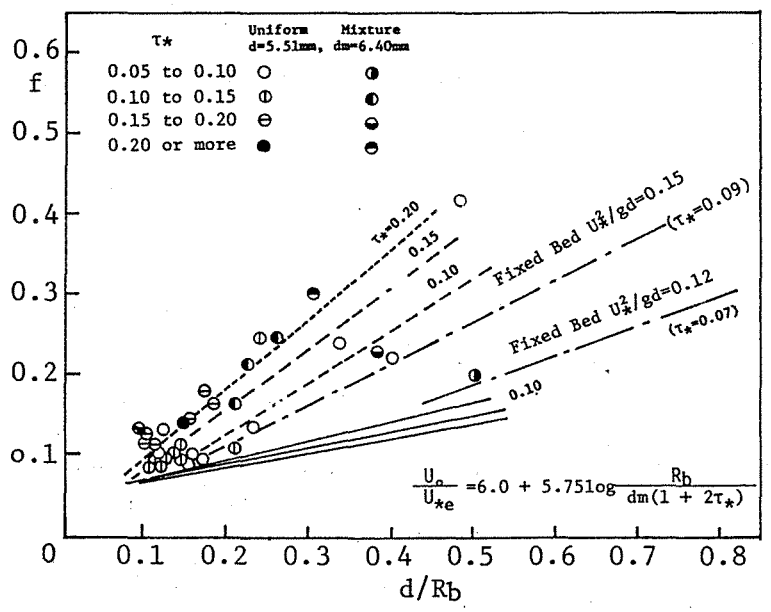

Fig. 2.10 Coefficient of Resistance of a Flow on a Movable Bed (1)

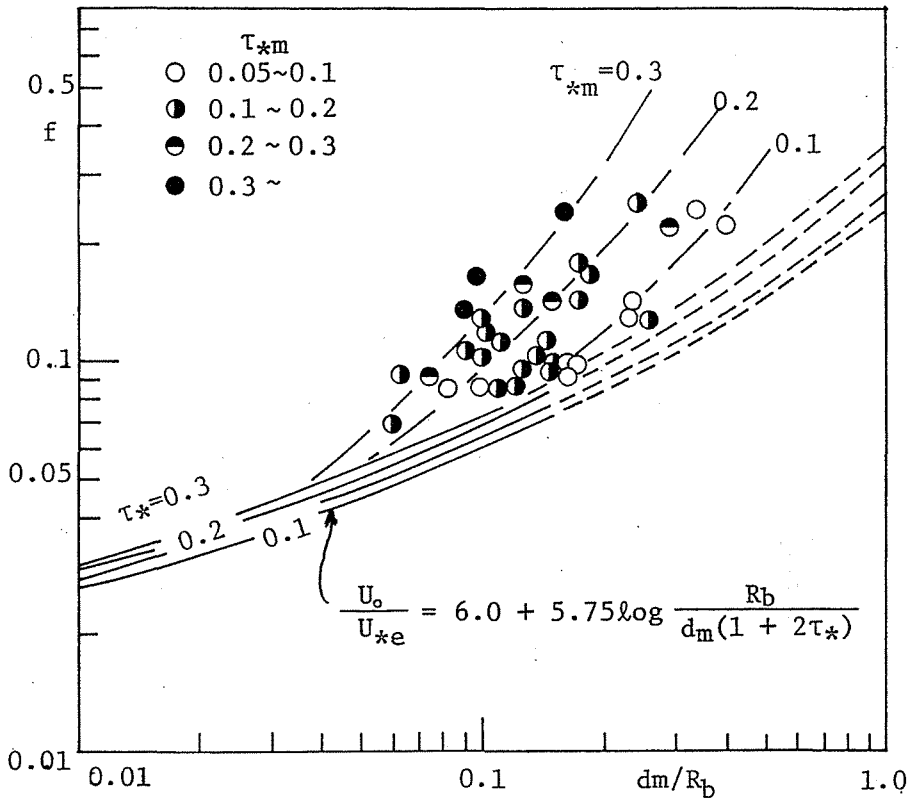

Fig. 2.11 Coefficient of Resistance of a Flow on a Movable Bed (2) (dm = Uniform sand gravel of 6.20mm)

Fig. 2.11, being the experimental results for uniform sand gravel with 6.20 mm in average diameter, exhibits almost the same resultt as Fig. 2.10. Namely, with respect to coefficient of resistance on a movable bed with the relative water depth being small in this way, the correction for the jump height of the sand particles is not important at all. What is of over-whelming importance is the increase of slope and the increase of relative roughness, and the coefficient of can be expressed with nearly the same relationship s for the fixed bed case. That depends on the river bed pattern being within the limits of the flat riverbed bed.

Section 4: Resistance and Characteristics of a Gravel Mixture Bed

A natural riverbed is composed of various large and small mixed gravel stones. This section describes the special characteristics of a mixed gravel bed and the resistance of the flow.

(1) Characteristics of a gravel mixture bed

With respect to the initation of motion of gravel and the resistance of the flow, the distribution of the number of gravel stones protruding from the riverbed surface h (di) is more important than the average grain size distribution up to a certain depth. Tsuchiya[2] considered the distribution of the number of gravel stones protruding from the surface, and assuming the gravel be uniformly distributed in the depth direction, proposed the equation, $h(di) = A^{f(di)}/di^2$. Here h(di) is the distribution percentage by the number of particles of grain diameter di in the riverbed, f(di) is the distribution percentage by total weight of particles of grain size di. A is a coefficient to make the right hand of the equation equal 100%. In order to investigate this h(di), glass beads of diameters 1, 2, 5, 7, 12.6, 16.4, 24.5 mm, and 18.3 mm porcelain beads were color coded by diameter, mixed, and laid to a 4 cm thickness. Photographs were then taken of the riverbed surface. The average grain diameter (dm) of these materials was 9.7 mm, and $\sqrt{d_{84}/d_{16}} = 2.84$. Fig. 2.12 shows the average distribution of particles laid as obtained from the photograph of the riverbed, and the calculated values from the above equation. From this it is obvious that it is difficult for small particles to exist at the surface, and this proves that other than being transported by the stream, small particles have a strong tendency due to vibration etc. to sink into the interstices, and it is difficult for them to be uniformly distributed by depth. In this case the average diameter of a particle on the riverbed surface was 11.09 mm. In this way, the average diameter of mixed gravel d_{ms} is considerably different for the surface and the whole, and thus it would be reasonable to use the average diameter for the riverbed surface when discussing the characteristics of the riverbed surface when discussing the characteristics of the riverbed. For that reason the average diameter at the surface d_{ms} will be used in this discussion hereafter.

A gravel mixture bed is complicated in many respects, and it is not well understood how best to describe its characteristics quantitatively. Among the characteristics, grain distribution has been studied previously, and has been expressed by average grain size or standard deviation. When considering flow resistance or initiation of motion of sand gravel, as in this study, information concerning the average position of each group of particles having different diameter from other group and the roughness of the riverbed surface is necessary. It is difficult to know the roughness of a riverbed for an actual river, but the grain size distribution is comparatively easy to measure. Thus, it is of significance to know the relationship between each parti-

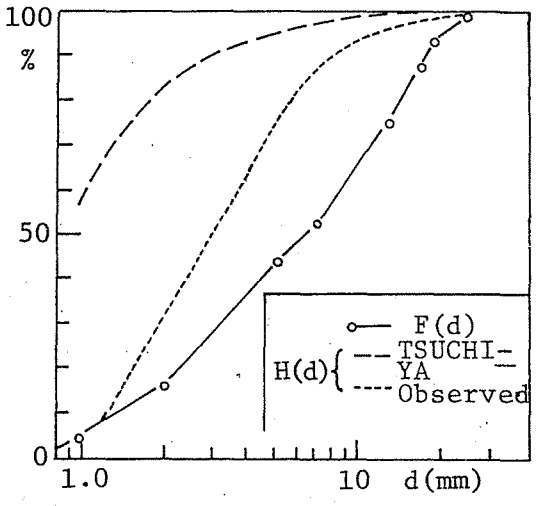

Fig. 2.12 Grain Size Distribution and Frequency Distribution of Protruding Gravel Stones

cle's existing height and grain size distribution and riverbed roughness. The past history can be thought to influence the relationship between riverbed surface condition and the grain size distribution, but as a first step in studying complicated riverbed surfaces, suggest the following argument that there is a unique relationship between grain size distribution and the condition of the riverbed surface, especially the roughness. Here riverbed surface roughness does not include sand waves in the riverbed, it is roughness of an order of grain size above riverbed wavy contour or the flat-riverbed.

As a method of expressing a riverbed surface's roughness one can take the standard deviation of riverbed height at certain observed intervals. Here, more simply, one observes the riverbed height Z at fixed intervals ΔX, and the average 8 the absolute value ΔZ of the difference in heights for bordering points is taken as the roughness. Here the measuring intervals are a problem.

Fig. 2.13 shows the variation of the average value of $\overline{\Delta Z}$ taking ΔX as 0.5 cm, 1.0 cm, 1.5 cm, 2.0 cm, 2.5 cm, 3.0 cm using the data observed at 5 mm intervals as the base. The riverbed was mixed gravel and river sand. From this we see that for small observation intervals ΔZ is small, but when the observation intervals are larger than the average grain diameter, the value of Z is fairly constant. Provided one can find a characteristic quantity ΔZ to express the riverbed surface's roughness. Fig. 2.14 presents observations of $\overline{\Delta Z}/d_{ms}$ for natural sand gravel having various grain size distributions.

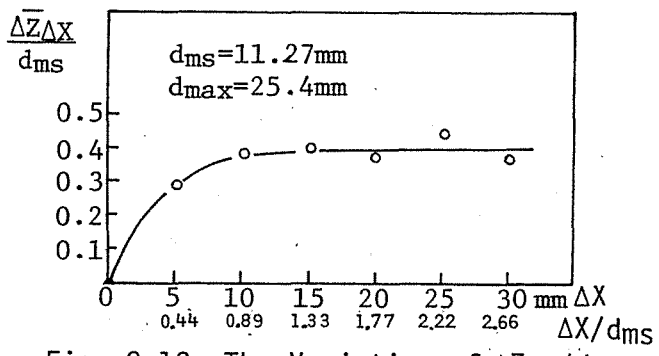

Fig. 2.13 The Variation of $\Delta Z_{\Delta X}/d_{ms}$ at Measuring Intervals

According to this, within the limits of average grain diameter at the riverbed surface being between 4.2 mm and 15.14 mm, or $\sqrt{d_{84}/d_{16}}$ from 1.34 to 2.70, $\overline{\Delta Z}/d_{ms}$ is constant at 0.27. Further, since for uniform gravel with d = 12 mm also $\overline{\Delta Z}/d_{ms}$ = 0.30, one can conclude the riverbed surface roughness is not proportional to the average grain diameter, nor related to the standard diviation of the grain size distribution. However, in Fig. 2.13 as the values approach 0.4 the difficulty of laying sand flat is indicated. Further, for

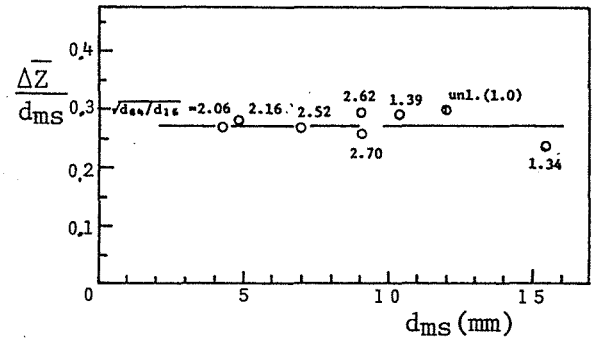

Fig. 2.14 Observed Values of $\overline{\Delta Z}/dms$ for Varoius Mixed Sand Gravel Beds

mixed gravel of glass beads, when dm = 9.70 mm, $\sqrt{d_{84}/d_{16}}$ = 2.74 $\overline{\Delta Z}/d_{ms}$ = 0.343 which is the same as $\overline{\Delta Z}/d_{ms}$ = 0.345 obtained for dm = 5.67 mm, $\sqrt{d_{84}/d_{16}}$ = 3.11. Furthermore, according to the reported results of grain diameter and riverbed height taken at the intersection points of a grid laid out with 5 cm intervals in the lateral direction and 10 cm intervals in the flow direction at Ashiarai Valley in the Jintsu River network in July 1973, for average grain diameter 9.16 mm, $\sqrt{d_{84}/d_{16}}$ = 3.03, $\overline{\Delta Z}$ is 2.83 cm and $\overline{\Delta Z}/d_{ms}$ is 0.31, thus confirming for a natural riverbed the fact the roughness is 0.3 times the average grain diameter. It is not well understood what relationship exists between the effective roughness with respect to the stream and $\overline{\Delta Z}$ defined in this way. However, it would be safe to assume it is proportional, as its first approximation. From the above, the resistance of a mixed gravel bed is expressed by d_{ms} the average grain diameter and is expected not to depend on grain size distribution.

Next let's investigate the height of particles having a particular grain diameter. In a mixed gravel bed of natural gravel, the heights of each grain size group of particles were observed. From that frequency distribution the author measured values of $(Z - Z_O)$, the distance from a theoretical riverbed surface of height Z at frequency distributions of 50% and 10%.

Fig. 2.15 indicates this height for each grain diameter. It was found that the dispersion of the distribution is large for small particles, but the value of (Zi - Zo)/di, with respect to grain diameter di, is about 0.4 for 10% and a constant value of 0.15 for 50%.

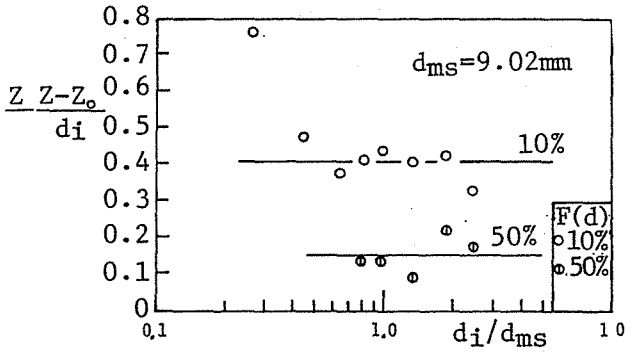

Fig. 2.15 Crest Height for Each Grain Size Group of Particles

(2) Resistance of a stream above a gravel mixture bed

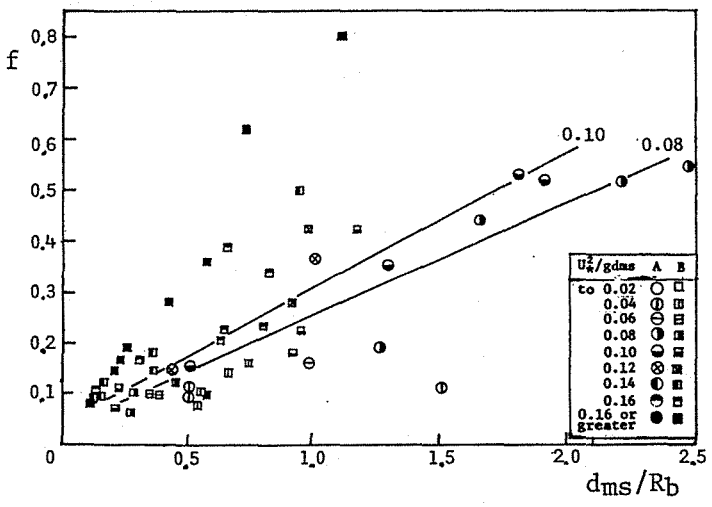

Fig. 2.16 Resistance Coefficient for Mixed Bed (1) (glass beads)

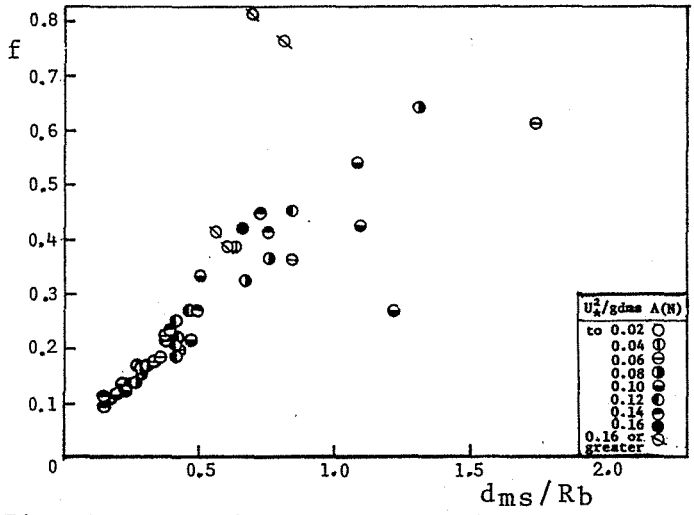

Fig. 2.17 Resistance Coefficient for Mixed Bed (2) (natural gravel)

It seems from studies concerning the characterisitics of mixed gravel bed, that the flow resistance law gives the same results as a uniform bed, provided one uses

the average diameter d_{ms} of the surface as a representative grain diameter. Figures 2.16 and 2.17 indicate the flow resistance coefficient for a mixed bed as d_{ms}/Rb arranged by value of U_*^2/gd_{ms}. The trend is practically the same as Fig. 2.5 the uniform bed case, and this shows the appropriates of using d_{ms} as a representaive quantity of the mixed riverbed. Both A and B in Fig. 2.16 are riverbeds made of glass beads of diameter 1 to 24.5 mm with, respectively, dm = 9.70 mm, $\sqrt{d_{84}/d_{16}}$ = 2.74, and dm = 5.67 mm, $\sqrt{d_{84}/d_{16}}$ = 3.11. Also, the A (N) of Fig. 2.17 is made of natural sand-gravel of diameters 0.84 to 25.4 mm and d_m = 7.78 mm and $\sqrt{d_{84}/d_{16}}$ = 2.74.

Section 5: Conclusion

This Chapter examined flow resistance which is basic when considering sediment. Since in river bed form the boundary region under consideration in the present study is upper flow reigime, it has advanced the discussion which was entirely concerned with flat river beds.

Concerning the flow velocity distribution above a rough surface, there is near the river bed a uniformly changing trend for the flow velocity distribution to depart from Prandtl's logarithmic rule. For a stream with a relatively large roughness, the rate for water depth in that area becomes large, and it, seems, rather, to become a controlling factor. There have been a number of studies concerning this tendency in stream velocity distribution. There are a large number of qualitative explantions, none of which are definitive. The author proposed that from the observed results the flow velocity distribution be divided into an upper and a lower regions at a height of 0.8 times the grain diameter, and that one apply a logarithmic law with slope 5.75 to the upper region and a logarithmic distribution with slope 2.64 to the lower region. When doing so the form of the equation treating the theoretical river bed changes, but the essential nature does not change. Further, in this study the theoretical bed is one where 25% of the surface has particles protruding. This corresponds to a position 0.15 diameters below the crest of a particle for uniform spheres densely spread.

Next, from experiements on large relative roughness, the increase in resistance coefficient f due to relative roughness, U^2/gd, Froude's number, and slope was made clear. Also, the nature of the variation in resistance coefficient was explained theoretically by a step-down model. Resistance on a movable bed was also investigated. The resistance coefficient for the fixed bed is the same as for a flat river bed. For large roughness the resistance is increased by grains of sand tossed up, and it was made clear that this addition is quite small compared with the influence of a steep slope.

Next, mixed gravel beds were considered. The grain size distirbution at the river bed surface is not the same as that for the river bed materials overall, and accordingly one must use the average grain diameter at the surface as a representative quantity for the river bed. Furthere, the roughness of the river bed is from 0.25 to 0.4 times the average grain diameter. And it was shown that the resistance coefficient can be regarded as the same as the resistance coefficient above a uniform bed having the same diameter.

REFERENCES

1) Kazuo Ashida, Atsuyuki Daido, Tamotsu Takahashi, and Takahisa Mizuyama: "Resistance of a Steeply Sloped Flow and its Critical Tractive Force", the Disaster Prevention Laboratory of the Kyoto University, Annual Report 16-B, April 1973, pp. 481-494.
2) Yoshito Tsuchiya: "Critical Tractive Force for Gravel Mixture", the Disaster Prevention Laboratory of the Kyoto University, Annual Report 6, July 1963, pp. 228-253.
3) Einstein, H.A. and S.A. Elsamni: "Hydrodynamic Forces on a Rough Wall, Review of Modern Physics, 21, 1949, pp. 520-524.
4) Cheng, E.D.H. and C.G. Clyde: "Instantaneous Hydrodynamic Lift and Drag Forces on Large Roughness Elements in Turbulent Open Channel Flow, Sedimentation", ed. by H.W. Shen, Chap. 3, 1972.
5) Christensen, B.A.: "Incipient Motion on Cohesionless Channel Banks, Sedimentation", Chap. 4, 1972.
6) O'Loughlin, E,M. and V.S.S. Annambhotla: "Phenomena Near Rought Boundaries, Jour. of Hydraulic Research, 7, No. 2, 1969, pp. 231-250.
7) Yuichi Iwagaki: "A Fundamental Study on Ground Erosion Mechanism due to Rainwater", Doctor thesis, 1955, pp. 1.22-1.38.
8) Ed. by Tojiro Ishihara: "Applied Hydraulics volume II", Maruzen Publishing Co., P.41.
9) Yalin, M.S. and G.D. Fanlayson: "On the Velocity Distribution of the Flow Carring Sediment in Suspension, Sedimentation, Chap. 8, 1972.
10) Isao Yamaoka: "An Effect of Rectangular Roughness on Bed in the Resistance of Waterway", the Hokkaido Development Agency's Civil Engineering Laboratory, Professional Report, 1962.
11) Zagni, A.F.E. and K.V.H. Smith: "Channel Flow over Peameable Beds of Graded Spheres", Proc. ASCE. HY2, 1976, pp. 207-222.
12) Shohei Adachi: "An Empirical Study on Artificial Roughness", JSCE, Professional paper 104, 1964, pp. 33-44.
13) Sayre, W.W. and M.L. Albertson: "Roghness Spacing in Rigid Open Channels', Trans, ASCE, vol. 128, partl, 1963.
14) Ed. by JSCE: "A Collection of Hydraulic Formulas", Gihodo Publishing Co., 1971, p. 36.
15) Mirajgaoker, A.G. and K.L.N. Charlu: "Natural Roughness Effects in Rigid Open Channels", Proc. ASCE. HY9, 1963.
16) Hitoshi Honma: "Torrential Flow Phenomena, Particularly on Fluid Resistance against a Torrential Flow (1)", Trans. JSCE 28-5, 1942, pp. 465-496.
17) White, C.M.: "The Equilibrium of Grains on the Bed of Stream", Proc. Roc. Soc. A-174, 1940.

18) Sutesaburo Sugio:
"A Law of Movable Bed Resistance", Water Engineering Series A-5, 1971.
19) Kazuo Ashida, Tamotsu Takahashi, and Takahashi Mizuyama:
"A Hydraulic Study for Channel Works Planning", the SHIN-SABO 97, Nov. 1975, pp. 9-16.
20) Schlichting, H.:
"Boundary-Layer Theory", McGraw Hill, 1968, p. 40.
21) Ed. by the Sub-Committee for flow resistance on a movable bed and bed transport forms in Hydraulic Committee of JSCE:
"Bed Transport Forms and Roughness of Bed Material in a Flow on a Movable Bed", Professional paper 210, 1973.
22) Chikara Kishi:
"Roughness in a Movable Bed Flow", Summer Seminar on Water Engineering, 1972.
23) Kazuo Ashida, and Masanori Michiue:
"A Fundamental Study of Resistance of a Flow on a Movable Bed and Bed Load Tansport Rate", JSCE, Professional paper 206, Oct. 1972, pp. 59-69.

CHAPTER 3 CRITICAL TRACTIVE FORCE FOR INITIATING THE TRANSPORT OF GRAVEL

Section 1: Outline

Uniform gravel or gravel mixture spread within a water channel doesn't move for a small discharge, but with an increase in the discharge the gravel begins to move from time to time. If the discharge is further increased, the movement becomes extraordinarily active. The border between this initiating and ceasing of the motion of gravel is called the transport threshold, and the shear stress of the gravel at that time is called the critical tractive force.

Because sediment begins to move when the critical tractive force surpasses the transport threshold, it goes without saying that the determination of that value corresponding to conditions in rivers, our objective, is a fundamental topic in order to treat rivers, which are channels for transporting not only water but also sediment. Accordingly, research has been carried out in the past on critical tractive force according to various definitions of transport threshold. The critical tractive force for deep streams on a gently sloping bed has become fairly clear. However, it is not yet clear whether the results of past research can apply to streams which have a water depth several times the bed gravel diameter only in flood times and which are steeply sloped, such as mountain streams. Rather, it is to be expected that the critical tractive force will differ.

This chapter clarifies the critical tractive force for initiating the transport of gravel or simply the initiating critical tractive force as it occurs in steply sloped streams, a topic practically untouched in past research. First, past research is summarized; next from experiments and theoretical considerations, the initiating critical tractive force is clarified for uniform gravel in a torrential flow and for gravel mixture having a wide grain size distribution as in mountain streams.

Section 2: Conventional Research on Critical Tractive Force

(1) Dimension analytical studies

The physical quantities governing transport phenomena of sediment due to flowing water are the water density ρ, the coefficient of viscosity μ, the gravel density σ, grain diameter d, water depth h, friction velocity U_*, and the gravitational constant g; an equation to describe the transport phenomena is expected to include these quantities. Now if one thinks about the equation describing the sediment discharge q_s, and derives a non-dimensional equation including the above quantities by dimension analysis, one can obtain.

$$\frac{q_s}{\rho U_*^3} = \Phi_3\left(\frac{U_* d}{\nu}, \frac{U_*^2}{(\sigma/\rho - 1)gd}, \frac{h}{d}, \frac{\sigma}{\rho}\right) \quad \cdots\cdots\cdots (3.1)$$

If one defines the transport threshold condition as $q_s = 0$, a non-dimensional equation to determine the critical tractive force is, from equation 3.1,

$$\tau_{*c} = \frac{U_{*c}^2}{(\sigma/\rho - 1)gd} = \Phi_4\left(\frac{U_{*}^2 cd}{\nu}, \frac{hc}{d}, \frac{\sigma}{\rho}\right) \quad \cdots\cdots\cdots (3.2)$$

Here the right hand side of the above equation represents the critical tractive force in a non-dimension fashion and the accompanying letter c indicates the critical value.

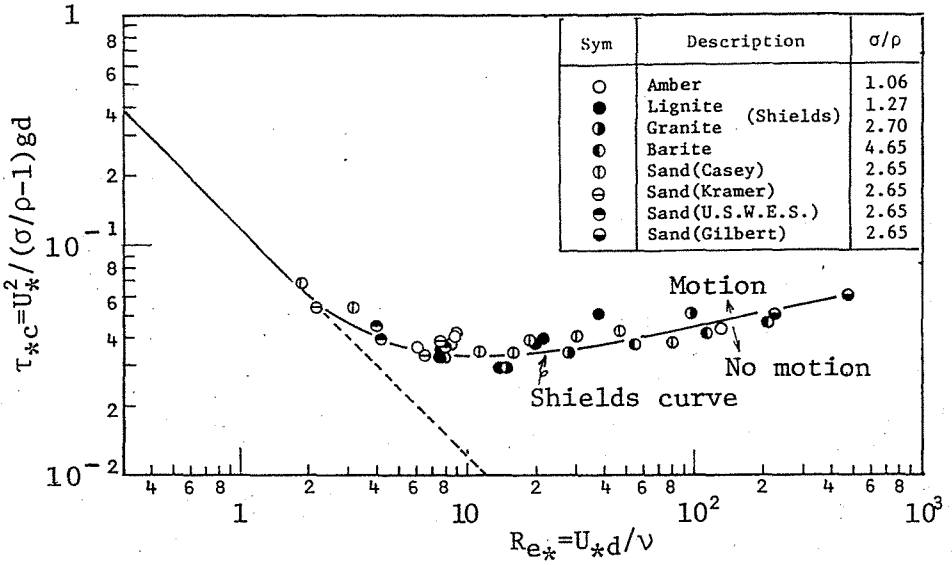

Fig. 3.1 Shields Diagram

Research on critical tractive force got its start in 1936 by Shields' studies. He left out the terms h_c/d and σ/ρ from eq. 3.2, plotted the empirical relation between τ_{*c} and Re_* (= $U_{*}cd/\nu$), and showed the results could be described virtually by a single curve. It was confirmed[1] that the same relationship held time for later experimental results comparing steep and mild slopes, which was widely used as Shields diagram.

According to Yalin[2], the reason the specific gravity term σ/ρ exerts no influence on the critical tractive force is that σ/ρ is a term due to inertia of sediment transport, and since the critical condition for initiating the transport lies in a static equilibrium condition, the term σ/ρ need not be considered. On the other hand, particles immediately before transport have been observed to shake and turn about due to the turbulence of flow, and one can not necessarily say the particle suddenly moves from rest. Ward[3] discusses the influence of σ/ρ, and modifies τ_{*c} by introducing an additional mass coefficient. However, in Fig. 3.1 points for different specific gravities fall on the same curve, so it seems σ/ρ does not exert an important influence.

Also, Yalin[2] and Gessler[4], concerning the reason the relative water depth hc/d does not influence the critical tractive force, suggest the stream near the river bed depends only on the distance from the bed and the friction velocity including turbulence, and is unrelated to depth. However, since the velocity

distribution and turbulent flow characteristics are not clear for a stream with a small relative depth on a steep slope, it is necessary to investigate the influence of relative depth. Let us consider conventional research concerning the influence of relative depth on critical tractive force. For example Bogárdi[5] classifies the experimental data by relative depth as

$$\tau_{*c} = \Phi_5 \left[\left(\frac{d}{\nu^{2/3} g^{-1/3}} \right)^{3/2}, \left(\frac{hc}{d} \right)^{1/2}, i^{1/2} \right] \quad \cdots\cdots\cdots (3.3)$$

from dimension analysis, and says for a constant value of $d/(\nu^{2/3} g^{-1/3})$ the non-dimensional critical tractive force expression τ_{*c} is proportional to $(d/h)^2$ or $i^{2/3}$. Here, i is the bed slope. This result is based on a certain prescribed water temperature and indicates that τ_{*c} for a certain particle size will increase if d/h or i increases. More correctly, the data used by Bogárdi fall within the limits $d/h < 0.2$, $i < 0.025$, $2 < Re_* < 10^4$, and the relationship between τ_{*c} and $(d/h)^2$ or $i^{2/3}$ exhibits a good deal of dispersion. Also, Sahap and Aksoy[6] give a modification table for τ_{*c} as a function of d/h within the range $d^{2/3}/\nu \sqrt{g\,(\sigma-\rho)/\rho} > 2.5 \times 10^3$. Neil[7] indicates, from experiments with d/h up to about 0.5, that the critical tractive force increases slightly due to an increase in d/h. Tabata and Ichinose[8] have carried out experiments on critical tractive force for large gravel, and have obtained the result that τ_{*c} increases as the slope increases.

As in the above examples, τ_{*c} in the past has primarily been treated as a coefficient only of Re_* on the right hand side of equation 3.2. However, it seems it is related to h/d also when the relative depth becomes small, and it is clear that research is necessary especially for the case when the depth is of the same order as the particle size.

(2) Mechanical analysis

Natural bed material is sand mixture and the flow in general is turbulent and the flow velocity changes. When the force working on an individual particle is greater than the resistance force of the particle, it starts to move, but the phenomenon is probabilistic because of the irregular nature of the configuration and shape of the particles and turbulence. Research on mechanical analysis of the critical tractive force, such as those comiled by Graf[9], is in general divided into those dependent on critical velocity and those dependent on drag force or lift force. Also, they are divided into deterministic studies concerned with the average value, and probabilistic studies considering variation. Further, they can be classified for uniform gravel or gravel mixture as the object of study. Here, a distinction is made between uniform gravel and gravel mixture in the investigations.

(a) Critical tractive force for uniform gravel

There are two basic points of view. One, such as Kurihara[10] and White[11], is taking the shear stress per unit area divided by the number of protruding particles per unit area as the value impinging on each particle which maintains an equilibrium. Another, such as Iwagaki[12], is taking equilibrium to be based on the balance between friction force and fluid force on an individual particle on the

sand surface. When the depth is sufficiently large compared to the particle diameter, τ_{*c} is the coefficient only for Re_*. The form of that coefficient has been considered by Kurihara and Iwagaki in terms of turbulent flow theory. Fig. 3.6 shows some of these theoretical curves. τ_{*c} has a minimum value near $Re_* \fallingdotseq 1.5$. For $Re_* \geqslant 400$ τ_{*c} is nearly constant at 0.047 ~ 0.06.

On the other hand, Carstens[13] gives

$$\frac{U_c^2}{(s-1)gd} \simeq 3.61(\tan\psi \cos\theta - \sin\theta) \qquad \cdots\cdots\cdots (3.4)$$

as a critical velocity equation. Here U_c is the flow velocity in the vicinity of gravel for the critical condition, S is the specific gravity of the gravel ($= \sigma/\rho$), ψ is the angle of internal friction of the gravel, θ is the water channel bed slope. Also there are many studies using the mean flow velocity U_o in place of the flow velocity near the gravel. Neil[7] has found an empirical equation

$$\frac{U_{oc}^2}{(s-1)gd} = 2.50\left(\frac{d}{hc}\right)^{-0.20} \qquad \cdots\cdots\cdots (3.5)$$

Next let us look at research concerned not with average values of hydraulic quantity, but with variation of the quantity, Kalinske[14] takes the velocity for actual purposes to be

$$|U - \overline{U}|_{max} \simeq 3\sigma_u \qquad \cdots\cdots\cdots (3.6)$$

according to a normal distribution. Here σ_u is the standard deviation of the variation around the average velocity $\overline{U}$. Also, from experimental results on the variation of flow velocity near the bed, the following equation is obtained.

$$\frac{\sigma_u}{\overline{U}_b} \simeq \frac{1}{4} \qquad \cdots\cdots\cdots (3.7)$$

Here, $\overline{U}_b$ is the flow velocity near the river bed. From eqs. 3.6 and 3.7, equation (3.8) is derived as follows.

$$U_{bmax} \simeq 1.75\overline{U}_b \qquad \cdots\cdots\cdots (3.8)$$

This indicates that the momentary velocity near the bed is about 1.75 times the average velocity and with respect to the tractive force the momentary value is three times the mean value.

Also, Chepil and Woodruff[15] introduce a turbulence coefficient expressed as

$$T = \frac{3\sigma_p + \overline{P}}{\overline{P}} \qquad \cdots\cdots\cdots (3.9)$$

to consider the threshold of transport. Here $\overline{P}$ is the average pressure near the particle and σ_p is the standard deviation of the pressure variation.

Christensen[16] reports that the conventional experimental values of critical tractive force are in agreement with a probability of 0.001 which corresponds to U'/σ_ν by letting $\sigma_\nu/\overline{U} = 0.16$ obtained from equation (3.10), the experimental results of Lalufer, Fage and Townsend, and Reichardt et al. that near the bed the value of $\sigma_\nu/\overline{U}$ is nearly equal to 0.15 to 0.18 and from the result clarified by Einstein and Elsamni[17] in their experiments on lift force that the flow velocity near the bed follows a normal distribution, where U' is the component of change of the flow velocity.

$$\frac{\tau}{\overline{\tau}_c} = \left(\frac{\overline{U} + U'}{\overline{U}}\right)^2 = \left(1 + \frac{\sigma_u}{\overline{U}} \frac{U'}{\sigma_u}\right)^2 \qquad \cdots\cdots\cdots (3.10)$$

Next, let us consider the probabilistic approaches studied by Einstein[18], Gessler[19), 20)], and Paintal[21].

Einstein introduced the transport of particles as a basis to derive a function for tractive force and replaced the probability P_s that a particle will start to move with the absolute probability $P_s t_1 = P_a$ using exchange time t_1. Here t_1 is considered proportional to the ratio d/w_o of diameter d to the fall velocity w_o of a particle of diameter d. Considering P_a represents the probability that the lift force L acting on a particle becomes greater than the particle's weight W, the requirement for $1 > w/L$ is given by equation (3.12) since W, L, and U are proportional to those given by equation (3.11).

$$\left.\begin{aligned} W &\propto g(\sigma - \rho)d^3 \\ L &\propto \rho U^2 d^2 (1 + \eta) \\ U &\propto U_* \end{aligned}\right\} \qquad \cdots\cdots\cdots (3.11)$$

$$|1 + \eta| > B\Psi, \text{ or } (1 + \eta)^2 > B^2\Psi^2 \qquad \cdots\cdots\cdots (3.12)$$

Here ψ is a non-dimensional quantity equal to $[(\sigma/\rho - 1)gd]\, U_*^{-2}$ called the flow intensity, η is a coefficient which varies with time. Let the standard deviation of η be η_o. Putting $\eta = \eta_o \eta_*$, for the threshold of transport the following is obtained.

$$[\eta_*]\text{limit} = \pm B_* \Psi - (1/\eta_o), \quad B_* = B/\eta_o \qquad \cdots\cdots\cdots (3.13)$$

Since the probability of η_* has a normal distribution, the following is obtained.

$$Pa = 1 - \frac{1}{\sqrt{\pi}} \int_{-B_*\psi-(1/\eta_o)}^{B_*\psi-(1/\eta_o)} e^{-t^2} dt \qquad \cdots\cdots\cdots (3.14)$$

Then the values are taken to be $1/\eta_o = 2.0$ and $B_* = 0.143$.

Also, Gessler considers a critical tractive force from a probabilistic point of view. Taking

$$q = \frac{1}{\sigma\sqrt{2\pi}} \int_{-\infty}^{(\tau_c/\tau)-1} \exp\left(-\frac{x^2}{2\sigma^2}\right) dx \qquad \cdots\cdots\cdots (3.15)$$

where q is the residual probability of the top layer, he found experimentally that the standard deviation σ of τ_c/τ is 0.57. Also, concerning time scale, he considers the transport probability per unit time, as a time coefficient, must be made non-dimensional such as the time of passage of a turbulent eddy, e.g. d/U_*. Noting that Kalinske or Einstein considers the velocity variation and but not the degree of exposure e of a particle, Paintal thinks the distribution E of the particles' height e above the average bed level should be considered together with the flow velocity variation. Thus he assumes for a particle to move it is necessary for the particle to possess a greater degree of exposure than the surrounding particles.

(b) Critical tractive force for gravel mixture

On this topic Kramer[22] and Sakai[23] find empirical equations for the characteristic quantities of gravel mixture, such as influence of the uniformity coefficient, with respect to threshold of transport for mean diameter gravel mixture particle. In this way a method of representing the gravel mixture by a certain particle to compare the transport threshold of the representative particle with that of uniform gravel was developed by Tsuchiya[24]. From the wake theory Tsuchiya considers a hiding coefficient, and obtains the result that the larger the standard deviation of the grain size distribution, the smaller the hiding coefficient. However, in order to explain actual problem, such as the armouring phenomenon seen in bed lowering, it is necessary to know the critical tractive force for each gravel diameter. The studies of Egiazaroff[28] are well known as studies of critical tractive force for different diameters. According to these studies, first for uniform gravel, letting the tractive force D and the resistance force F be

$$D = \frac{\rho}{2} C_D U_d^2 \frac{\pi}{4} d^2 \qquad \cdots\cdots\cdots (3.16)$$

$$F = \frac{\pi}{6} d (\sigma - \rho) g \tan\phi \qquad \cdots\cdots\cdots (3.17)$$

for spherical particles of diameter d, then setting D = F and $\tan\psi = 1$ one obtains an equation for the threshold of transport.

$$\tau_{*c} = \frac{2}{3} \frac{\lambda' c}{C_D \zeta_c^2} \qquad \cdots\cdots\cdots (3.18)$$

Here,

$$\left(\frac{U_o}{U_*}\right)^2 = \frac{2}{\lambda'} \qquad \cdots\cdots\cdots (3.19)$$

$$\zeta = \frac{U_d}{U_o} \qquad \cdots\cdots\cdots (3.20)$$

Also, Ud is the flow velocity at the height ad above the bottom surface. Using a logarithmic distribution function for the flow velocity distribution, the following is obtained.

$$\frac{\lambda'}{\zeta^2} = \frac{2}{\{5.75 \log(30.2a)\}^2} \qquad \cdots\cdots\cdots (3.21)$$

Next, letting a = 0.63 so that the value of τ_{*c} within the bounds of a perfect turbulent flow can agree with the conventional experimental value of 0.06, the following equation is obtained.

$$\tau_{*c} = \frac{0.024}{C_D} \qquad \cdots\cdots\cdots (3.22)$$

In the region of a perfect turbulent flow, letting $C_D = 0.4$ makes $\tau_{*c} = 0.06$. For $Re_* < 1000$, C_D becomes a function of Re_*, and accordingly τ_{*c} also becomes a function of Re_*. Next, assuming the above methods can be applied to each grain diameter for the case of gravel mixture, let $y = ad_i$ be the flow velocity of a particle of diameter d_i. Assuming a = 0.63, the critical tractive force τ_{*ci} for grain diameter d_i is

$$\tau_{*ci} = \frac{2}{3C_D} \cdot \frac{0.06}{\left(\log 19 \frac{d_i}{d_m}\right)^2} \qquad \cdots\cdots\cdots (3.23)$$

Assuming $C_D = 0.4$ for a perfect turbulent flow, we get

$$\tau_{*ci} = \frac{0.1}{\left(\log 19 \frac{d_i}{d_m}\right)^2} \qquad \cdots\cdots\cdots (3.24)$$

which agrees well with experimental values. Ashida, Michiue and Egashira[26] find for $d_i/d_m < 0.4$ that τ_{*c} from Egiazaroff's equation is too large, and they modified it empirically to $\tau_{ci}/\tau_{cm} = 0.85$ (constant). Further, for $d_i/d_m > 0.4$ they change the expression to

$$\frac{\tau_{ci}}{\tau_{cm}} = \frac{1.64}{(\log 19 \frac{d_i}{d_m})^2} \cdot \frac{d_i}{d_m} \qquad \cdots\cdots (3.25)$$

(See Fig. 3.2)
Here τ_{ci} and τcm are the tractive forces which are not non-dimensional values for diameters di and dm. Hirano[27] reports similar results. Further, taking τ_{*c} = 0.05 and C_D = 0.5 for a perfect turbulent flow, a = 0.617 is the result.

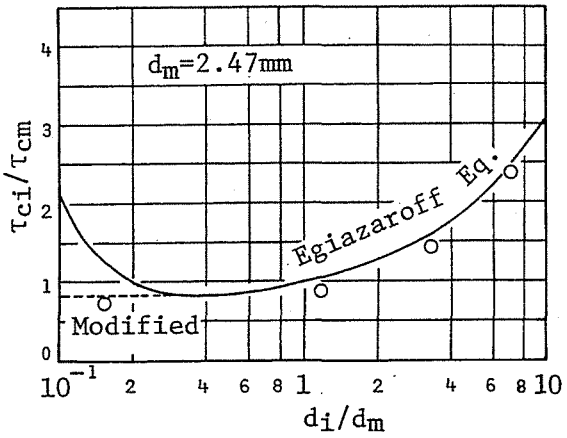

Fig. 3.2 Critical Tractive Force for Gravel Particles of Different Diameters

The conventional research on critical tractive force has been outlined so far. It clarifies the problems remaining which must be elucidated. These include the necessity of detailed information on the relative positions of grains on a bed, the fluid force, characteristics of turbulent flows, and the flow velocity distribution near a river bed, just for critical tractive force for uniform gravel. For example, C_D which is used by Iwagaki and Egiazaroff is a drag coefficient for spheres in a uniform flow. It is necessary to sudy C_D for a shear flow over a gravel bed. Concerning this, Coleman[28] obtained the result that there is almost no difference between C_D for a shear flow and that for a uniform flow, but Garde and Sethurman[29] indicate that C_D for spheres rolling on the slope on which the particles are spread in a still fluid is considerably larger than that for a uniform flow. For the threshold of transport, Coleman's experimental conditions are close to the actual ones, but it is necessary to gather more experimental results. Also, concerning the lift conefficient CL, Chepil[30] reports CL/CD = 0.85 over a wide range of Reynolds Numbers. Chen[31] indicates that C_D and C_L tend to decrease with an increase in d/h. However, these results are not yet definitive, and hereafter direct measurements of the fluid force are necessary.

Next, it has been pointed out that from a practical view point the modified Egiazaroff equation can be applied to find the critical tractive force for gravel mixture. Experiments are necessary on gravel mixture having a wider grain size distribution than the experimental range for which the appropriateness of application has been recognized. Also, one should investigate whether the critical tractive force for the mean diameter dm given by this equation always agrees with that for a uniform diameter. The reason according to Kramer et. al. is that τ_{*c} for the mean diameter varies with the uniformity constant. According to Tsuchiya there is a tendency for the critical tractive force, for the median diameter $\sqrt{d_{84}/d_{16}}$ being from 1 up until about 1.5, to be slightly smaller than that for a uniform diameter, and above 1.5 there is a tendency for it to be larger.

Considering the facet of theoretical treatment for the threshold of transport, first there is a problem of defining the threshold of transport. One definition of the threshold of transport holds that when that threshold is crossed the sediment discharge increases sharply. This has much practical value, but since it has a certain amount of ambiguity especially for gravel mixture, it is necessary to clarify the definition of the threshold of transport in order to advance the discussion of determining the threshold of transport. Concerning studies of probabilistic models, other than the aforementioned relative positions of bed grains and characteristics of a turbulent flow near a bed, it is necessary to clarify the physical significance of time, in order to convert probabilities of grains leaving per unit area per unit time into absolute probabilities.

The main problems with past researches are enumerated above. Since there have been practically no studies on critical tractive force for the case of a steeply sloped stream with a small relative water depth, it is necessary first to elucidate the phenomena by experiment, other than exploring the above problems.

Section 3: Critical Force for Initiating the Transport of Uniform Gravel

(1) Outline of the experiment

(a) Range of conditions and procedure for the experiment

The experiments were carried out on a 20 cm wide, 20 m long, 40 cm deep water-circulating steel flume whose slope could be changed within the limits of $0 \sim 0.20$.

As shown in Fig. 3.3, within the flume there is a movable bed section flanked by two rigid bed sections. The rigid bed is made by placing the gravel in a varnished aluminum box. The transport of the movable bed section gravel was observed. The length of the movable bed section was such that the exposed surface had several hundred spheres, and the thickness such that there were two layers above a rigid bed section.

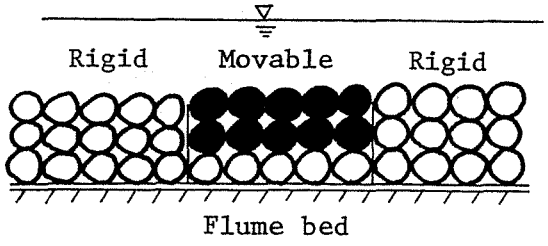

Fig. 3.3 A Conceptual Scheme of Gravel Bed

Three kinds of gravel were used in the experiments as indicated in Table 3.1.

Table 3.1 Properties of Gravel Particles used in the Experiments

No.	Mesh	Sieve diameter ds	Nominal diameter dn	Shape factor	Specific weight s	tanφ	Length of movable bed
1	22.2~20.0mm	21.10mm	22.5mm	0.945	2.490	1.0	2.0m
2	12.7~ 9.5	11.10	12.0	1.008	2.656	1.0	1.0
3	5.66~4.76	5.21	6.4	—	2.507	1.3	0.5

There are various conceivable ways to describe the diameters of complex natural gravel particles. In the following data analysis the nominal diameter will be used. The reason is that it seems the weight of a particle is an important resistance force against transport. Further, the internal friction angle of the gravel used in the experiments is taken as the angle where the grains in the movable bed box on a tilt board in the air begin to move.

As for experimental procedure, first the channel was set to a prescribed slope, the movable bed section was covered with a screen metal, and a certain amount of water was supplied. When it reached uniform flow the wire net was removed, and the number of pieces of gravel which leave the movable bed box was observed at the first 30 seconds after and 3 minutes after the screen was removed. Pertaining to the measurement of hydraulic quantity the hydraulic gradient was measured by a total pressure tube and the flow discharge by a venturi tube depth, and temperature were also measured.

(b) Methods for judging the transport threshold

What conditions constitute the threshold of transport has been variously debated. Here is introduced an experiment carried out with a small discharge of water as explained in the previous paragraph, the number of grains transported was read, and the number was returned to the original amount. Then, the same experiment was repeated with increasing amount of water. Fig. 3.4 shows the relationship between water depth and number of grains transported after 30 seconds and 3 minutes. The maximum water depth at which the number of transported particles would be zero is taken to be the water depth at the threshold of transport for that slope.

From Fig. 3.4 we see there is not a remarkable difference between the numbers of particles transported for 30 seconds and for 3 minutes for the same water depth. Since the way the gravel is first spread on the movable bed controls the amount of transport, care must be exercised in determining the critical tractive force. Further, looking at what other researches have dealt with judging the transport threshold, Tabata[8] uses the point on a graph similar to Fig. 3.4 where the bed load gravel amount increases abruptly. Also, Tsuchiya[24] takes for the transport threshold the condition that the percent of gravel which begins to move in unit time for a unit bed area becomes 0.5% sec. Also, it seems methods to define it from the amount of sediment transport are widely used. If one compares these criteria[32], one can say the definition as 0 particles transported used here is lower than others.

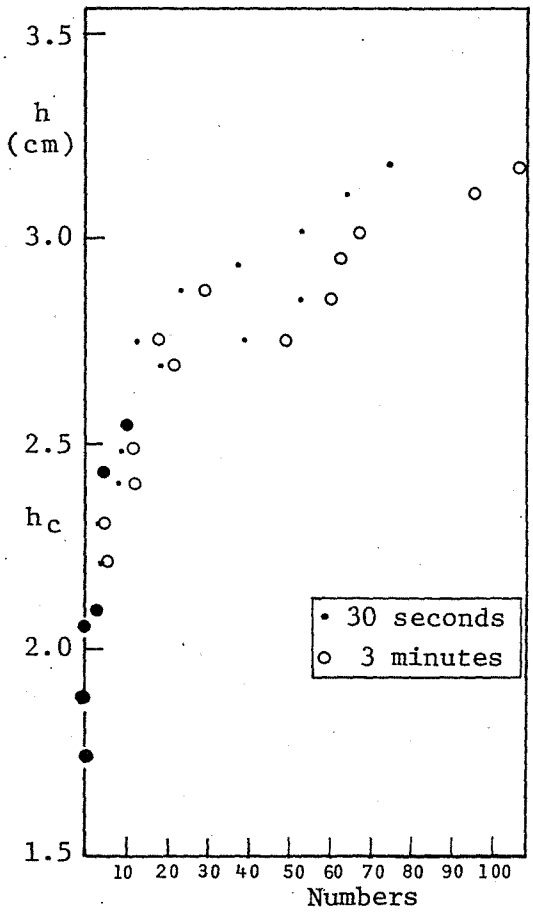

Fig. 3.4 An Example Explaining the Realtionship between the Number of Movable Gravel Particles and the Depth

(c) Standard bed surface level

Since the object of this study is large gravel in a shallow stream, the determination of the standard surface of the bed exerts a large influence on the results. As stated in the previous chapter, many methods have been proposed for determining the standard bed level. While searching, through trial and error, for such height that the initiating critical tractive force for three different grain diameters is appropriate in the figure showing the relationship between τ_{*sc} and d/h, it was found that the appropriate height should be chosen such that 25% of the whole bed surface is above the standard bed level, which was employed in the previous case of resistance. Thus, this was adopted in the experiment as the definition of the standard bed level.

Furthermore, within the confines of this experiment, there occurred no gravel movement in such state that gravel pieces protrude above the water surface.

(2) Experimental results and examination on the results

(a) Experimental results

The experimental results of the critical tractive force as stated above, are shown in Fig. 3.2, where the influence of the roughness of the wall surface was removed by using Einstein's method[34].

Table 3.2 Experimental Results

No.	d_n(mm)	i	hc(cm)	Q(l/s)	Rb(cm)	τ_{*sc}
1.1	22.5	0.02	9.15	22.3	7.00	0.0431
1.2		0.05	3.55	7.4	3.25	0.0527
1.3	22.5	0.075	2.50	4.9	2.37	0.0607
1.4		0.10	2.15		2.06	0.0743
1.5		0.15	1.53	3.05	1.48	0.0894
1.6		0.20	1.30	1.7	1.29	0.1178
2.1	12.0	0.01	9.75	13.5	8.20	0.0402
2.2		0.025	3.65	5.0	3.40	0.0427
2.3		0.05	2.05		1.95	0.0535
2.4		0.075	1.45		1.42	0.0608
2.5		0.10	1.20	0.85	1.19	0.0691
2.6		0.125	1.15	0.7	1.14	0.0846
3.1	6.4	0.01	5.45	6.5	4.76	0.0386
3.2		0.025	2.40	2.4	2.30	0.0461
3.3		0.05	1.30	0.85	1.28	0.0546

The R_b in the table is the hydraulic radius for the bed. Fig. 3.5 shows the relationship between τ_{*sc}, the non-dimensional expression of the critical tractive force which is obtained through the modification of the effect of slope and d/hc.

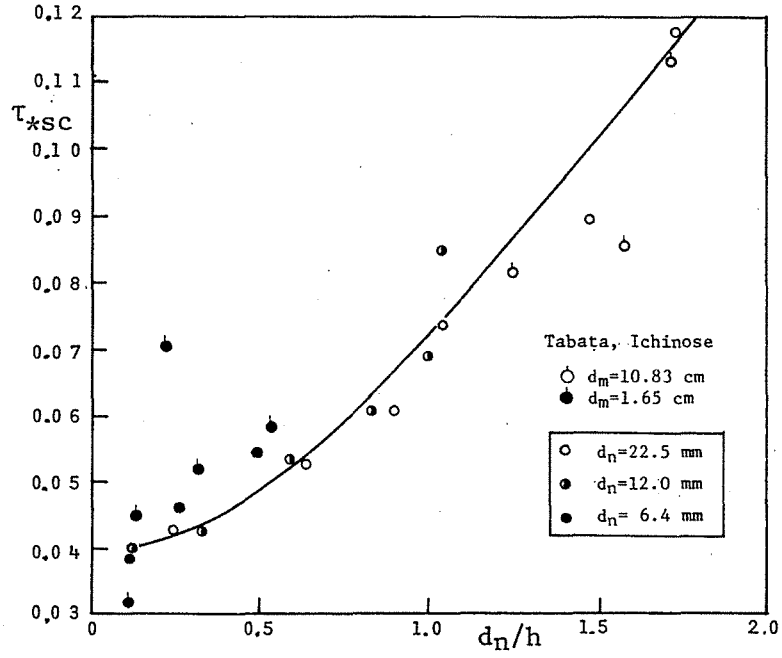

Fig. 3.5 The Change of Critical Tractive Force for Relative Roughness

The figure proves that, regardless of the grain size of the gravel, as the depth becomes shallower, that is, as the slope becomes teeper, the critical tractive force becomes sharply greater. This relationship is expressed in an empirical equation as follows.

$$\left.\begin{array}{l} d/h \geqq 0.22 \\ \tau_{*sc} = 0.034 \times 10^{0.32(d/h)} \\ d/h \leqq 0.22 \\ \tau_{*sc} = 0.04 \end{array}\right\} \quad \cdots\cdots (3.26)$$

Here τ_{*sc} is, as will be explained later on, equal to $\tau_{*c}/[\tan\varphi \cos\theta - (\sigma/\sigma-\rho) \sin\theta]$, the non-dimensional expression of critical tractive force for a modified slope. The experimental results in a Shields diagram are shown in Fig. 3.6.

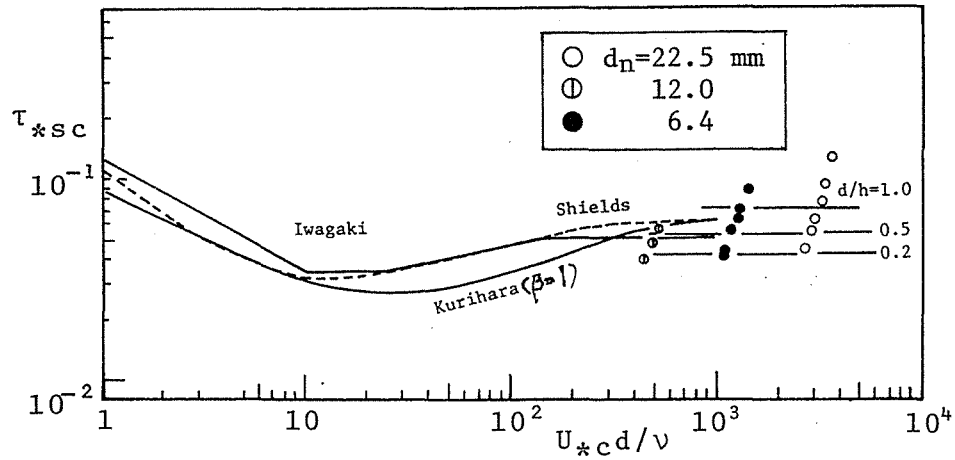

Fig. 3.6 Shields Diagrams of Experimental Values

Further, data obtained by Tabata and Ichinose[8] are also plotted in Fig. 3.5. The distribution of those data is wide spread. It would be due to the difference in definition of the critical tractive force, or due to the difference in method of finding standard bed level.

However, a tendency to the increase in τ_{*sc} with reference to d/h is nearly uniform. A primary reason for the appearance of such results as shown in Fig. 3.5 is considered to be due to the effect of the change in flow velocity in the vicinity of the gravel with reference to relative roughness. Next, the author intends to explain the feature of this change in the critical tractive force with reference to the relative roughness, using the previously mentioned resistance law and velocity distribution in a torrential flow.

(b) Theoretical examination on experimental results

First, an equation for gravel equilibrium will be derived[35].

As shown in Fig. 3, 7, the following equation (3.27) is available for solid particles in the transport threshold condition.

$$D + W\sin\theta = (W\cos\theta - L - B)\tan\psi \qquad \cdots\cdots (3.27)$$

where, θ: the slope of the water channel, D: Drag force, L: Lift force, B: Buoyancy, W: Gravel weight, and φ: Internal friction angle of gravel.

Neglecting the influence of pressure gradient, these forces can generally be expressed as:

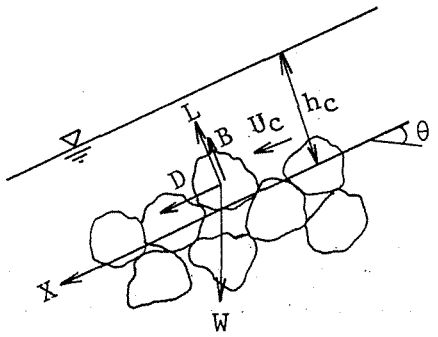

Fig. 3.7 Equilibrium Conditions of Gravel

$$D = C_D \cdot k_1 \cdot d^2 \cdot \rho \frac{U_c^2}{2} \quad \cdots\cdots (3.28)$$

$$L = C_L \cdot k_2 \cdot d^2 \cdot \rho \frac{U_c^2}{2} \quad \cdots\cdots (3.29)$$

$$W = \sigma g \cdot k_3 \cdot d^3 \cdot \quad \cdots\cdots\cdots (3.30)$$

$$B = \rho g \cdot k_3 \cdot d^3 \cos\theta \quad \cdots\cdots\cdots (3.31)$$

where, C_D : Drag coefficient
C_L : Lift coefficient
K_1 & K_2 : Constants representing areas
K_3 : Constant representing a volume
U_c : Critical flow velocity in the vicinity of gravel

Plugging equations (3.28), (3.29), (3.30), and (3.31) in equation (3.27) the following equation is obtained.

$$\frac{U_c^2}{(S-1)gd} = \frac{2k_3(\tan\psi\cos\theta - \frac{S}{S-1}\cdot\sin\theta)}{C_D k_1 + C_L k_2 \tan\psi} \quad \cdots\cdots\cdots (3.32)$$

where, $S = \sigma/\rho$.

Letting $U_c = CU_{*c}$ ..... (3.33)
and inserting equation (3.33) into equation (3.32), the following equation can be obtained.

$$\frac{U_{*c}^2}{(S-1)gd} \cdot \frac{1}{(\tan\psi\cos\theta - \frac{S}{S-1}\cdot\sin\theta)}$$

$$= \frac{1}{C_D} \cdot \frac{2k_3}{k_1 + \frac{C_L}{C_D} k_2 \tan\psi} \cdot \frac{1}{C^2} \quad \cdots\cdots\cdots (3.34)$$

where, U_{*c} is the critical friction velocity and the former half of the left hand side of the above equation (3.34) becomes Shields parameter τ_{*c}. The method for obtaining a flow velocity at the transport threshold in the mode of equation (3.32) is called the critical velocity equation, and the method by means of equation (3.34) for $C_L = 0$ and that for $C_D = 0$ are called the drag force theory and the lift force theory, respectively. There has been little study using equations (3.32) and (3.34) with consideration for all the elements, but in most cases of this category only two elements θ and $\tan\varphi$ are set at 0 and 1.0, respectively.

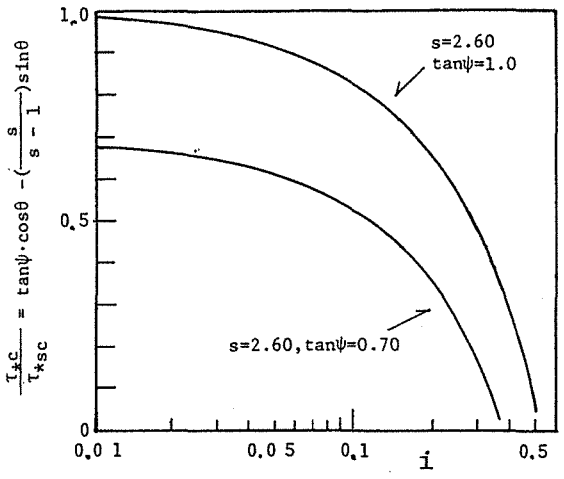

Fig. 3.8 The Effect of Modifying τ_{*c} to τ_{*sc}

The left hand side of equation (3.34) is the expression which was obtained by modifying the Shields parameter for a steep slope, and let it be τ_{*sc}. Fig. 3.8 shows the extent of the effect of this modification, where the extent increases considerably along with slope. To simplify the expression for τ_{*sc}, let the shape of gravel particles be spherical and introduce hiding coefficient ϵ, the τ_{*sc} can be expressed as follows.

$$\tau_{*sc} = \tau_{*c} \cdot \frac{1}{(\tan\psi\cos\theta - \frac{S}{S-1}\cdot\sin\theta)}$$

$$= \frac{1}{C_D} \cdot \frac{4}{3} \cdot \frac{1}{\varepsilon(1 + \frac{C_L}{C_D}\tan\ )} \cdot \frac{1}{C^2} \qquad \cdots\cdots\cdots (3.35)$$

The right hand side of equation (3.35) contains the drag coefficient, the lift coefficient, the hiding coefficient, and the resistance coefficient, and is in general considered a function of Reynolds number and relative roughness, but in a perfect turbulent flow it can be considered independent of Reynolds number.

To obtain the critical tractive force from the equilibrium equation (3.35) for the critical condition, it is first necessary to determine the flow velocity that would be effective for initiating the movement of a particle. Now, let the flow velocity at the crest of the particle be U_t, it is incorporated into the following equation through equation (2.2).

$$\frac{U_t}{U_*} = \frac{U_\delta}{U_*} + \psi \cdot \ln \frac{0.015}{\delta} \qquad \cdots\cdots\cdots (3.36)$$

From equations (2.9), (2.10), and (3.36), U_t/U_* can be figured out if given a value of U_o/U_*, where the value of U_o/U_* can be obtained from the diagram of the resistance coefficient in Fig. 2.5 with reference to d/h and U_*^2/gd.

Let the right and left hand sides of equation (3.35) be X and Y, respectively, that is,

$$X = \frac{1}{C_D} \frac{4}{3} \frac{1}{\varepsilon(1 + C_L \tan\psi)} \frac{1}{C^2} \qquad \cdots\cdots\cdots (3.37)$$

$$Y = \frac{U_*^2}{(S-1)gd} \frac{1}{(\tan\psi\cos\theta - \frac{S}{S-1}\sin\theta)} \qquad \cdots\cdots\cdots (3.38)$$

and C be equal to U_t/U_*, the values of X and Y can be obtained for a combination of given values of U_*^2/gd and d/h. Curves thus obtained are plotted in Fig. 3.9.

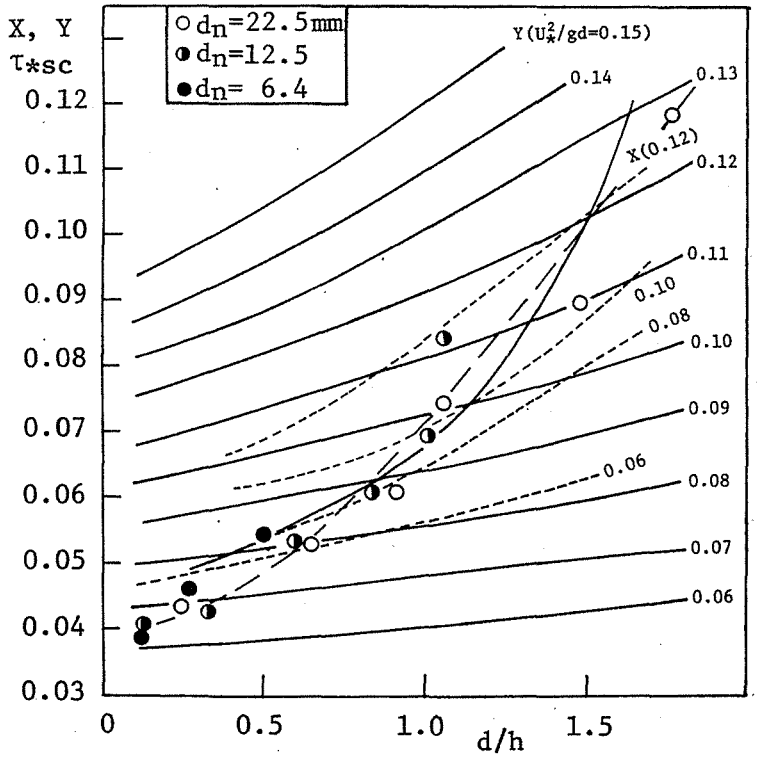

Fig. 3.9 The Result of Calculating the Critical Tractive Force

The intersection of two curves in the figure represents the critical tractive force τ_{*sc}. The curve drawn by connecting the intersections thus plotted agrees comparatively well with the experimental curve, where $C_D \cdot \epsilon [1 + (C_L/C_D)\tan \varphi] = 1.0$ is assumed.

Section 4: Critical Tractive Force for Initiating the Transport of Gravel Mixture

In the previous section, it was made clear that a non-dimensional critical tractive force for the modified effect of slope is a function of relative roughness. Needless to say, since a natural river bed consists of gravel mixture, the experiment used in this section adopted gravel mixtures of a wide range of grain size in order to examine the effect of gravel mixtures and the influence of relative roughness on the critical tractive force.

(1) Outline of the experiment

(a) Experimental flume

The experiment was carried out using a 15-meter long flume with a variable slope in which a 3-meter long and 20-centimeter wide steel channel was inserted, and two reaches one meter in length from the upper and lower ends of which were provided with rigid beds and the remaining reach between the two rigid beds was provided with a movable bed (See Fig. 3.10).

(b) Experimental gravel mixture bed

The bed was formed of gravel mixture of glass beads having seven different diameters, 1, 2, 5, 7, 12.6, 16.4, and 24.5 mm and ceramic particles of 18.3 mm. The experiment adopted two different kinds of gravel mixtures called mixture A and mixture B, having different grain size distributions, as shown by solid lines in Figs. 3.11 and 3.12.

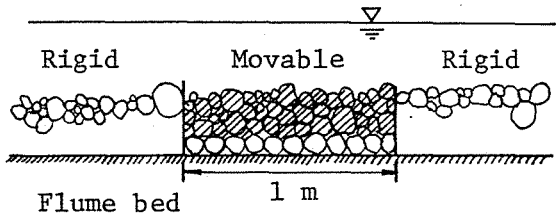

Fig. 3.10 A Conceptual Scheme of Gravel Mixture

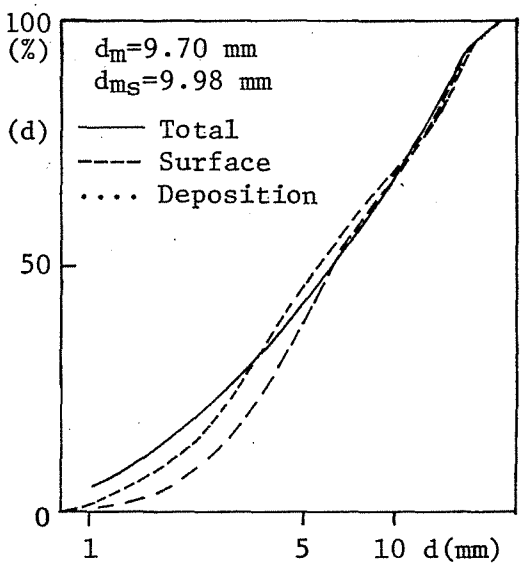

Fig. 3.11 Grain Size Distribution of Gravel Mixture A

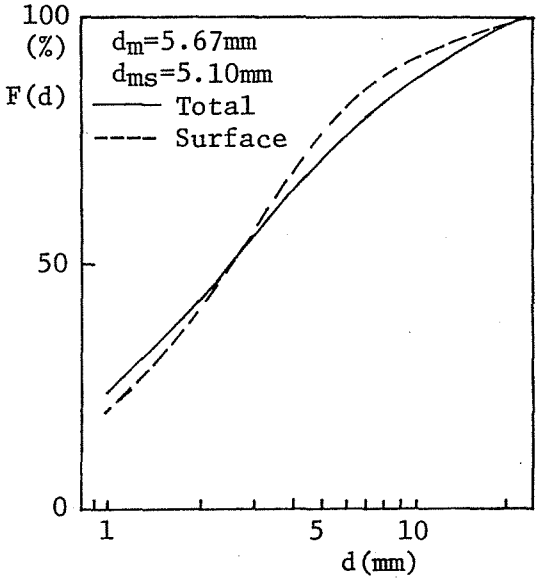

Fig. 3.12 Grain Size Distribution of Gravel Mixture B

Fig. 3.13 shows the grain size distribution of another mixture called mixture A(N).

The curve named "deposition" put down in Fig. 3.11 represents the grain size distribution of particles on the surface of the sediment supplied from the upper stream area and deposited. Table 3.3 presents various kinds of glass beads and natural gravel, and Table 3.4 the characteristics of gravel mixtures A, B, and A(N), such as the mean diameter d_{ms}, the standard deviation $\sqrt{d_{84}/d_{16}}$, the mean diameter of a particle on the surface of bed material d_{ms}, the internal friction angle φ, and the bed roughness ΔZ.

The internal friction of gravel mixture was represented by the critical angle of an inelined box at which the entire gravel mixture filled in the box starts moving simultaneously in the air, which is similar to he case of uniform gravel.

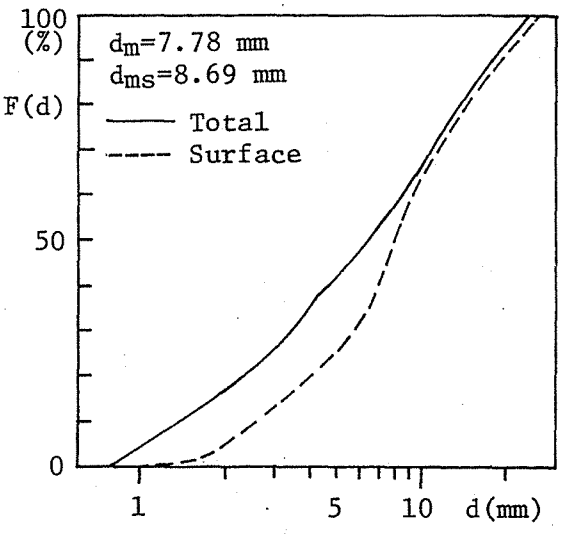

Fig. 3.13 Grain Size Distribution of Gravel Mixture A(N)

In the experiment, each gravel mixture consisting of selected particles having nearly the mean diameter is laid out as thick as one layer on the bottom of an aluminium box one meter long in order to form rigid beds on which sand mixture is further laid out as thick as 4 cm to form a movable bed. In addition, particles were color coded for each diameter to make it easy to distinguish them in diameter during the experiment.

Table 3.3 Bed Materials used in the Experiments

d_i (mm)	σ/ρ	Description
1, 2, 5, 7	2.50	Glass beads
12.6, 16.4	2.60	Glass beads
18.3	2.40	Porcelain
24.5	2.53	Glass beads
0.84 ~ 5.4	2.55	River sand

Table 3.4 Properties of Gravel Mixtures used in the Experiments

Mixture	dm(mm)	dms	tanφ	$\sqrt{d_{84}/d_{16}}$	$\sigma_{\Delta x=1cm}$	$\sigma_{\Delta x=1cm}/d_{ms}$	$\Delta Z_{\Delta x=1cm}$	$\Delta Z_{\Delta x=1cm}/d_{ms}$
A	9.70	9.98	0.625	2.74	0.401	0.402	0.342	0.343
B	5.67	5.13	0.510	3.106	0.354	0.690	0.177	0.345
A(N)	7.78	8.69	0.983	2.74	0.464	0.534	0.370	0.426

(c) Procedure for the experiment

The experiment was carried out in the aforementioned gravel mixture bed with its slope being changed into 8 gradients in a range of $\sin\theta = 0.02$ to 0.198.

The experimental procedure was made such that like the procedure for the case of uniform gravel the movable bed was covered with a metallic net, the net is taken away from the movable bed and lifted up when the flow becomes uniform, and the number of moved gravel particles which flowed out to the lower stream area was counted every 30 seconds for 3 minutes. During this interval the depth was measured by using a point-gauge, the flow discharge by a triangular weir, and the water temperature as well. This experiment was repeated while slightly changing the flow discharge each time. Fig. 3.14 provides for an example showing the relationship between the flow depth and the number of moved particles of gravel mixture A.

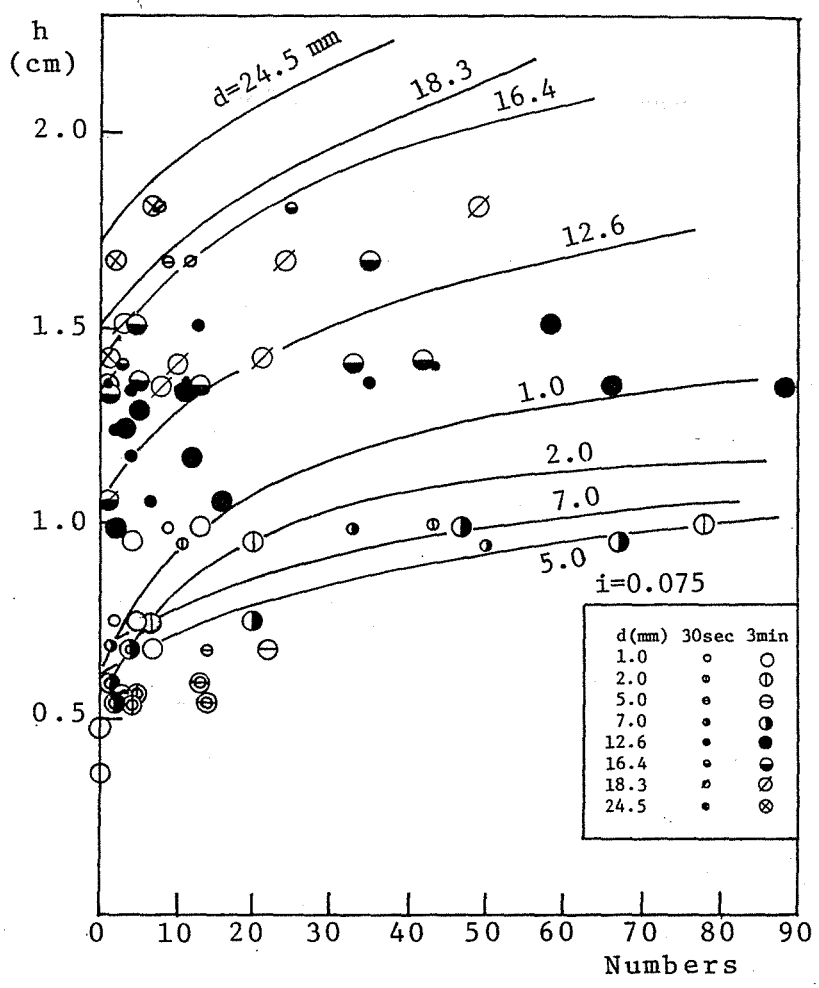

Fig. 3.14 An Example Explaining the Relationship between the Number of Movable Gravel Mixture Particles of Different Diameters and the Depth

In defining the threshold of transport the state of first initiating the motion of particles during the first 30 seconds for the gravel consisting of particles of larger than the mean diameter and the state for the gravel whose particles are of less than the mean diameter of first initiating the motion of particles except for those which moved due to the turbulent flow caused by lifting the metallic net were adopted, respectively. The reason for setting the above definition was that since the object of the experiment is to obtain the critical tractive force for the primitive bed condition, it is necessary to remove the influence of the turbulent flow caused by lifting the metallic net covering the gravel consisting of small particles and to protect large size particles from a tendency of being moved easily when small particles in the neighborhood of large particles are washed away and the bed surface becomes loose and/or when local scouring occurs in a place downstream from the place of large particles.

In the experiment for a steep slope, as stated in Chapter 1, the flow discharge per unit river width was small in quantity, the flow concentration developed as time for water supply elapses, and further a tendency to meander, the bed collapse, and the laminar sliding of bed were observed. This paper does not deal with the initiation of motion for drifting.

The standard bed surface level used in this experiment was set to such height that 25% of the whole bed surface area protrudes above the standard bed surface level, similar to the case of uniform gravel. According to Tsuchiya[24], the standard bed level is considered to be lower as the grain size distribution spreads more widely. However, since it is hard to determine the standard bed surface level for gravel mixtures theoretically, it was defined in the same fashion as introduced in the case of uniform gravel. In addition, side wall modification was done in accordance with the Einstein's method.

(2) Experimental results and examination on the results

(a) Results of the experiment

In considering the resistance of a gravel mixture or its critical tractive force, the grain diameter of the gravel mixture needs to be represented non-dimensionally with a certain representative diameter of the gravel mixture particles. Although Yalin[2] adopts the maximum diameter d_{max} for its representative value, it is hard to agree with his idea since the percentage of grain size distribution that is occupied by the maximum diameter is extremely small. Accordingly, it is expected to find a grain diameter that occupies a considerable percentage of grain size distribution as the representative value. Further, since the initiating critical tractive force is closely related with the resistance law, it is possible to choose an equivalent roughness like quantity which indicates what representative grain diameter does the uniform gravel have when its resistance value is equivalent to that of a given gravel mixture. It has been proved from the result of Chapter 2 that this representative grain diameter is the mean diameter. Egiazaroff chose the mean grain diameter for a representative value of roughness and converted individual grain diameters of gravel mixtures into a non-dimensional value with the use of the mean grain diameter. Here, again the results will be arranged using the mean grain diameter, where the mean grain diameter defined herewith is the mean grain diameter of bed surface as described in Chapter 2.

Results of the experiments for sand mixtures A, B, and A(N) are indicated in Figs. 3.15, 3.16, and 3.17 with d_i/d_{ms} representing the ratio of an individual grain diameter to the mean grain diameter for the effect of grain diameter of gravel mixture and with d_{ms}/h for influence of the relative roughness.

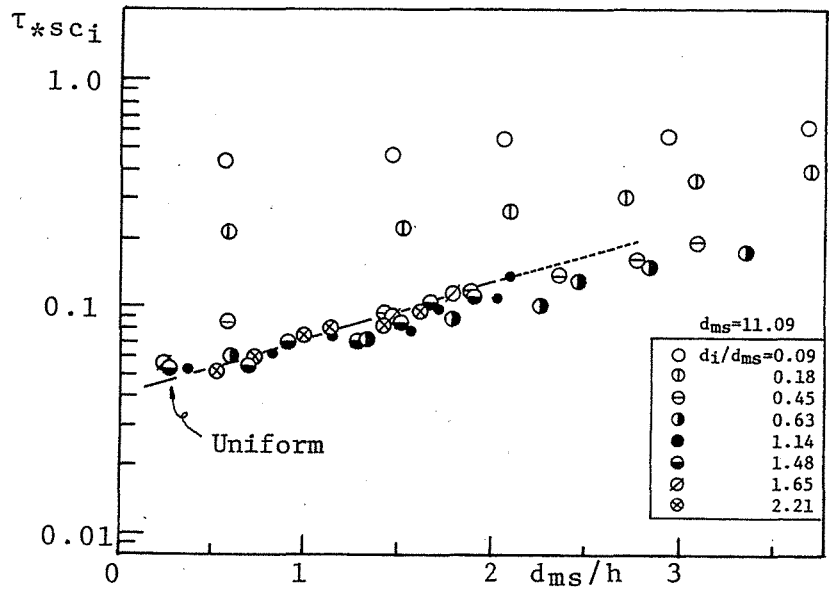

Fig. 3.15 The Change of Critical Tractive Force for Gravel Mixtures A of Different Diameters with reference to d_{ms}/h

Those results show the same tendency as seen for uniform gravel that $\tau_{*s}C_i$, the initiating critical tractive force by grain diameter for each individual diameter d_i increases as increase in d_{ms}/h, though the extent of the increase appears to be less than that for the uniform gravel. In addition, the diagrams show that the initiating critical tractive force increases as decrease in grain diameter if the value of d_{ms}/h is kept constant, and as a result the gravel is hard to move, where the critical tractive force is given by eq. (3.39).

$$\tau_{*sci} = \frac{U_{*ci}^2}{(S-1)gd_i} \cdot \frac{1}{(\tan\psi\cos\theta - \frac{S}{S-1}\sin\theta)} \quad \cdots\cdots \quad (3.39)$$

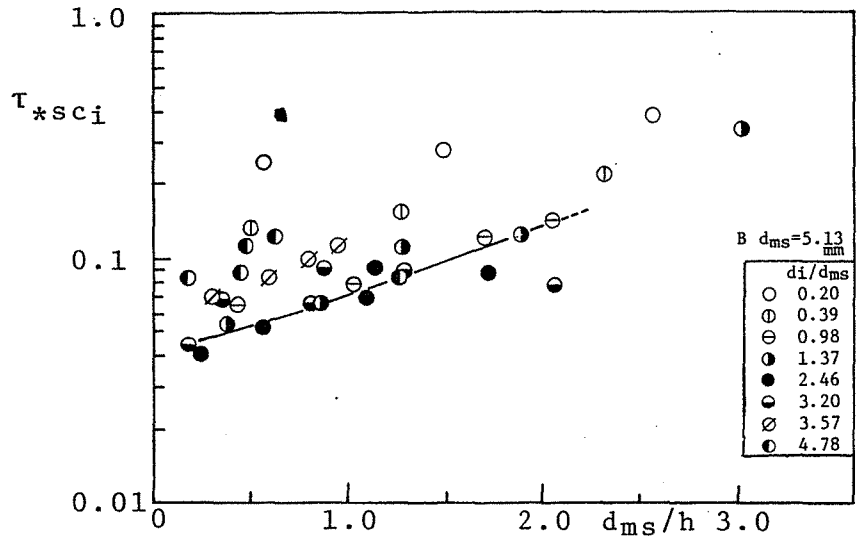

Fig. 3.16 The Change of Critical Tractive Force for Gravel Mixtures B of Different Diameters with reference to d_{ms}/h

In Fig. 3.15 showing the result of the experiment for glassbeads gravel mixture, there exists the relation $\tau_{*sci} \fallingdotseq \tau_{*scm} \fallingdotseq \tau_{*sco}$ for the particles having diameters greater than the mean diameter, where τ_{*sci} is the initiating critical tractive force for d_{ms} and τ_{*sco}, the initiating critical tractive force for uniform gravel. In the experiment for gravel mixture B shown in Fig. 16, if $d_i/d_{ms} < 2.4$ the smaller particles are hard to move and if $d_i/d_{ms} > 2.4$, while if $d_i/d_{ms} > 2.4$ the larger particles are hard to move. These results are in disagreement with the result of Egiazaroff's study whereby there is a tendency for the particles having greater diameters than the mean diameter to become mobile. This difference seems to be due chiefly to the way of laying out the gravel, so many different variations were experimented, but always with the same results.

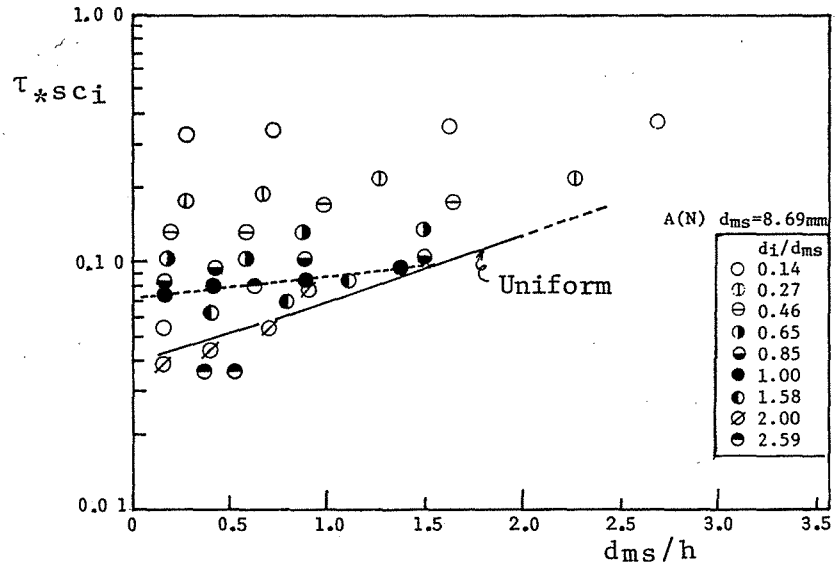

Fig. 3.17 The Change of Critical Tractive Force for Gravel Mixtures A(N) of Different Diameters with reference to d_{ms}/h

In contrast to this, in the case of natural gravel A(N) shown in Fig. 3.17, as d_i/d_{ms} increases τ_{*sci} becomes unilaterally smaller, which is in perfect agreement with a tendency of Egiazaroff equation. From this, it can be deduced that this difference is due to the difference in experimental bed materials used. Namely, in the case of glass beads, because of their spherical shape and smooth surface large particles are hard to keep staying at the upper part of the gravel layer and tend to sink into the bed. On the other hand, in the case of natural gravel particles their irregular shapes make them possible to stay at the upper part of the gravel layer. This is clarified from the fact that both tan ψ of mixture A and that of mixture B are considerably smaller than that of mixture A(N) (See Table 3.4). Further, in the case of mixture A and B shperical shapes and smooth surface of beads would also cause their resistance to be small. Thus, unlike natural gravel particles, beads, though they were used in expectation of easy and simple handling in experiments due to uniformalization of gravel particles and so on, have proved unsuitable for materials to examine the mixture effect of gravel particles. Accordingly, the result of the experiment for A(N) shown in Fig. 3.17 will mainly be described in the following.

First, pertaining to the initiating critical tractive force for the mean-diameter particles, when the depth is sufficient, τ_{*scm} becomes 0.07 which, compared with 0.04 for uniform gravel, is quite large. From this, it is proved that when grain size distribution becomes wide, particles of the mean diameter or so are hidden by larger particles and become hard to move. Thus, the extent of increase in the initiating critical tractive force for the mean-diameter gravel mixture particles, as opposed to that for uniform gravel, in comparison with Tsuchiya's result is shown in Fig. 3.18.

The conventional studies, of which results are shown in Fig. 3.18, have been carried out for gravel mixtures having not only a relatively wide range of grain size distribution but a considerable dispersion of the distribution, so the tendency to increase in the initiating critical tractive force is not so remarkable. Experiments other than the author's has taken d_{50} as representative grain diameters. Because the grain size distribution in mixture A(N) used in this research was not expressed in a logarithmic normal distribution fashion d_m is used instead, but it can be safe to say that the general tendency for the initiating critical tractive force is towards increase.

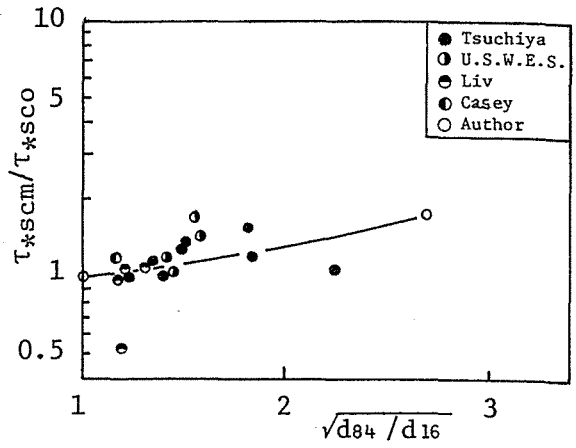

Fig. 3.18 The Change of Critical Tractive Force for Gravel Mixture of a Mean Diameter with reference to $\sqrt{d_{84}/d_{16}}$

As can be seen from Fig. 3.17, the increase in τ_{*scm}, the initiating critical tractive force for particles of the mean diameter, by d_{ms}/h is smaller than that for uniform gravel particles and appears to be in agreement with τ_{*sco}, the initiating critical tractive force for uniform gravel when d_{ms}/h is around 1.5. Therefore, the comparison of τ_{*sco} and τ_{*scm} to the same value of d_{ms}/h was taken and shown in Fig. 3.19.

Since it is considered from the results of Tsuchiya's study[24] that as far as the standard deviation of grain size distribution is less than 1.5 or so, the mixture effect of gravel particles comes out, in the case of $\sqrt{d_{84}/d_{16}}$ = 1.5 the value of the ratio τ_{*scm}/τ_{*sco} would follow the dotted estimated line shown in he figure. The ratio τ_{*scm}/τ_{*sco} for $d/h \to 0$ is shown in Fig. 3.18, whereas the variation of the ratio with d/h must be deduced by referring to experimental values obtained.

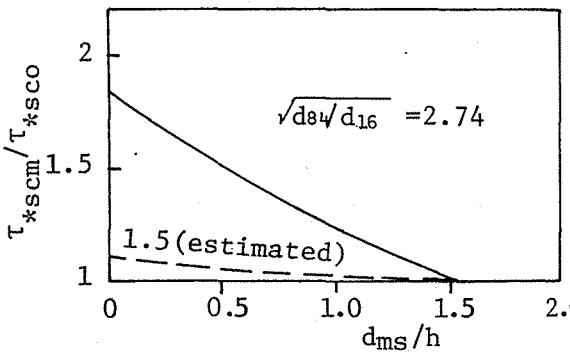

Fig. 3.19 The Change of Critical Tractive Force for Gravel Mixture of a Mean Diameter with reference to d_{ms}/h

Next, in order to further clarify the influence of d_i/d_{ms} on the initiating critical tractive force, the value of τ_{*sci} for the same d_{ms}/h was obtained through interpolation or exterpolation, and normalized by the mean grain diameter to obtain the variation of τ_{ci}/τ_{cm} to d_i/d_{ms}, as shown in Fig. 3.20.

In the figure, a modified Egiazaroff equation derived by Ashida and the case that τ_{*sci} always equals τ_{*scm} ($\tau_{ci} = \tau_{cio}$) are also shown. From this, a tendency can be seen that when d/h << 1, the initiating critical tractive force is in agree with the modified Egiazaroff equation, and as d/h increases the smaller particles become more mobile while the larger particles become harder to move and the critical tractive force variation becomes close to that for uniform gravel sand. However, since there exists a problem with definition of the threshold of transport or so, it is difficult to compare the above with other research results. From this, it may be concluded that the modified Egiazaroff equation can apply to calculation of the initiating critical tractive force for this case even in a range of d/h ≒ 1.

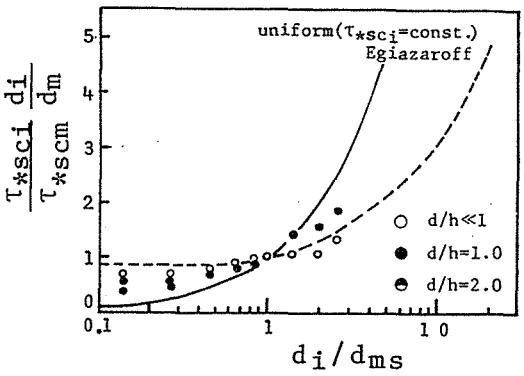

Fig. 3.20 A Comparison Critical Tractive Force by Grain Diameters and Modified Egiazaroff Equation

Putting together all the things stated so far, in case the depth is sufficient the τ_{*scm} becomes great compared with the τ_{*sco} as the grain size distribution widens, while critical tractive force by grain diameter can be given by the modified Egiazaroff equation. Further, as increase in the relative roughness the initiating critical tractive force for the mean grain diameter increases and at the same time the function form of the initiating critical tractive force for the mean grain diameter also changes. At the present stage, there is still a lack of experimental information for gravel mixtures having wide grain size distribution, so it is too early to conclude that the results shown in Figs. 3.19 and 3.20 are generally true, and further information needs to be collected.

Here, some additional explanation would be preferred. The content of Fig. 3.17 is separately explained in Figs. 3.19 and 3.20. First, in Fig. 3.19, the fact that the initiating critical tractive force for the mean-diameter gravel particles comes close to the value of critical tractive force for uniform gravel as d_{ms}/h increases means that as d_{ms}/h increases the hiding effect lessons. It can be inferred from this that the water flowing between the larger particles plays a significant role along with increase in slope. This brings to mind the changes in the theoretical bed. Pertaining to Fig. 3.20, in the case of the changes in τ_{*scm} with grain size distribution and d_{ms}/h as seen in this research, it is not a very pertinent expression, but becomes significant only when considered in conjunction with Figs. 3.18 and 3.19.

Next, it is intended to try to explain in terms of dynamics the variation characteristics of the initiating critical tractive force clarified so far by referring to the case of uniform gravel.

(b) Examination on the results

The variation characteristics of the initiating critical tractive force by grain diameter will be explained according to the information of gravel mixtures and flow velocity distribution given in Chapter 2. Assuming that the observed flow velocity distribution pattern for uniform gravel bed can apply to that for gravel mixture, its velocity distribution pattern can be provided by the following equations.

$$\frac{U}{U_*} = A + \psi \cdot 1n\frac{y}{\delta} \qquad \text{for } 0 < y < \delta \qquad \cdots\cdots\cdots (3.40)$$

$$\frac{U}{U_*} = A + \frac{I}{\kappa} \cdot 1n\frac{y}{\delta} \qquad \text{for } y \geq \delta \qquad \cdots\cdots\cdots (3.41)$$

where $K = 0.4$, $\psi = 0.87$, $A = U_\delta/U_*$, and $\delta = 0.8\ d_{ms}$. From Fig. 2.15, if the crest of a particle of diameter d_i is at $y = 0.4\ d_i$, it can be said that particles of less than $d_i = 2d_{ms}$ are in the lower part of the flow velocity distribution, and those of greater diameter protrude above the upper layer. For $d_i/d_{ms} < 2$, the flow velocity at the crest can be derived from eq. (3.40) as follows.

$$\frac{U_{ti}}{U_*} = \frac{U_\delta}{U_*} + 0.87 \cdot 1n\frac{1}{2}\frac{d_i}{d_{ms}} \qquad \cdots\cdots\cdots (3.42)$$

Also, for $d_i/d_{ms} \geq 2$, from eq. (3.41) the following is obtained.

$$\frac{U_{ti}}{U_*} = \frac{U_\delta}{U_*} + 2.5 \cdot 1n\frac{1}{2}\frac{d_i}{d_{ms}} \qquad \cdots\cdots\cdots (3.43)$$

U_δ/U_* can be obtained from equations (2.9) and (2.10), using the resistance coefficient given in Fig. 2.5 or Fig. 2.17, and flow velocity U_{ti}/U_* at th crest can be obtained from eqs. (3.42) and (3.43).

On the other hand, the equation for the threshold of transporting a particle of diameter d_i is obtained from eq. (3.35).

$$\tau_{*sci} = \frac{U_{*ci}^2}{(S-1)gd_i} \cdot \frac{1}{\left(\tan\psi\cos\theta - \frac{S}{S-1}\sin\theta\right)}$$

$$= \frac{1}{C_D} \cdot \frac{4}{3} \frac{1}{\varepsilon_i\left(1 + \frac{C_L}{C_D}\tan\right)} \cdot \frac{1}{C_i^2} \qquad \cdots\cdots\cdots (3.44)$$

where suffix i represents a value for d_i. Let the function of the right hand side of equation (3.44) be X, and the function of the left hand side be Y,

$$X = \frac{1}{C_D} \cdot \frac{4}{3} \cdot \frac{1}{\varepsilon_i\left(1 + \frac{C_L}{C_D}\tan\psi\right)} \frac{1}{C_i^2} \qquad \cdots\cdots\cdots (3.45)$$

$$Y = \frac{U_*^2}{(S-1)gd_i} \cdot \frac{1}{\left(\tan\psi\cos\theta - \frac{S}{S-1}\sin\theta\right)} \qquad \cdots\cdots\cdots (3.46)$$

X and Y are determined by d_{ms}/h, U_*^2/gd_{ms}, and d_i/d_{ms}. The initiating critical tractive force for d_i/d_{ms} and that for d_{ms}/h can be obtained by plotting intersections of the X and Y curves. Here is a problem of how to determine coefficients contained in the right hand side of equation (3.45). At present, there are no definitive physical quantities for drag coefficient and lift coefficient, and further unclear for hiding coefficient. In calculating the initiating critical tractive force for uniform gravel described in the preceding section, $C_D\,[1 + (C_L/C_D)\tan\psi] = 1.0$ was assumed. Here, a kind of hiding coefficient ϵ_i is introduced into the calculation so as to explain the experimental result for gravel mixture A(N), where ϵ_i' is given by the following equation.

$$\varepsilon_i' = C_D\varepsilon_i\left(1 + \frac{C_L}{C_D}\tan\psi\right) \qquad \cdots\cdots\cdots (3.47)$$

Assuming that neither drag coefficient nor the lift coefficient change, the above equation represents the ratio of hiding coefficient for gravel mixture to that for uniform gravel.

When the variation of ϵ_i' with reference to d_i/d_{ms} is given as shown in Fig. 3.21, the variation of τ_{*sci} with respect to d_{ms}/h and d_i/d_{ms} are as shown in Fig. 3.22 which thus indicates the variation characteristics of τ_{*sci}. This way, however, causes many complicated phenomena to be intensified in the hiding coefficient, and it is, therefore necessary to further to clarify the phenomena from the microscopic standpoint.

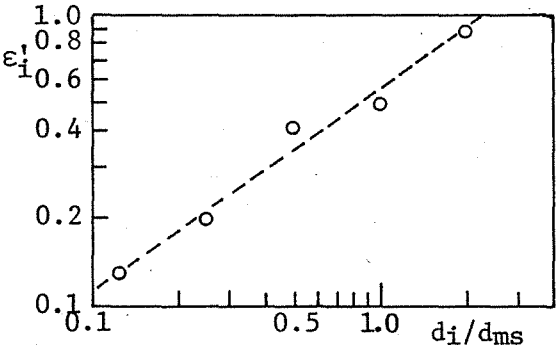

Fig. 3.21 The Relationship between ε_i' and d_i/d_{ms}

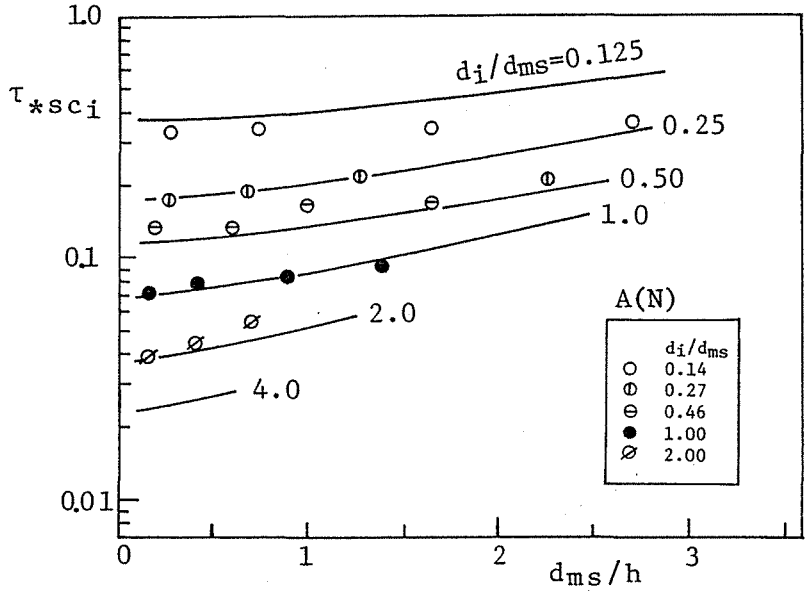

Fig. 3.22 A Comparison of Calculated Values of Critical Tractiev Force for Gravel Mixture and Its Experimental Values

Section 5: Conclusion

The aforementioned study on the critical tractive forces for initiating the transport of both uniform gravel and gravel mixture in a steeply sloped flume has brought about the following results.

First, concerning uniform gravel,

I) Shield parameter τ_{*sc} which was used to modify the effect of slope, is a function of relative roughness in a range of perfect turbulent flow, and its function form was obtained empirically. According to this τ_{*sc} increases abruptly as d/h increases.

II) The variation characteristics of the initiating critical tractive force thus obtained from the above could be explained theoretically using the gravel equilibrium equation and the law of resistance.

In order to examine further, it is necessary to observe the characteristics of a turbulent flow occurring in a stream which has a great relative roughness and a steep slope, and to observe forces acting upon bodies placed in that stream.

Next, concerning gravel mixture,

I) The initiating critical tractive force for gravel mixture particles of the mean diameter is much greater than that for uniform gravel due to the shield effect of larger pieces of the gravel. This ratio increases with the increase of $\sqrt{d_{84}/d_{16}}$, and the relation of up to a value of $\sqrt{d_{84}/d_{16}} = 2.8$ was made clear experimentally. Furthermore, it is necessary to examine anew the effects on a gravel mixture which has a wider grain size distribution.

II) The initiating critical tractive force by grain diameter and the ratio of it to the mean diameter are given as a function of d_i/d_m and that of d/h, and the critical tractive force can be expressed approximately in a modified Egiazaroff equation when d/h is small and as d/h becomes larger it becomes closer to the initiating critical tractive force for uniform gravel.

III) From the above two conclusions, the initiating critical tractive force for an individual grain diameter can be obtained, and the relationship between the above two conclusions could be explained theoretically with the assumption of hiding coefficient for an individual diameter.

REFERENCES

1) ASCE Progress Report:
"Sediment Transportation Mechanics"; Initiation of Motion, Jour. ASCE, HY2, March 1966, pp. 297.
2) Yalin, M.S.:
"Mechanics of Sediment Transport, Pergamon, 1972.
3) Ward, B.D.:
"Relative Density Effects on Incipient Bed Movement", Water Resources Research, vol. 5, No. 5, Oct. 1969.
4) Gessler, J.:
"Beginning and Ceasing of Sediment Motion", Chap. 7, River Mechanics, vol. 1, 1972.
5) Begárdi, J:
"Bestimug der Grenzzustande bei der Geschiebewegung", Die Wasserwirtshaft, 7. 1968.
6) Sahap, Aksoy:
"The Influence of the Relative Depth on Threshold of Grain Motion", IAHR, ISRM, 1973.
7) Neill, C.R.:
"Mean-velocity Criterion for Scour of Coarse Uniform Bed Material", Proc. 12th Congress of IAHR, 1967.
8) Shigekiyo Tabata, and Masahiko Ichinose:
"An Empirical Study of Critical Tractive Force of Large Gravel", the SHIN-SABO 79, May 1971.
9) Graf, W.F.:
"Hydraulics of Sediment Transport, McGraw Hill, 1971
10) Michinori Kurihara:
"On the Critical Tractive Force" The Fluid Mecahnics Laboratory of the Kyushu University, Laboratory Report, vol. 4, No. 3, 1948.
11) White, C.M.:
"The Equilibrium of Grains on the Bed of Stream", Proc. Roc. Soc., A174, 1940
12) Yuichi Iwagaki:
"A Fluid Mechanical Study of the Critical Tractive Force", JSCE, Professional paper 41, 1956.
13) Carstens, M.R.:
"Accelerated Motion of Spherical Particles, Trans. A.G.U., vol. 33, 1952.
14) Kalinske, A.A.:
"Movement of Sediment as Bed Load in Rivers, Trans. A.G.U., vol. 28, No. 4, 1947.
15) Lyles, Woodruff:
"Boundary-Layer Structure Effects on Detachment of Noncohesive Particles", Chap. 2, Sedimentation, 1972.
16) Christensen, B.A.:
"Incipient Motion on Cohesionless Channel Banks, Sedimentation", Chap. 4, 1972.
17) Einstein, Elsamni:
"Hydrodynamic Forces on a Rough Wall, Review of Modern Physics, 21, 1949, pp. 520-524.
18) Einstein, H.A.:
"Formulas for the Transportation of the Bed Load, Trans. ASCE, vol. 107, 1942.
19) Gessler, J.:
"Critical Shear Stress for Sediment Mixtures, IAHR, Proc. 14th Congress Paris, 1971.
20) Gessler, J.:
"Behavior of Sediment Mixtures in Rivers", IAHR, ISRM, Bangkok, 1973.

21) Paintal, A.S.:
"A Stochastic Model of Bed Load Transport", Jour of Hydraulic Research, vol. 9, No. 4, 1971.
22) Kramer, H.:
"Sand Mixture and Sand Movement in Fluvial Models", Proc. ASCE, 1934.
23) Takao Sakai:
"Critical Tractive Force for Bed Gravel", JSCE, Jour. 31, 2, Feb. 1946.
24) Yoshito Tsuchiya:
"Critical Tractive Force for Gravel Mixture", the Disaster Prevention Laboratory of the Kyoto University, Annual Report 6, July 1963, pp. 228-253.
25) Egiazaroff, I.V.:
"Calculation of Nonunifiorm Sediment Concentrations", Proc. ASCE, HY4, July 1965.
26) Kazuo Ashida, Masanori Michiue, and Shinji Eto:
"Initiation of Motion of Gravel Mixture", Annual summary of lecture., 1971.
27) Muneo Hirano:
"Deformation of Gravel Mixture Bed and Equilibrium of Bed", JSCE, Professional paper 207, Nov. 1972.
28) Coleman, N.L.:
"The Drag Coefficient of a Stationary Sphere on a Boundary of Similar Spheres", LA HOLILLE BLANCHE, No. 1, 1972.
29) Garde, R.J., Sethurman, S.:
"Variation of the Drag Coefficient of a Sphere Rolling along a Boundary, LA HO-LILLE BLANCHE, 1, No. 7, 1969, pp. 727-732.
30) Chepil, W.S.:
"The Use of Evenly Spaced Hemispheres to Evaluate Aerodynamic Forces on a Solid Surface", Trans. A.G.U., vol. 39, No. 3, June 1958, pp. 397-404.
31) Chen, C.N.:
"Mechanic of Removal of a Spherical Particles from a Flat Bed", IAHR, 1973.
32) Muneo Hirano:
"On the Bed Lowering Accompanying Armouring, JSCE, Professional paper 195, Nov. 1971.
33) Atsuyuki Daido:
"Critical Tractive Force for Gravel Particles Protruding above Flow", ISCE, 27th Annual Summary of Lecture, 1972.
34) Sutesaburo Sugio:
"Registance Law for a Movable Bed", Water Engineering Series A-5, 1971.
35) Kazuo Ashida, Atsuyuki Daido, Tamotsu Takahashi, and Takahisa Mizuyama:
"Resistance of a Steeply Sloped Flow and its Critical Tractive Force", the Disaster Prevention Laboratory of the Kyoto University, Annual Report 16-B, April 1973, pp. 481-494.

CHAPTER 4 BED LOAD TRANSPORT RATE

Section 1: Outline

Research concerning bed load transport rate began with the Duboy's bed load equation in 1879. After that a number of empirical equations were found from dimension analytical examinations and much experimental data. From the use of bed load models many bed load equations were proposed. However, there is still no bed load equations which can be applied with full confidence to place where the grain size ranges widely and the slope is steep, as in mountain rivers. The present study concerns just such cases. As a prerequisite to that, first, let us summarize some of the conventional representative bed load equations.

I) Einstein[1]'s bed load function

From observations and experiments Einstein made the following assumptions a) Transport of bed sand occurs when the momentary lift force becomes greater than the sand weight, b) Regular intense exchange of particles exists between bed material and bed load, c) The movement of individual particles can be expressed in terms of a kind of step function having relatively long intermissions. d) The displacement for one step is due only to grain diameter regardless of flow velocity. e) The increase in bed load transport rate is due to the mean time variation between the steps and the thickness of laminar flow. Thus, he derived the following bed load equation (4.1).

$$1 - \frac{1}{\sqrt{\pi}} \int_{-0.143\psi-2.0}^{0.143\psi-2.0} e^{-t^2} dt = \frac{43.5\Phi}{1 + 43.5\Phi} \quad \cdots\cdots\cdots (4.1)$$

Here Φ is a nondimensional quantity for bed load called the bed load transport intensity, and is expressed as equation (4.2).

$$\Phi = \frac{q_B}{\{(\sigma/\rho - 1)gd^3\}^{1/2}} \quad \cdots\cdots\cdots (4.2)$$

Here q_B is the sand discharge per unit area per unit time. Also ϕ is called the flow intensity and is expressed as equation (4.3).

$$\psi = \frac{(\sigma/\rho - 1)gd}{U_*^2} = \frac{1}{\tau_*} \quad \cdots\cdots\cdots (4.3)$$

Einstein proposed applying the tractive force, partitioned by hydraulic radius, that is effective in transport of bed load when bed ripples are formed. This is given by the following equation.

$$\frac{U_o}{U_{*e}} = 5.75 \log\left(\frac{12.27 \times R'}{d_{65}}\right) \quad \cdots\cdots\cdots (4.4)$$

Here U_o is the cross sectional average velocity, U_{*e} is the effective shear velocity ($= \sqrt{gR'I}$), X, a coefficient, which is a function of Reynolds number for bed load as $d_{65}U_*/11.6\nu$), and R' is the hydraulic radius effectively acting on the sediment.

II) Kalinske' research[2)]

Let n_b be the number of sand particles per unit area of bed surface and $\overline{V}_s$ be the average velocity of bed load. The bed load transport rate can be expressed as

$$q_B = \frac{\pi}{6} d^3 \overline{V}_s n b \qquad \cdots\cdots\cdots (4.5)$$

Kalinske assumes the momentary velocity V_s of a particle is proportional to $(U - U_c)$ and lets.

$$V_s = b(U - U_c) \qquad \cdots\cdots\cdots (4.6)$$

Here, b is a constant close to 1, U the flow velocity near the gravel, U_c the flow velocity near the gravel at the time of transport threshhold. Also, he assumes the variation of speed to follow a normal distribution, and expresses eq. (4.5) as eq. (4.7).

$$\frac{q_B}{U_* d} = 2.6F_1(\tau_c/\tau_o) \qquad \cdots\cdots\cdots (4.7)$$

Here, $F_1(\tau_c/\tau_o)$ represents a function of τ_c/τ_o.

III) Sato, Yoshikawa and Ashida's equation

Sato, Yoshikawa and Ashida consider the momentum from pressure on lower particles due to turbulence to be equal to the momentum from gravity acting on particles within the bed load region, and derive the following equation.

$$\Phi = \psi F_2(\tau_o/\tau_c)\tau_*^{3/2} \qquad \cdots\cdots\cdots (4.8)$$

Where $F_2(\tau_o/\tau_c)$ is a coefficient which is a function of τ_o/τ_c, and τ_* is equal to $U_*^2/(\sigma/\rho\text{-}1)gd$. Also, from experiments ψ has been determined to be

$$\begin{aligned} &n \geqq 0.025; \quad \psi = 0.62 \\ &n \leqq 0.025; \quad \psi = 0.62(40n)^{-3.5} \end{aligned} \qquad \cdots\cdots\cdots (4.9)$$

Here n is Manning's roughness coefficient.

IV) Meyer-Peter, Müller's equation[3)]

Meyer-Peter et al. proposed the following empirical equation based on a wide range of experiments.

$$\Phi = 8(\tau_{*}e - 0.047)^{3/2} \qquad \cdots\cdots\cdots (4.10)$$

Here $\tau_{*e} = U_{*}^{2}e/(\sigma/\rho-1)gd$, $U_{*}e$ is the effective shear velocity $(=(n_b/n)^{3/4} U_{*})$, n_b is a Stlicker type roughness coefficient expressing sand drag, $n_b = 0.034 d_{90}^{1/6}$, n is the stream's overall roughness coefficient.

V) Ashida, Michiue's equation[4)]

Ashida and Michiue, from experiment and Bagnold's theory, proposed the following equation.

$$\Phi = 17\tau_{*}e^{3/2}\left(1 - \frac{\tau_{*c}}{\tau_{*}}\right)\left(1 - \frac{U_{*c}}{U_{*}}\right) \qquad \cdots\cdots\cdots (4.11)$$

Further, the effective shear velocity $U_{*}e$ is determined from the following equation.

$$\frac{U_o}{U_{*}e} = 6.0 + 5.75\log\frac{R}{d(1 + 2\tau_{*})} \qquad \cdots\cdots\cdots (4.12)$$

Einstein, Meyer-Peter & Müller, Ashida and Michiue's equations are shown in Fig. 4.1.

The above are representative bed load equations. With the exception of Kalinske's equation, each equation takes into account directly or indirectly the effect of riverbed roughness. In order to express in unified way the sediment discharge, including the case when bed ripples are formed, consideration of effective tractive force has merit. How to determine this quantity is at present the most important subject in research of bed load transport rate.

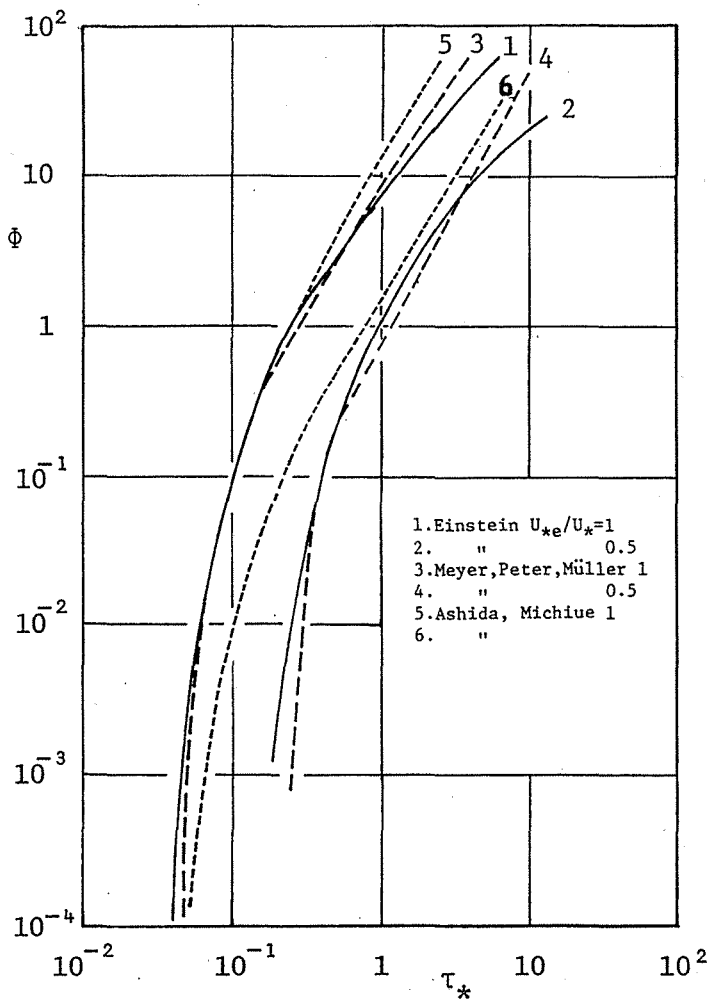

Fig. 4.1 Bed Load Equations

VI) Bed load equation for gravel mixture

There has not been much research on sediment transport for gravel mixture. This is due to the bed materials used in experiments being largely uniform gravel or close to it, and also to the fact particle distributions in actual flat rivers are not very wide and to the fact the overall value is close to the result obtained using the mean diameter. However, in mountain rivers the grain size distribution is wide, and there are many cases where stationary particles are present. Also, to try to explain the advance of armouring with time under non-equilibrium conditions, a bed load equation by diameter is necessary.

Einstein introduced a modification coefficient because fine particles are hidden by coarse ones, and proposed a bed load equation by diameter for gravel mixture. However, later research indicated this modification coefficient over-

estimated the hiding effect. Further, Egiazaroff developed another bed load equation for different diameters which combines a bed load equation and one more equation for critical tractive force by diameter developed by Egiazaroff as introduced in Chapter 3. This equation was used in the discussion of riverbed deformation accompanying armouring phenomena[5), 6)]. For example, combining the above equation with Sato-Yoshikawa-Ashida's equation, bed load quantity q_{Bi} for diameter d_i is given as follows.

$$\frac{q_{Bi}}{f_o(d_i)U_* d_i} = \psi F_2(\tau_o/\tau_{ci})\frac{U_*^2}{(\sigma/\rho - 1)gd_i} \qquad \cdots\cdots\cdots (4.13)$$

Here $f_o(d_i)$ is the percentage of the gravel particles of diameter d_i which occupies part of bed material. τ_{ci} is a modified Egiazaroff equation representing the critical tractive force for diameter d_i, which is given in Fig. 3.2.

Now, what problems arise for the case of mountain rivers in comparison with these researches? First, in mountain rivers bed gravel has a wide grain size distribution including large diameters, and there are many cases where large gravel particles are present which do not move under ordinary flood. Also, the resistance increases for a torrential flow, as was made clear in the studies of critical tractive force, and as a result the critical tractive force increases. For that reason the bed load transport rate is expected to decrease. The wash load for river beds having stationary particles has been studied, for example by Ashida[7)], but the influence of slope has not been studied. So, below first a bed load equation will be introduced, and then the influence of slope and the bed load transport rate for gravel mixture will be considered.

Section 2: Bed Load Transport Rate for Uniform Gravel

(1) Examination on bed load equations

First, assume the flow resistance law for the gravel in transport is the same as for the rigid bed case. This, for the case of steep slope, is not an unreasonable assumption as related in Chapters 2 and 3, and to a gentle slope it can apply according to Kishi[8)].

Since Bagnold's[9)] conception as a model of sand flow is clear with respect to physical meaning, it is utilized here. He formed the following hypothesis and confirmed it by research on streams containing cohesionless particles.

$$\tau_o = \tau_G + \tau_F \qquad \cdots\cdots\cdots (4.14)$$

Here, τ_o is the entire shear stress transmitted to the riverbed, τ_G is the shear stress caused by protruding particles, τ_F is the shear stress caused in the stream body. τ_G can be written

$$\tau_G = N(\sigma - \rho)g\cos\theta \cdot \mu_f \qquad \cdots\cdots\cdots (4.15)$$

letting N be the volume of sediment per unit area, θ the riverbed slope, μ_f the sand's coefficient of dynamic friction of a particle, δ and ρ the densities of sand and water respectively, and g the gravitational constant.

Consider the concentration of bed load of uniform diameter to be in equilibrium and assume the particles in the riverbed surface and the movable particles to exchange from time to as they move, then at the time the stationary particle in the surface begins to move the tractive force acting on that particle must be greater than that at the transport threshold. On the other hand, the particle which continued moving until that point must stop on the riverbed. In other words, in order that the equilibrium condition be maintained while the exchange takes place the critical tractive force for initiating the transport of particles and the critical tractive force for ceasing the transport must be equal, and the shear stress τ_F acting on the bed surface must reach just such condition that both critical forces be equal. However, since in general movable particles protrude from the surface more than stationary particles on the surface, they are in a state where it is easier to move than stationary particles. So, it seems there is a large probability of continuing to move in that state. In other words, the ceasing critical tractive force is smaller than the initiating critical tractive force. When the tractive force acting on the stationary particles within the riverbed surface is less than the initiating critical tractive force, the bed load equilibrium condition is reached. Accordingly,

$$\tau_F = K\tau_c \qquad \cdots\cdots\cdots (4.16)$$

The constant K is expected to be a value smaller than 1. Here, τ_c is the initiating critical tractive force. There is no practical method of estimating K at present, but because the bed load equilibrium breaks down and the movable sediment is deposited if τ_F falls below the ceasing critical tractive force as a lower limit τ_F is assumed equal to the ceasing critical tractive force.

Next, let us consider the relationship between the threshold of ceasing and the threshold of initiation. The critical transport velocity U_c for the transport threshold can be expressed for spherical particles from eq. (3.32):

$$U_c^2 = \frac{4}{3}\frac{1}{C_D}\frac{1}{\varepsilon}\frac{1}{\left(1+\frac{C_L}{C_D}\tan\psi\right)}(S-1)gd\left(\tan\psi\cos\theta - \frac{S}{S-1}\sin\theta\right) \qquad \cdots\cdots\cdots (4.17)$$

Here, $S = \sigma/\rho$. On the other hand, the average transport velocity of movable particles, from the equation for equilibrium condition of forces becomes

$$\frac{1}{2}\rho C_D(U_b - \overline{V}_s)^2\frac{\pi}{4}d^2 + \sigma g\frac{\pi d^3}{6}\sin\theta = (\sigma-\rho)g\cos\theta\frac{\pi d^3}{6}\cdot\mu_f \qquad \cdots\cdots\cdots (4.18)$$

Here, U_b is the representative flow velocity for movable particles, $\overline{V}s$ is the average transport velocity of the particles. From eq. (4.18)

$$U_b - \overline{V}_s = \sqrt{\frac{4}{3}\frac{1}{C_D}\{(S-1)\mu_f\cos\theta - S\sin\theta\}gd} \quad \cdots\cdots (4.19)$$

When $\overline{V}_s = 0$, U_b is the critical flow velocity for ceasing the transport, so let it be U_{cs} and the equation becomes

$$U_{cs}^2 = \frac{4}{3}\frac{1}{C_D}(S-1)gd\cdot\cos\theta\left(\mu_f - \frac{S}{S-1}\tan\theta\right) \quad \cdots\cdots (4.20)$$

Inserting eq. (4.17) into eq. (4.20) the following equation is obtained.

$$U_{cs}^2 = \varepsilon\left(1 + \frac{C_L}{C_D}\tan\psi\right)\frac{\mu_f - \frac{S}{S-1}\tan\theta}{\tan\psi - \frac{S}{S-1}\tan\theta}\cdot U_c^2 \quad \cdots\cdots (4.21)$$

Since the results for the experiments concerning critical tractive force on a steep flume in Chapter 3 were well explained by taking $C_D\ \varepsilon\ [1+(C_L/C_D)\tan\varphi] = 1.0$, this is applied here. Letting $C_D = 0.5$, $\tan\varphi = 1.0$, $\varepsilon\ (1 + 2C_L) = 2.0$ and eq. (4.21) becomes

$$U_{cs}^2 = \frac{2\left(\mu_f - \frac{S}{S-1}\tan\theta\right)}{1 - \frac{S}{S-1}\tan\theta}\cdot U_c^2 \quad \cdots\cdots (4.22)$$

Since the critical flow velocity U_c for initiating the transport is evaluated as the flow velocity at the crest of a particle, if we evaluate the ceasing critical flow velocity U_{cs} at the same height, the relation expressed by eq. (4.22) becomes:

$$U_{*cs}^2 = \frac{2\left(\mu_f - \frac{S}{S-1}\tan\theta\right)}{1 - \frac{S}{S-1}\tan\theta}\cdot U_{*c}^2 \quad \cdots\cdots (4.23)$$

Here U_{*cs} is the ceasing critical frictional velocity, U_{*c} is the initiating critical frictional velocity defined by the separated particle 0. According to the experimental results concerning Bagnold's μ_f, $\mu_f = 0.32 - 0.5$ and for the fully inertial range $\mu_f = 0.32$. Assuming $\mu_f = 0.5$ in Eq. 4.23, when $\tan\theta = 0$, $U_{*cs} = U_{*c}$. However, since $U_{*cs} < U_{*c}$ as is clear from the previous discussion, μ_f is expected to be less than 0.5. So here, from experimental results, the value is postulated to be $\mu_f = 0.425$. From eq. (4.23), the following equation is derived.

$$U_{*cs} = \alpha U_{*c} \qquad \cdots\cdots\cdots (4.24)$$

the values of α for each slope, letting S = 2.60, are those given in Table 4.1.

From eq. (4.19) the following equation is obtained.

$$U_b - \overline{V}_s = U_{cs} \qquad \cdots\cdots\cdots (4.25)$$

For a flat riverbed letting N be the volume of movable sand and V_s be the average transport velocity of the particles, q_B the sand discharge can be expressed as $q_B = N\overline{V}_s$. In general when there are ripples on a riverbed, especially when such ripples are formed in the lower regime, there is a separation region of the flow extending downstream a certain range from the crests of the ridges. In such sections there is no bed load present. Thus, as in Fig. 4.2, if one considers the wavelength λ of the ridge to be divided into a wake region λ_2 and a region λ_1, where bed load is present, then the sediment discharge q_B is given by

$$q_B = \frac{\lambda_1}{\lambda} N\overline{V}_s \qquad \cdots\cdots (4.26)$$

Putting eq. (4.25) into eq. (4.26), the following equation is obtained.

$$q_B = \frac{\lambda_1}{\lambda} N(U_b - U_{cs}) \qquad \cdots\cdots (4.27)$$

Table 4.1 Values of α for Different Gradients

$\tan\theta = i$	α	α^2
0	0.922	0.85
0.015	0.906	0.821
0.022	0.899	0.807
0.025	0.898	0.806
0.049	0.867	0.751
0.100	0.791	0.626

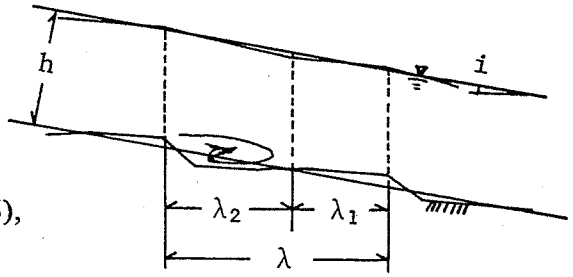

Fig. 4.2 A Typical Shape of Sand Wave

where, U_b is the flow velocity at the riverbed surface in the section λ_1. Writing the effective tractive force in section π_1 as τ_{o1}, the following equation in derived from equations (4.14), (4.15) and (4.16).

$$\tau_{o1} = N(\sigma - \rho)g\cos\theta \cdot \mu_f + K\tau_c \qquad \cdots\cdots\cdots (4.28)$$

Making use of the definition that separation distance is 0 for τ_c, and letting $K = \alpha^2$, and letting

$$U_{b_1} = \beta_1 U_{*1} \qquad \cdots\cdots\cdots (4.29)$$

the following can be obtained.

$$q_B = \frac{\lambda_1}{\lambda} \frac{\beta_1}{(S-1)g\cdot\cos\theta\cdot\mu_f} \cdot U_{*1}^3 \left(1 - \frac{\alpha^2\tau_{*c}}{\tau_{*_1}}\right)\left(1 - \alpha\sqrt{\frac{\tau_{*c}}{\tau_{*_1}}}\right)$$

$$\cdots\cdots\cdots (4.30)$$

In equation (4.30) the values of λ_1/λ, U_{*1}, and β_1 are unknown, and it is necessary to estimate them. If the shapes of bed ripples are known, they can be calculated, but at the present stage there are difficulties in postulating such shapes so the bed load transport rate above the ripples will not be discussed hereinafter.

First, consider the case of flat bed with a mild slope. In such cases a logarithmic law is applicable to flow velocity distribution.

$$\beta_1 = 8.5 + 2.5\cdot\ell n\frac{y}{k_s} \qquad \cdots\cdots\cdots (4.31)$$

$$\cdots\cdots (4.31)$$

Here, y is the height agove the theoretical riverbed surface, K_s is the relative roughness. Taking the particle diameter d of bed material as K_s, the theoretical riverbed surface lies 0.25d below the crest of a particle for a gently sloped flume. Since the height at which β_1 is evaluated is that of the crest of the particle as explained above, y = 0.25, and finally from eq. (4.31) we obtain $\beta_1 = 5.03$. Considering $\tan\theta \approx 0$ for a gently sloped flume, and because $\alpha \fallingdotseq 0.92$, the sediment discharge equation, for a flat bed, letting $\lambda_1/\lambda = 1$, becomes

$$\Phi = 12\tau_*^{3/2}\left(1 - 0.85\frac{\tau_{*c}}{\tau_*}\right)\left(1 - 0.92\sqrt{\frac{\tau_{*c}}{\tau_*}}\right) \qquad \cdots\cdots\cdots (4.32)$$

Fig. 4.3 is a comparison of equation (4.32) with the conventional experimental results[9] for a flat bed. The degree of the agreement is good, where τ_{*c} is let equal to 0.04.

(2) Bed load transport rate in a steeply sloped flume

The above is the case for a comparatively mild slope. When the bed slope is steep the influences of α in equation (4.30), of the fact that the critical tractive force becomes great, and of β_1 varying due to the variation of the resistance law, all become important, and the curve of Fig. 4.3 is likely to change.

As reported in Chapter 2, the frictional resistance coefficient f, according to experiments for resistance on a steep slope, is a function of d/h and τ_*, and it becomes extremely large compared with that for mild slopes. Also, according to actual observations of flow velocity distribution, near the bed surface there is a uniform flow velocity region (of thickness δ), and above it there is a logarithmic distribution rule with K = 0.4, i.e. for $y \leqslant \delta$

$$\frac{U}{U_*} = A + \psi \cdot 1n\frac{y}{\delta} \qquad \cdots\cdots\cdots (4.33)$$

for $y > \delta$

$$\frac{U}{U_*} = A + \frac{1}{\kappa} \cdot 1n\frac{y}{\delta} \qquad \cdots\cdots\cdots (4.34)$$

In the range $\delta/h \leqslant 1.0$, finding the resistance coefficient from eq. (4.34) or eq. (4.33), the following is obtained.

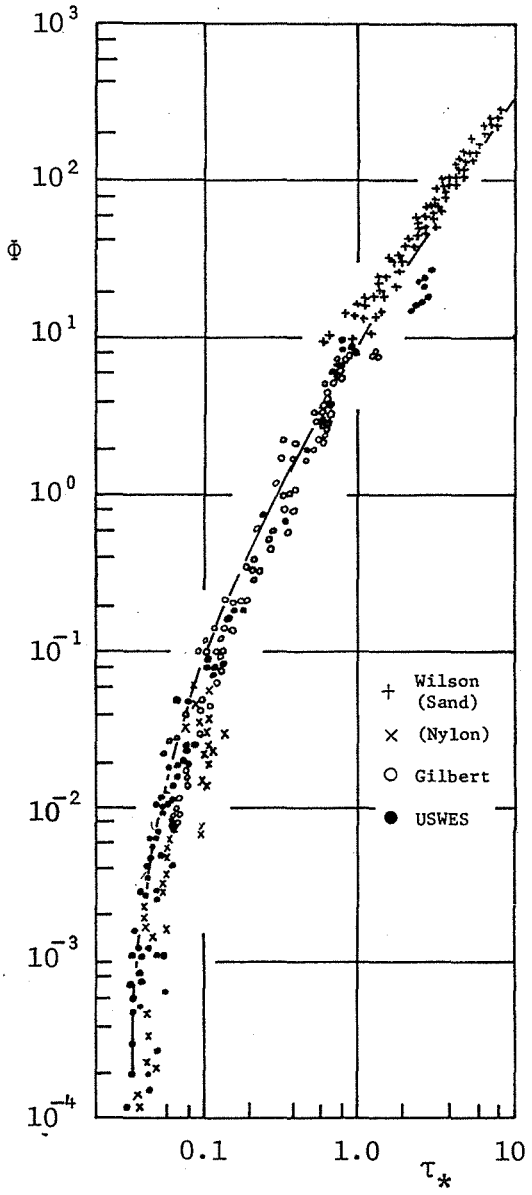

Fig. 4.3 A Comparison of Bed Load Transport Rate on a Flat Bed and Equation (4.32)

$$\sqrt{\frac{8}{f}} = A - 2.5\left(1 - \frac{\delta}{h}\right) - \psi\frac{\delta}{h} - 2.5 \cdot 1n\frac{\delta}{h} \qquad \cdots\cdots\cdots (4.35)$$

Since f is a function of τ_* and the relative depth d/h, in the final analysis it is expected that A, δ, ϕ are functions of the relative water depth and τ_*, or of the slope and τ_*. However, because the range of experimental data is limited, it is difficult to discuss the nature of the variation characteristics of A, ϕ, and δ in general. Here, as in Chapter 2, we assume $\phi = 0.87$, and $\delta = 0.8d$ are assumed. Using equations (4.33) and (4.35) and the resistance coefficient from Fig. 2.11 at a height y = 0.15d, we can find values of β_1 are obtained from equation (4.30). Fig. 4.4 gives the results of these calculations

Here Fig. 4.4 corresponds to the following equation which well explains the bed load transport rate for a steeply sloped blume (See below).

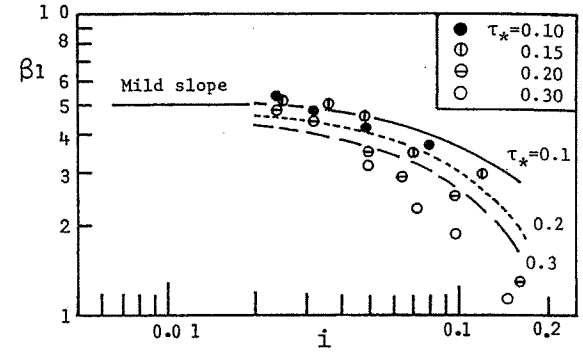

Fig. 4.4 Calculated Values of β_1

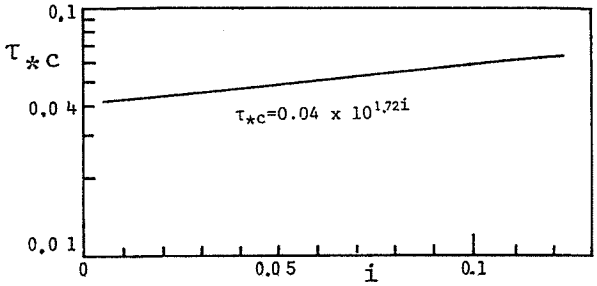

Fig. 4.5 The Change of Critical Tractive Force for Bed Slope of Different Gradients

$$\beta_1 = (5 - 10\sqrt{i})\tau_*^{-\sqrt{i}} \quad \cdots\cdots\cdots (4.36)$$

$$\cdots\cdots (4.36)$$

Equation (4.36), as can be seen from Fig. 4.4, well explains the bed load transport rate for $i > 0.05$. Also, the variation of τ_{*c} due to slope, from Chapter 3's experimental results, corresponds to eq. (4.37), shown in Fig. 4.5, (provided $\sigma/\rho = 2.60$, $\tan\varphi = 1.0$, and $i = \tan\theta$.)

$$\tau_{*c} = 0.04 \times 10^{1.72i} \quad \cdots\cdots\cdots (4.37)$$

$$\cdots\cdots (4.37)$$

Accordingly, the bed load equation for a steeply sloped flat riverbed is

$$\Phi = \frac{12 - 24\sqrt{i}}{\cos\theta} \cdot \tau_*^{(1.5-\sqrt{i})} \left(1 - \alpha^2 \frac{\tau_{*c}}{\tau_*}\right)\left(1 - \alpha\sqrt{\frac{\tau_{*c}}{\tau_*}}\right)$$

$$\cdots\cdots\cdots (4.38)$$

Plotting the equation (4.38) with the author's experimental values gives Fig. 4.6.

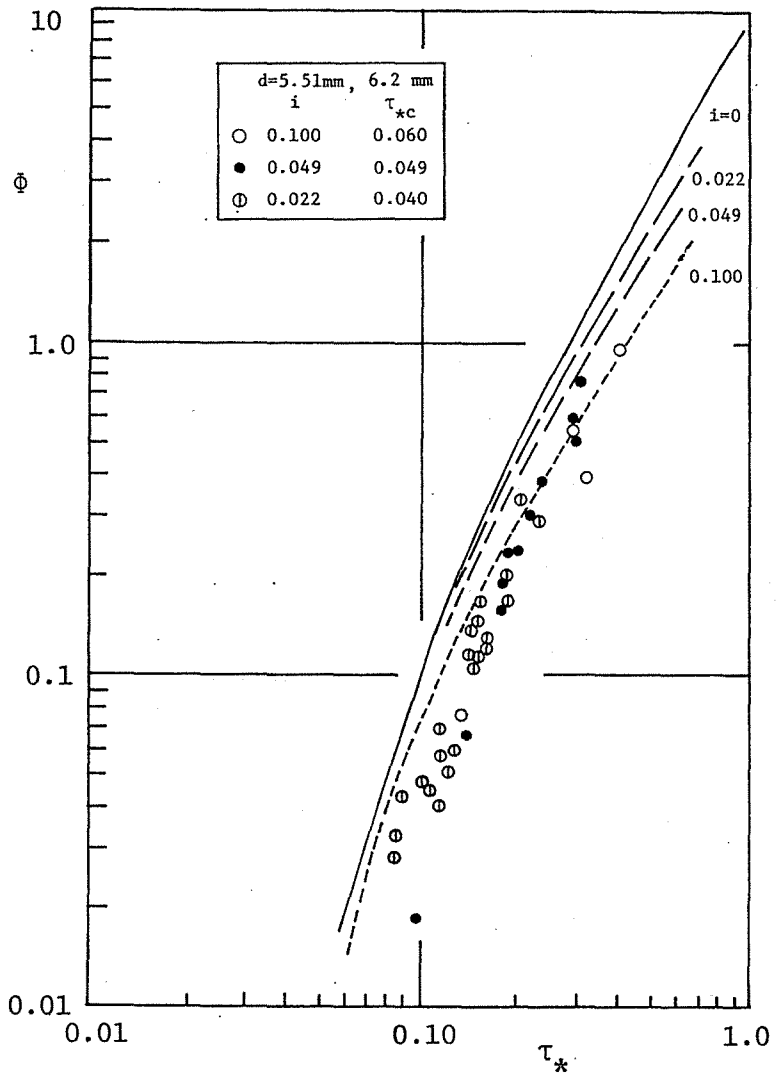

Fig. 4.6 A Comparison of Bed Load Transport Rate on a Steeply Sloped Flume and Equation (4.38)

Eq. (4.38) does not fit the experimental values well for $i_o = 0.022$, but it gives a mostly satistactory result.

Section 3: Bed Load Transport Rate for Gravel Mixture

(1) Critical tractive force for ceasing the transport of gravel mixture

According to experiments on the initiating critical tractive force for transport of gravel mixture, the critical tractive force is nearly a constant irrespective of grain diameter for $d_i/d_m < 1$, and it increases with grain diameter for $d_i/d_m > 1$.

Accordingly, under constant hydraulic conditions, it is impossible that the tractive force corresponding nearly to that at the threshold of transport acts on indivudual grains of different diameters stationary on the bed surface, and the equilibrium of bed load can not occur if a tractive force acting on the bed material is within that at the threshold of transport for each grain diameter.

Fig. 4.7 is a comparison of experimental result by Hirano, Ashida and Michiue with the theoretical result obtained by incorporating the modified Egiazaroff equation into Sato-Yoshikawa-Ashida's equation[4]. They are in good agreement for $d_i/d_m < 0.7$; the experimental values are greater than calculated values for $d_i/d_m \geqslant 0.7$, and as d_i/d_m increases the agreement worsens. This indicates that the method of incorporating the modified Egiazaroff equation into the bed load equation for gravel mixture as the critical tractive force in the bed load equation is in appropriate. In bed load transport experiments for gravel mixture, it has been observed that large particles do not easily exchange with bed material, but they continue to move. These facts specially suggest that the critical tractive force for ceasing the transport of particles having a diameter greater than the mean diameter is smaller than the critical tractive force for initiating the transport. Consider the tractive force transmitted from the flow to bed, in the same way as for uniform gravel, as becoming the critical tractive force for ceasing and as causing the equilibrium of bed load to be maintained. If that is so, the condition that bed load must be in

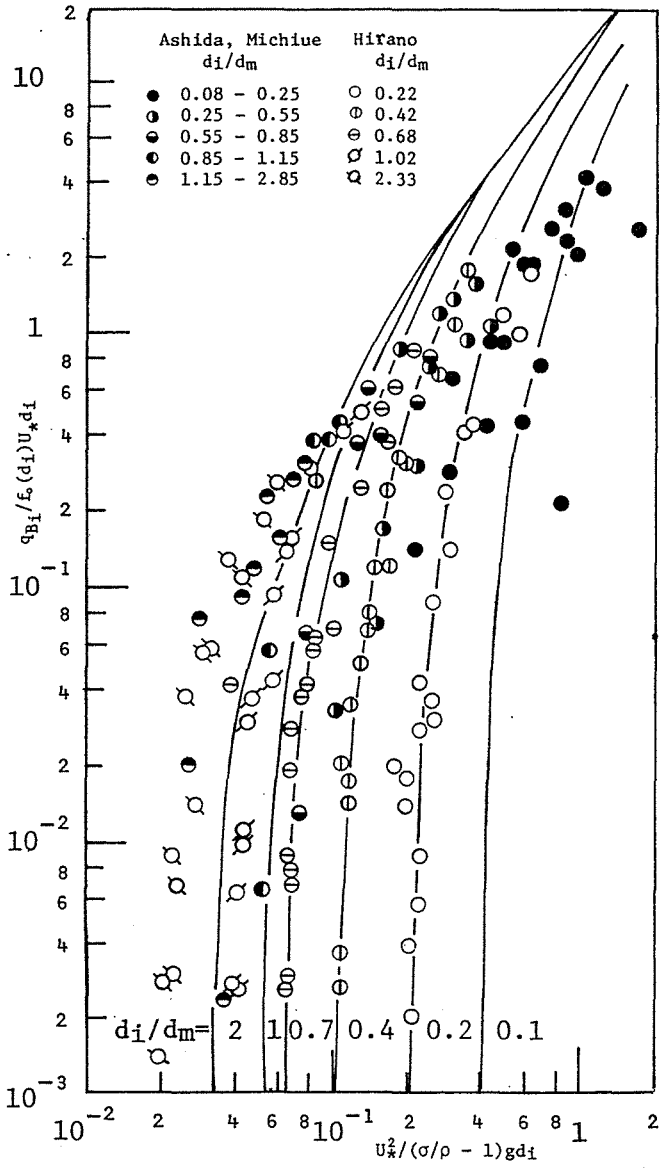

Fig. 4.7 A Comparison of Experimental Values of Critical Tractive Force for Gravel Mixture and Its Calculated Values

equilibrium for each different diameter requires the critical tractive forces for ceasing the transport of individual different size particles to be smaller than the critical tractive force for initiating the transport and also to be equal to each other irrespective of grain diameter. Thus, the experiments were carried out to determine the critical tractive force at the threshold of ceasing the transport.

A rigid bed was made by spreading uniform sand of 3.5 mm in diameter (k) 1 cm thick in a 17 m long and 50 cm wide variable slope water flume, and then varnished. Here, taking the value for gravel mixture bed as equivalent to the value for a uniform gravel bed whose mean diameter equal to that of gravel mixture is based on the experimental result related in Chapter 2 that if they are equal in mean diameter, they are also the same in degree of bed roughness independent of grain size distribution. This time the observed roughness ($\triangle\overline{Z}$) from radius pitch was 1.59 mm. Sand was dropped a particle at a time on to the rigid bed surface, and the transport velocity ($\overline{V}_{si}$) was observed by following each particle. The ceasing threshhold was defined as the friction velocity, at which the transport velocity becomes zero on a graph of the average transport velocity versus the friction velocity. It is determined from the graph by means of exterpolation.

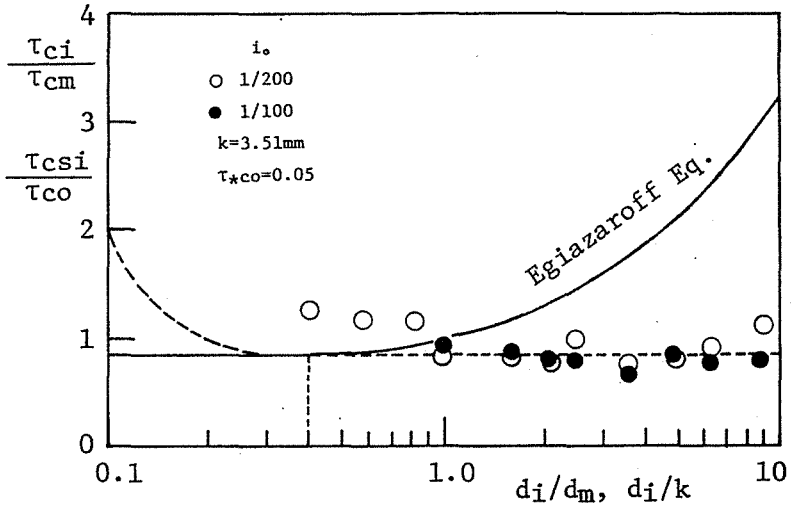

Fig. 4.8 Critical Tractive Force for Ceasing the Transport of Gravel Mixture Particles by Grain Diameters

Fig. 4.8 indicates the results along with Egiazaroff's transport threshold for each diameter. From the graph it can be seen that the critical tractive force for the initiation is nearly constant independent of diameter. Further, for $d_i/d_m < 1$ an effect of the rigid bed appears and the sand grains are caught by troughs of the rough bed surface and the ceasing critical tractive force becomes greater. However, for a movable bed, thinking along the same lines as for the modified Egiazaroff equation, the initiating threshold can be considered to be in agreement with the ceasing threshold of the mean diameter since as long as the larger particles are in transport the hiding effect almost vanishes.

(2) Bed load equation for gravel mixture

As reported above, it was confirmed that the ceasing critical tractive orce for gravel mixture is nearly constant independent of diameter. Thus, the same method used in Chapter 2 is applied to examine the bed load equation for gravel mixture on a flat bed.

$$U_{bi} - \overline{V}_{si} = U_{csi} \qquad \cdots\cdots\cdots (4.39)$$

The bed load q_{Bi} for each diameter is:

$$q_{B_i} = N_i \overline{V}_{si} \qquad \cdots\cdots\cdots (4.40)$$

Here U_{bi} is the flow velocity acting on particles of diameter d_i which is a value independent of diameter if it is evaluated at the crest of bed surface similarly to the case of uniform gravel. $\overline{V}_{si}$ is the average velocity of transporting particles of diameter d_i. U_{csi} is the average velocity at the ceasing threshold for d_i. N_i is the amount of particles of diameter d_i transported per unit area. Accordingly, the following equation is obtained.

$$\tau_o = \sum_i N_i(\sigma - \rho)g\cos\theta \cdot \mu_{fi} + K\tau_{cm} \qquad \cdots\cdots\cdots (4.41)$$

Here, τ_{cm} is the critical tractive force for initiating the transport of particles of the mean diameter. Provided $k\tau_{cm}$ is nearly equal to the ceasing critical tractive force, $k = \alpha^2$ and $\alpha^2 = 0.85$ are obtained from Fig. 4.8 in a milder slope, the value is the same as for uniform gravel. The degree of bed roughness was the same for both uniform gravel and gravel mixture in case the average diameter is normalized. Although the coefficient of dynamic friction μ_{fi} is presupposed to vary with diameter, here it is taken to be constant for all diameters and assumed equal to a value of 0.425 in the case of uniform gravel.

Further, concerning the number of movable particles of diameter d_i per unit area, for a selective discharge in which especially large particles do not move, the number is presupposed to be unrelated to the grain size distribution of the bed material. However, here the condition is first considered that the largest particles are also in motion, and assuming the number to be proportional to $f_o(d_i)$, the percentage of particles of diameter d_i which occupies part of the bed material.

$$N_i = f_o(d_i)\sum_i N_i \qquad \cdots\cdots\cdots (4.42)$$

Equation (4.41) becomes

$$\tau_o = \frac{N_i}{f_o(d_i)}(\sigma - \rho)g\cos\theta \cdot \mu_f + \alpha^2\tau_{cm} \qquad \cdots\cdots\cdots (4.43)$$

From equations (4.31) and (4.32) we get

$$q_{Bi} = \frac{\tau_o - \alpha^2 \tau_{cm}}{(\sigma - \rho) g \cos\theta \cdot \mu_f} (U_b - U_{csi}) f_o(d_i) \qquad \cdots\cdots\cdots (4.44)$$

Since the height at which both U_b and U_{csi} are evaluated are that of the crest of a particle in the bed, the following equation can be obtained.

$$U_b - U_{csi} = \beta_1 (U_* - U_{*csi}) \qquad \cdots\cdots\cdots (4.45)$$

Equation (4.44) is transformed into the following.

$$\frac{\Phi_i}{f_o(d_i)} \left(\frac{d_i}{d_m}\right)^{3/2} = \frac{\beta_1}{\cos\theta \cdot \mu_f} \cdot \tau_{*m}^{3/2} \cdot \left(1 - \alpha^2 \frac{\tau_{*cm}}{\tau_{*m}}\right) \left(1 - \alpha \sqrt{\frac{\tau_{*cm}}{\tau_{*m}}}\right)$$

$$\cdots\cdots\cdots (4.46)$$

Here $\Phi_i = q_{Bi} / \{(\delta/\rho - 1) g d_i^3\}^{1/2}$ and

$\tau_{*m} = U_*^2 / (\delta/\rho - 1) g d_m$

The value of coefficient β_1 in eq. (4.46) can be considered the same as for uniform gravel from the fact that the bed roughness is the same as for uniform gravel.

Thus, the following equation is obtained.

$$\frac{\Phi_i}{f_o(d_i)} \left(\frac{d_i}{d_m}\right)^{3/2} = \frac{12 - 24\sqrt{i}}{\cos\theta} \cdot \tau_{*m}^{(1.5 - \sqrt{i})} \left(1 - \alpha^2 \frac{\tau_{*cm}}{\tau_{*m}}\right)$$

$$\times \left(1 - \alpha \sqrt{\frac{\tau_{*cm}}{\tau_{*m}}}\right) \qquad \cdots\cdots\cdots (4.47)$$

This equation can be transformed as follows.

$$\Phi = \frac{12 - 24\sqrt{i}}{\cos\theta} \cdot \tau_{*m}^{(1.5 - \sqrt{i})} \left(1 - \alpha^2 \frac{\tau_{*cm}}{\tau_{*m}}\right) \left(1 - \alpha \sqrt{\frac{\tau_{*cm}}{\tau_{*m}}}\right)$$

$$\cdots\cdots (4.48)$$

$$q_{Bi} = q_B \cdot f(d_i) \qquad \cdots\cdots\cdots (4.49)$$

The bed load transport rate can be determined by deriving the overall bed load transport rate from equation (4.48) for the mean diameter, then taking the value of d_i/d_m.

Considering first the case of a mild slope, assuming $i \fallingdotseq 0$ and $\alpha^2 = 0.85$, Fig. 4.9 can be obtained from the data of Fig. 4.7. Equation (4.47) explains the experimental results well. More precisely, τ_{*cm} varies according to $\sqrt{d_{84}/d_{16}}$ as discussed in Chapter 3, but here the value $\tau_{*cm} = 0.05$ is employed.

Next, for the case of a steep slope, assume the influence of slope on critical tractive force for gravel mixture can be expressed the same as for uniform gravel. In Fig. 4.10 values from equation (4.48) and the author's experimental values for the mean diameter 6.40 mm $\sqrt{d_{84}/d_{16}} = 3.45$, and the mean diameter 7.6 mm $\sqrt{d_{84}/d_{16}} = 4.83$ are shown.

Further, Fig. 4.11 is an example of the grain size distribution of bed load and that of bed material. The dispersion is great, but the homogeneousness is good which indicates the argument is appropriate.

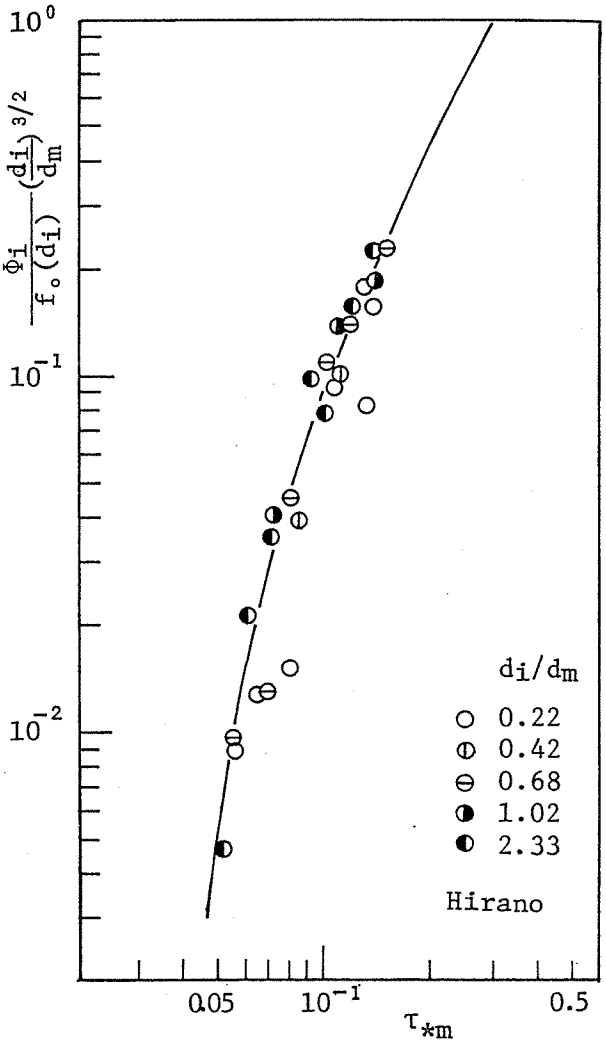

Fig. 4.9 A Comparison of Bed Load Transport Rate for Gravel Mixture and Equation (4.47)

Section 4: Time Variation of Bed Load Transport Rate for Gravel Mixture

The average bed load transport rate for gravel mixture can be expressed as equation (4.48) or equation (4.49). However, if one finds the bed load transport rate or short time intervals experimentally, or observes the bed load transport rate every mo-

ment, the grain size distribution of bed load expressed as equation (4.49) is not necessarily equal to that of bed material, but it seems cyclically to become rough and fine. So, using a gravel mixture having the grain size distribution shown in Fig. 4.12, further examinations were made concerning bed load transport rate for gravel mixture.

First, consider the coarsening of bed load to occur in the beginning of water supply. This phenomenon is called a selection of sand particles. For example, Kinoshita[11] reports on sand discharge in the case of bars formation, "In the beginning of coarse-grained particles of bed load are transported, and as time passes they diminish, and instead transport of the next largest diameter particles follows."

Figures 4.13 and 4.14 show, respectively, the grain size distribution and transport rate of the bed load for the case of sand used in the experiments designated "A" in Fig. 4.12, where sediment in transport coarsens in the beginning of water supply.

These experiments were carried out on a channel of width 20 cm. These graphs prove that large diameter particles are transported at a rate nearly equal to the rate of their presence in the bed material, and that almost no small diameter particles are discharged at all. In this way, one can consider a difference in transport velocity for each diameter to be the reason that in the beginning of water supply coarse grained particles are transported while fine grained ones

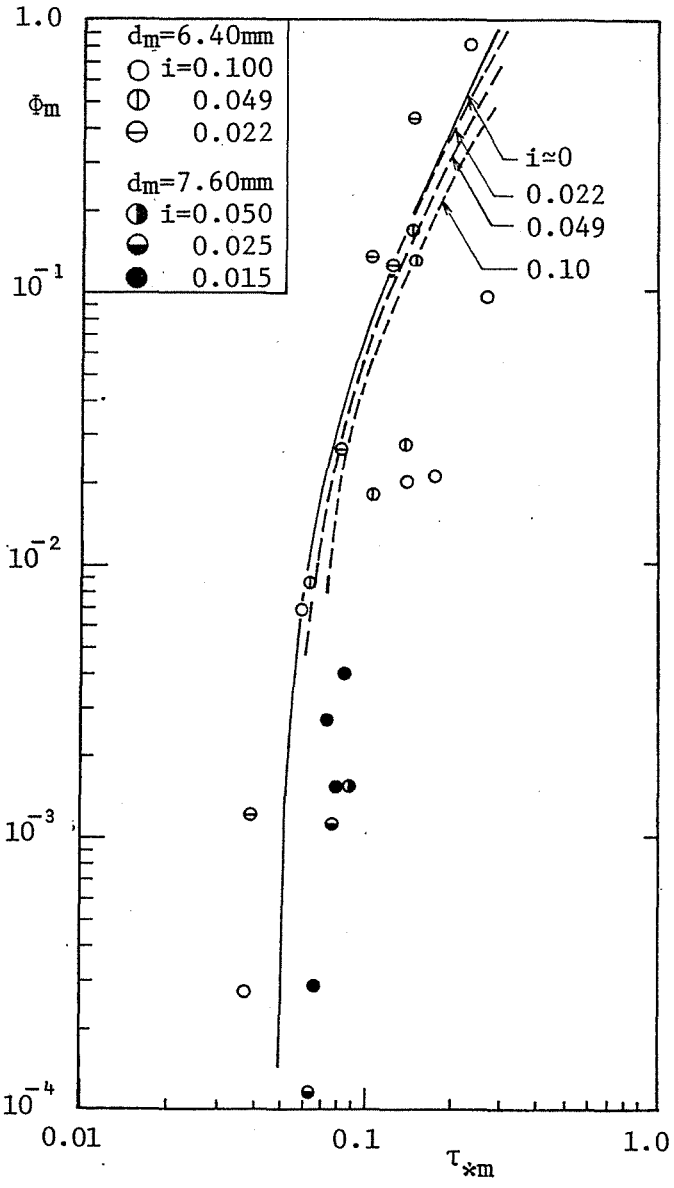

Fig. 4.10 Bed Load Transport Rate for Gravel Mixture on a Steeply Sloped Flume

are not. Thus, using gravel mixture of minimum diameter 0.74 mm, and of maximum diameter 16 mm, indicated as "B" in Fig. 4.12, the gravel transport forms were observed from the side. The gravel mixture was color coded for each diameter, and photographs were taken and analyzed of sand movement in a channel whose slope was varied between 0.02 and 0.15. The gravel was spread 20 cm wide, 9 cm thick and 6.7 m long. There was no sand supply. There follows a summary of the observations through the experiment.

a. When the crest of a movable particle, in the case where tractive force is not particularly large, is only a diameter distant from the bed surface, and the gravel transport forms where gravel moves above the rigid bed having the roughness being on the order of the mean diameter.

b. The velocity of the particles in transport is essentially the same independent of diameter.

c. When the largest particles move the smaller particles fall down and are hidden by the larger ones. When making observations from the side, in the beginning of water supply almost no small particles in transport could be seen, and even when they do move they soon go in bed troughs or wake regions of gravel on the bed surface, thereby making them difficult to move.

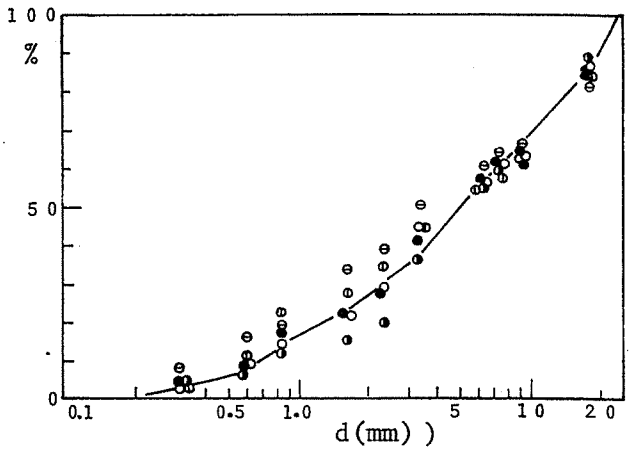

Fig. 4.11 Grain Size Distribution of Bed Material and That of Bed Load

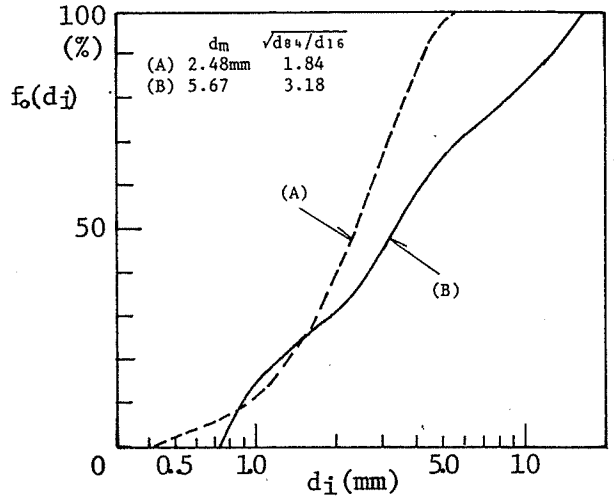

Fig. 4.12 Grain Size Distribution of Sand Materials used in the Experiments

d. When the tractive force and slope increase, (in these experiments $i_o > 0.1$, $\tau_*m > 0.33$) the particles, rather than moving independently, the medium size particles begin to move buried in the larger moving particles, and the coarsening of transported particles mentioned above is extremely pertinent.

The falling of smaller particles within gravel mixture in this way has been studied by Daido[12] in relation to mud flow. Here we see this phenomenon occurs for bed load also. It seems this phenomenon becomes more noticeable as the grain diameter distribution becomes wider.

The above observations prove that the coarsening of movable particles is due to the effect that smaller particles are hidden by larger particles. So, evaluating this hiding effect by the term $\alpha^2 \tau_*cm$ in eq. (4.48), and finding this from Fig. 4.14, one gets τ_{ci} indicated in 4.15. This shows a trend that for $d_i/d_m < 0.4$, as for the Egiazaroff Equation, the smaller the particle the more difficult it is to trransport. On account of this selection phenomenon the grain size distribution of the bed material and that of bed load vary every moment, but taking the average value of a certain considerable time duration both distributions are in agreement with each other. However, the rate of bed deformation is probably different from that calculated on the average. Fig. 4.16 is one example of bed load trnansport rate by diameter.

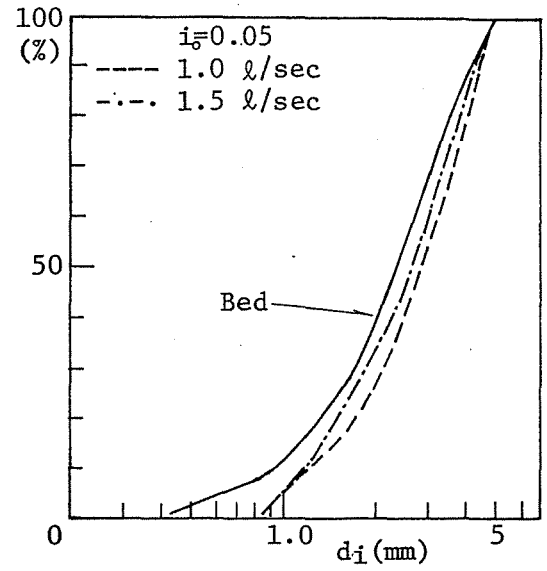

Fig. 4.13 Grain Size Distribution of Sand Materials in the Beginning of Water Supply

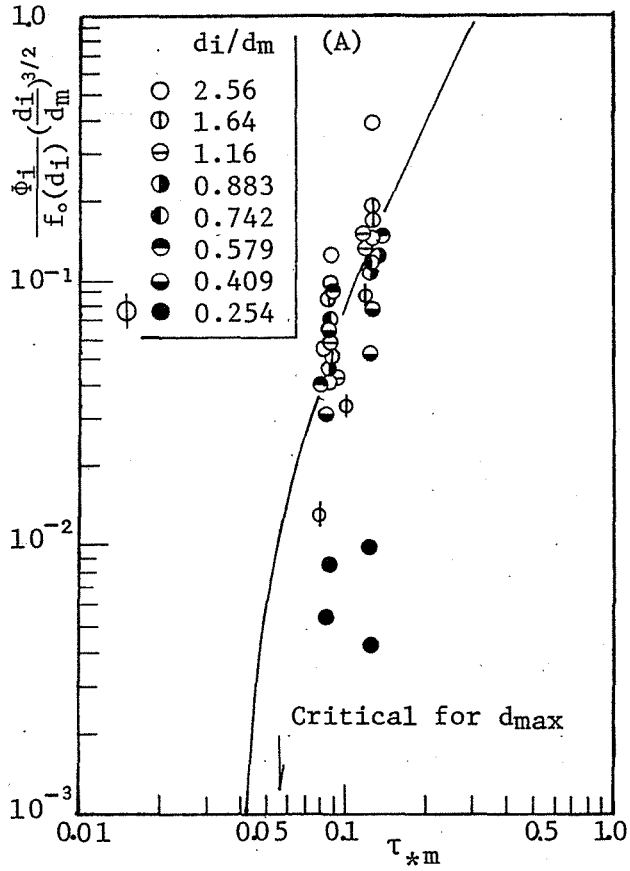

Fig. 4.14 Bed Load Transport Rate in the Beginning of Water Supply

The above is largely the case of transport of gravel particles of all diameters including the largest ones. Next, to the case of particles below a certain grain size moving while larger stationary particles are present, equation (4.47) is also applicable provided that the bed load is in an equilibrium condition. It can be said to be so from the fact if includes such data as in Fig. 4.9. However, as the percentage of contained unmovable particles increases it seems a hiding effect will appear. Here the percentage of contained unmovable particles is varied from 0%, 5% and 10% (the weight percentage), and the variation of sand discharge by diameter was checked.

In Fig. 4.17 since the amount of data obtainable is limited, it is difficult to make out a definitive conclusion, but the two cases of 0% and 5% unmovable particles are the same in sand discharge while for 10% the sand discharge becomes fairly smaller. From this it is found that large gravel which is often seen in mountain stream beds is not simply functioning as roughness, but also has the possibility of having a hiding effect when its percentage increases.

Next, in case where unmovable particles are present, the actual tractive force is smaller than the critical tractive force for initiating the transport of the largest particles, and there is little or no supplied sand from the upper stream, the bed roughness is coarsened with time and the so called armour coat is formed. To such cases where the sediment is not in equilibrium, equation

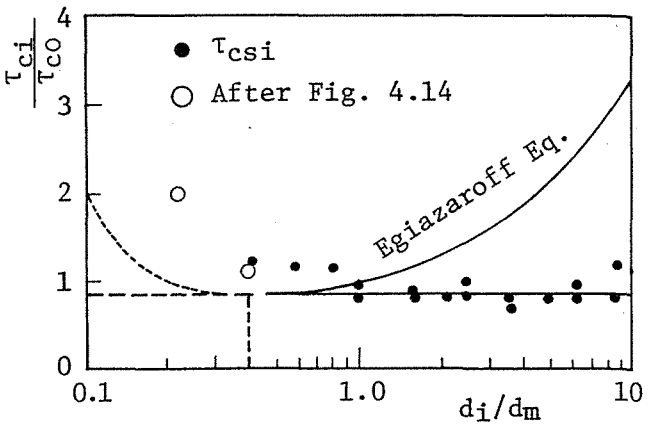

Fig. 4.15 The Critical Tractive Force Obtained from Fig. 4.14

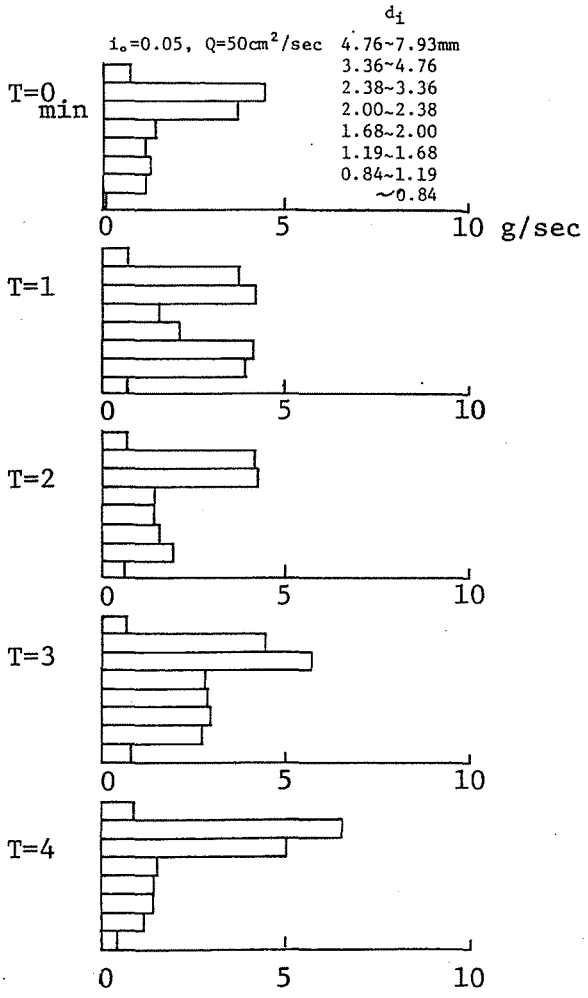

Fig. 4.16 Time Variation of Bed Load Transport Rate for Different Grain Diameters

(4.47) can not apply. Further, in a channel of finite length when armour coat has advanced from upstream over a long time period and the sediment in the lower stream extremity is nearly in equilibrium, equation (4.47) can apply to the case. However, even in that case equation (4.47) is not valid for the largest particles. The tractive force domain in which armour coats form is typically indicated with domain A of Fig. 4.18 between the transport threshold for the largest particles and the ceasing threshold. From the above observations, Ashida, Michiue[5] and Hirano's[6] examinations of tracing the process of the formation of armour coats using equation (4.13) and similar equations are considered expedients, and the reason why there arose no problem with their examinations is considered to be due to the phenomenon that the armour coat formation was carried out mainly by particles smaller than the mean diameter.

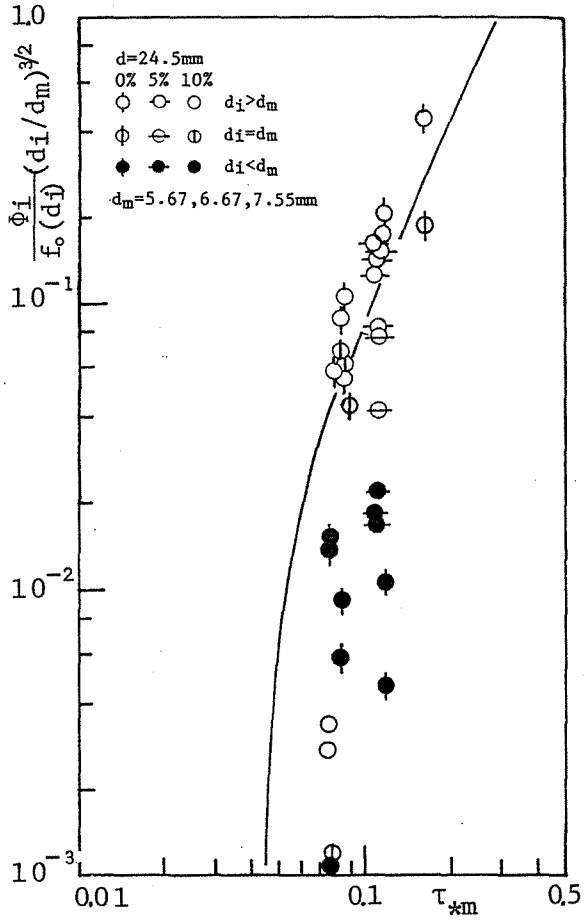

Fig. 4.17 The Hiding Effect of Unmovable Gravel Particles

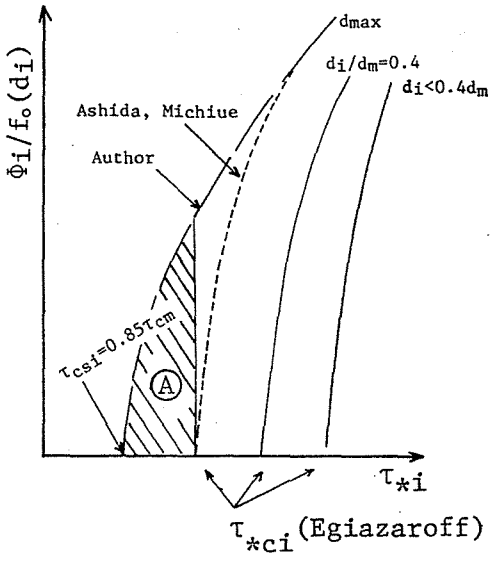

Fig. 4.18 A Conceptual Scheme of an Armour Coat Formation Region

Section 5: Conclusion

This chapter has been oriented toward bed load transport rate for uniform gravel and that for gravel mixture in a steeply sloped channel.

First, section 1 gave representative conventional bed load equations and offered explanation of them, and then indicated that a bed load equation applicable to mountain streams, where a steep slope and wide grain size distribution of bed materials must be taken into account, had not yet been proposed.

Section 2, using Bagnold's model as a base, derived a new bed load equation which is available well with the conventional data. And, using the results of critical tractive force and resistance law from Chapters 2 and 3, section 2 proposed another bed load equation for a steep slope which is in good agreement with the author's experimental values.

Section 3 examined a bed load equation for gravel mixture. First, experiments were carried out on the ceasing critical tractive force for the gravel, and from these experiments it was proved that the force is a constant value independent of grain diameter. From the analysis of these results, a new bed load equation for gravel mixture under equilibrium condition was offered assuming the critical tractive force to be constant. This equation fits the experimental values better than the conventional bed load equations by diameter. Also, one equation was proposed for a steep slope which is in satisfactory agreement with the author's experimental values.

Section 4 examined the bed load transport rate for gravel mixture in greater detail. During transport smaller particles are hidden by larger particles. That elucidates the marked appearance of coarsening sediment in the beginning of water supply. Also, evaluating this hiding effect in terms of the critical tractive force in the bed load equation, the result is obtained for $d_i/d_m < 0.4$, as for Egiazaroff equation, the smaller the particle the greater the critical tractive force is. Next, the influence of unmovable large particles on bed load transport rate was investigated and it was found that as the percentage of contained unmovable particles increases, a hiding effect arises and the transport rate decreases. Finally, an explanation of armour coat formation was added.

There are a number of problems remaining with the above investigations, but new equations were found applicable to mountain rivers characterized by gravel mixture bed and steep slope.

REFERENCES

1) Einstein, H.A.:
"The Bed-Load Function for Sediment Transport", IAHR, Stockholm, 1948.
2) Kalinske, A.A.:
"Movement of Sediment as Bed Load in Rivers", Trans. A.G.U. Vol. 28, No. 4, 1947, pp. 615-620.
3) Meyer-Peter, Müller:
"Formulas for Bed Load Transport", IAHR, Stockholm, 1948.
4) Kazuo Ashida, and Masanori Michiue:
"A Fundamental Study of Resistance of a Flow on a Movable Bed and Bed Load Transport Rate", JSCE, Professional paper 206, Oct. 1972, 59-69.
5) Kazuo Ashida, and Masanori Michiue:
"Sediment Transport Rate and Bed Transformation", the Disaster Prevention Laboratory of the Kyoto University, Annual Report 14-B, 1971.
6) Muneo Hirano:
"On the Bed Lowering accompanying Armouring", JSCE, Professional paper 195, Nov. 1971.
7) Hiroshi Asada:
"Some Ways of Technical Consideration on Sediment Transport in Mountain Rivers", the SHIN-SABO 89, Nov. 1973, pp. 4-13.
8) Ed. by the Sub-Committee for flow resistance on a movable bed and bed form in Hydraulic Committee of JSCE:
"Bed Transport Forms and Roughness of Bed Material in a Flow on a Movable Bed", Professional paper 210, 1973.
9) Bagnold, R.A.:
"The Flow of Cohesionless Grains in Fluids, Philosophical Trans. Royal Society of London, Vol. 249, 1957.
10) Paintal, A.S.:
"A Stochastic Model of Bed Load Transport, Jour. of Hydraulic Research, 9, No. 4, 1971, pp. 527-554.
11) Ryosaku Kinoshita:
"Bed Transformation Survey in the Ishikari River", the Natural Resources Bureau of the Science and Technology Agency, Professional material 36, pp. 527-554, 1961.
12) Atsuyuki Daido:
"A Phenomenon of Selecting Gravel Transport with Water", JSCE, 30th annual summary of lecture, 1975, II-157.

CHAPTER 5 APPLICATION OF STUDIES IN THE PREVIOUS CHAPTERS TO EROSION CONTROL PLANNING

Section 1: Outline

This Chapter considers problems of applying the results of research on bed load transport rate, critical tractive force, resistance law for a stream, and channel pattern of mountain rivers presented in the previous chapters to erosion control planning.

Erosion control planning is, ideally, a complete treatment of sand's behavior in all parts of a stream area, from production of mud flow in upstream areas to erosion at the ocean's shores. However, considering just the amount of sediment supplied from the upper stream, there are many problems for which it is very difficult to make accurate predictions for planning purposes. These include probabilistic phenomena such as land collapse and mud-flows, and production of large amounts of sediment from such phenomena. Futher in order to make a prediction of sediment supply within the basin, many problems must be resolved. Accordingly, planning erosion control for an entire drainage system is the ideal, but it must be said the actual conditions are extremely difficult.

However, it is important to aim at establishing more reasonable erosion control policy, using fundamental knowledge such as discussed in this thesis, even for partial planning within a drainage system.

A representative example one can consider hydrologically is river bed deformation, in a channel section of finite length, for caused when sediment is no longer supplied from upstream because of a dam. In conventional research on such case, the object of investigation was formation of an armour coat or river bed lowering. In erosion control, there are many cases when channel works are planned to fix the channel in a farm area. Especially recently there are many instances of executing channel works as repair which were small rivers 1 – 2m wide, work in areas, where mud flow occurred. In such cases, first, how much should it be widened, and next, what level of construction is necessary to allow the planned discharge to flow safely downstream. One can consider applying the present research to such problems.

Further, one can consider sediment discharge from comparatively flat sandy exposed slopes. One can not find the sediment discharge from exposed slopes if the gully pattern is not understood. However, in downstream slope areas comparatively stable gullies are formed which do not change much from year to year. In such places, given information on rainfall, slope and materials of the incline, one can determine the amount of flow from an appropriate runoff analysis and, applying the results of this study, determine the water depth and channel width. If one assumes that the slope does not vary much and that there is sufficient sand capable of being transported, one can calculate the sediment outflow.

One can also discuss the regulating effect of an erosin control dam. It is said that in general the slope of a dune from mud-flow is 3° to 5°. One can study what type of channel is formed on the lobe for subsequent flood waters and how much sediment flows out.

In these ways the present research can apply to important portion of erosion control planning; the next section examines applications particularly to channel works planning.

Section 2: Application to Channel Works Planning[1)]

The aim and methods of executing channel works are summarized by Tabata and Abe,[2)] but conceptions vary from person to person. The places where many channel works are built are fan areas where sediment has been deposited as a result of vigorous sediment transport from upstream mountain areas. They are sediment deposit regions when viewed from the perspective of sediment balance for the entire drainage system. Accordingly, the channel within a fan area is unstable. A high degree of river bed lowering and channel deformation imply a 2 dimensional outflow of deposited sediment and they exert a deteriorating influence on the river downstream. Also, in mountain regions the fan areas are really the only habitable areas available. Channel deformation or flood not only means the loss of habitable areas, but in such places these assailants possess an enormous momentary destructive force which sometimes cause disasters involving losss of human life. Disaster prevention methods for such areas must include, first, the prevention of floods and torrential outflows such as mud-flows from the upper stream, and next, safe drainage of flood wasters along with prevention of erosion and fixation of the channel. Accordingly, execution beforehand of measures to prevent dangerous sediment outflow from the upstream region is a precondition in order to make it fulfill its function adequately. According to River Erosion Control Technical Standards, design prerequisites are, "In the upstream extremity of a channel works planning region a check dam, as a rule, is required;" "The flood discharge considered in planning a channel works must be the flood discharge reduced by the percentage of sediment included, since erosion control works are assumed to be completed beforehand."

If the sand supply to a channel which is nearly in equilibrium, allowing the outflow of upstream sediment to flow downstream or the channel to deform over and over, is suspended, the channel will begin to move to a new equilibrium position. However, provided one presupposes a new equilibrium condition in advance, forms a new appropriate channel, and then stops the sand supply, erosion can be prevented and a design flood supply can be accepted safely. The purpose of planning the function of a channel works is to design a stable and safe channel within the limits set by the length of the work section and the elevations of the upper and lower ends of the stream.

(1) The width of a channel works

A channel works' width must be wide enough to be able to prevent both banks from being eroded by a design flood easily and narrow enough so that the water does not meander within the channel. Provided such an appropriate width is utilized, construction of very strong revetments becomes unnecessary, as was pointed out in Chapter 1 concerning a stable channel section, for regime rivers the channel width is proportional to the 1/2 power of the flow discharge. This relationship, as shown in Fig. 1.6, can apply to a very wide range of flow discharge, from a small discharge in the experimental water channel to a large

volume in actual rivers, irrespective of bed slope or bed material. This relationship can be written as:

$$B = 3.5 \sim 7Q^{1/2} \quad \text{(Unit: m/sec)} \quad \cdots\cdots\cdots \quad (1.4)$$

The reason is unclear, but if the channel width was made larger separation of flow would occur, and if made smaller, erosion of banks would occur and the channel would be enlarged.

Here the case is one without sediment. In the degree of sediment concentration which is similar to that of general bed load, suspended load, or the like, the sediment does not act greatly as a resistance against the flow. So, provided one selects a channel width satisfying equation (1.4), it is safe to assume that the width is sufficiently stable for sidebank erosion even when there is no sediment. Thus, in designing a channel works, the channel width given by equation 1.4 is the largest value which must be considered.

Tabata and Abe[2), 3)], concerning each area's erosion control dam, show the relationship between the basin area and relative flow discharge with reference to the design flood discharge. They also show the relationship between the width of many channel works actually in operation and the basin area. Here, considering the previous relationship as a relationship between basin area and relative flow discharge for channel works, and rearranging as one between channel width and design flood discharge, one gets Fig. 5.1 which compares this with Equation 1.4.

Further, both the standard values of channel width and the desing discharge given in the Ministry of Construction's River Erosion Control Technical Standards are also indicated in Fig. 5.1.

As is clear from the figure, for large flow discharges above 2000 m^3/sec, equation (1.4) and actual river width are in good agreement. For small discharges the river width is narrower than that given by equation (1.4). One reason for using these narrow widths in channel works is that the so called dominant discharge, which determines the width of a natural river channel, is apt to become the cause of meandering within the channel. A channel width given by equation (1.4) for design flood (Pickup, G.[4)]) is too large for the 1.5yr probability flood discharge, the kind of floods which occur several times a year or once in several years. Another reason is that in places where channel works can be operated, being originally narrow, it is impossible actually to make the width given by eq. (1.4), say, 50m for a 100 m^3/sec design flood discharge.

Thus, in practice, using channel width smaller than given by eq. (1.4) necessitated a policy of desposing strong revetments to prevent sidebank erosion in design flood times. When determining the specific channel width, one must consider restrictions due to conditions of land utilization and the difficulty of maintenance after put in operation. Of course, the narrower the channel, the greater the capacity to erode the bankers and one must increase the strength of revetments. Since the equilibrium slope decreases, as explained below, one must increase the embedment depth of the revetments.

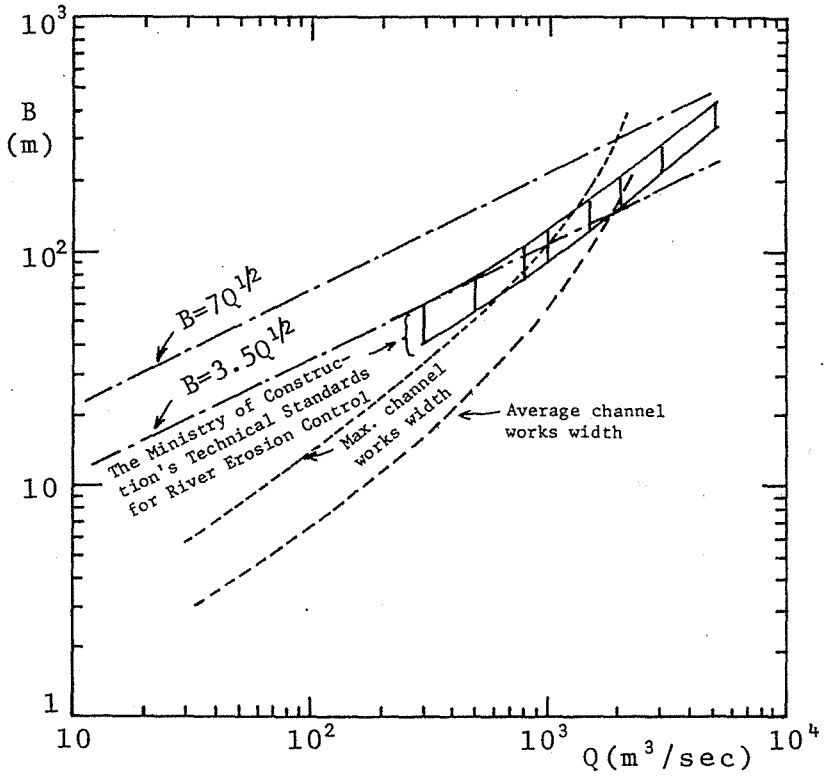

Fig. 5.1 The Relationship between River Width and Flood Discharge

(2) Equilibrium slope

In general, the equilibrium slope where sediment discharge is the same at any cross section is dtermined by the supplied sediment discharge. Under the condition of no supplied sediment from the upper stream area as in planning channel works, the maximum value of the longitudinal slope is the so called static equilibrium slope, where at every point in the longitudional direction no sediment exists. The static equilibrium slope for a given bed material can be obtained by analysis of critical tractive force for various diameters of the material. Especially for the case of gravel mixture having a wide grain size range as in general mountain streams, when grains below 90 – 95% grain diameter are selectively swept away, the average lowering of the riverbed becomes small, and reaches equilibrium when the riverbed surface becomes covered with relatively coarse grains (armour coating).

The critical tractive force for a riverbed composed of uniform grains, for a steeply sloped small relative depth flow, is given in this study by quation (3.26). For gravel mixture, there is Egiazaroff equation (3.25). As was stated in Chapter three it is necessary to apply some modification to eq. (3.2) for the cases of large grain distribution range and small relative depth. However, here assuming that the logarithmic equation obtained by putting equation (3.26) into τ_{*cm} of equation (3.25) can be applied as it is, the following equation can be obtained.

Assuming that the armour coat begins to form when gravel of $d_i=d_{90}$ stops moving, one can find the critical tractive force $\tau_{*c_{90}}$ corresponding to that from equation (5.1).

$$\tau_{*ci} = 0.04\left(\frac{\log_{10}19}{\log_{10}19\frac{d_i}{d_m}}\right)^2 \times 10^{1.76\,I} \qquad \cdots\cdots\cdots (5.1)$$

One can see from dimension analysis that the Darcy-Weisbach frictional resistance coefficient f for a steeply sloped small relative depth flow is a function of d/h and U_*^2/gd. This functional relationship can be found as in Fig. 2.6. The following show some of the methods for finding a static equilibrium slope, for a prescribed flow discharge and channel width, using these quantities.

First, assume an appropriate slope (I), from a grain size distribution of a given bed material and find d_{90} and dm. Calculate $\tau_{*c_{90}}$ from equation (5.1). Next, insert this τ_{*c} into equation (5.2).

$$\tau_{*c_{90}} = U^2_{*c_{90}}/(\sigma/\rho - 1)gd_{90} \qquad \cdots\cdots\cdots (5.2)$$

and find $U^2_{*c_{90}}/gd_{90}$.

$$U^2_{*c_{90}}/gd_m = (U^2_{*c_{90}}/gd_{90})(d_{90}/d_m) \qquad \cdots\cdots\cdots (5.3)$$

From the above equation (5.3) find the value of $U^2_{*c_{90}}/gdm$, and calling this U_*^2/gdm find its value from a group of curves given in Fig. 2.6. Because the curves giving the assumed (I) are also indicated in Fig. 2.4, one can find the intersection of both curves. Reading off the coordinate of dm/h and f of the intersection, and using h and f, one can calculate the discharge from

$$Q = h\sqrt{8/f}\sqrt{ghI}\cdot B \qquad \cdots\cdots\cdots (5.4)$$

If Q obtained in this way does not agree with the prescribed discharge, reiterate the calculations assuming different values of I until they do agree. The average slope calculated as above varies with the given values of B and Q and bears no relationship for the original bed slope.

Here, let us examine channel works width and equilibrium slope by taking a practical example, the Iwatsubodani channel works plans within the jurisdiction of the Jintsu River Drainage System Erosion Control Works Office. The Iwatsubodani Channel Works was planned for the 460 m stretch the Hikage Erosion Control Dam downstream to the confluence point with the main stream of the Hirayu River, the already constructed Hikage Dam being taken as the check dam. Its purpose was to prevent lateral erosion and riverbed lowering. The alignment was determined as a consequence almost from necessity by restrictions such as roads.

The channel width, too, dependent on conditions such as land use, was determined to be 10 m for the upper stream section and 15 m for the lower. With an overall drop of 42 m the present average bed slope is 0.0913. The grain size distribution of the bed material is shown in Fig. 5.2.

The mean diameter (d_m) is 5.7 cm and the 90% diameter (d_{90}) is 16.2 cm. The problem is the design flood discharge. In the case of the Iwatsubodani using the 150-year probability rainfall it gets 215 m^3/sec.

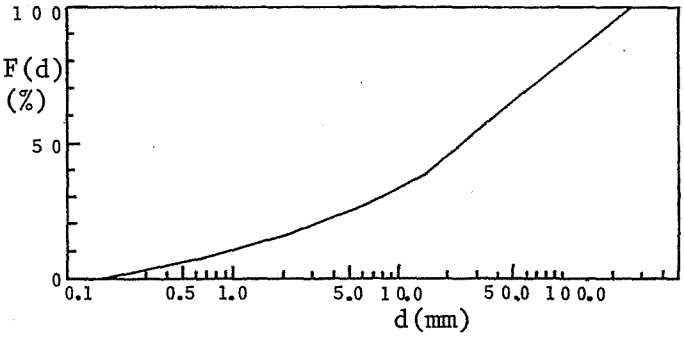

Fig. 5.2 Grain Size Distribution at Iwatsubodani

From the above data the static equilibrium slope can be obtained, where it is assumed that for sake of simplicity the channel section is a rectangle and that curves in the alignment exert no influence. Further, make the calculations using 10 m or 15 m as the value of the channel works width B_0. Now, from equation 5.1, assuming $d_{90}/md = 2.84$, $\tau_{*c_{90}}$ becomes 0.0218 for $I \approx 0$. The $\tau_{*c_{90}}$ for a slope I is given by $\tau_{*c_{90}} = 0.0218 \times 10^{1.76\,I}$. For example, if I = 0.10, the $\tau_{*c_{90}}$ is 0.0327. From equation 5.2 we get

$$U^2_{*c_{90}}/gd_{90} = \tau_{*c_{90}}\ (\sigma/\rho - 1) = 0.0349 \times 10^{1.76\,I}$$

Here, σ/ρ is taken to be 2.60. Also from equation (1.4), letting the flow discharge per unit width be q m^3/sec/m, the following is obtained.

$$B = (12.3 \sim 49)\,Q/B = (12.3 \sim 49)\,q \qquad (m)$$

One can find the channel width B from the flow discharge per unit width. Insert whichever width is smaller, B the channel width or B_0 the channel works width, into eq. (5.4) and find the flow discharge Q (m^3/sec).

The results of these calculations are shown in Table 5.1 and Fig. 5.3. From these results we see that provided the flood time continues sufficiently long for riverbed deformation, the equilibrium slope will become an extremely mild slope of 0.0014 for a design flood discharge of 215 m^3/sec even if the channel works width is 15 m. In terms of height this is a gain of 0.74 m, and we see it is necessary to take care of the remaining 41.26 m by a falling works or the like.

Table 5.1 Examples of Calculating the Equilibrium Slope

I	0.1	0.05	0.025	0.0125	0.005	0.0025	0.001
$\tau_* c_{90}$	0.0327	0.0267	0.0241	0.0229	0.0222	0.0220	0.0219
$U_*^2 c_{90} / g d_{90}$	0.0523	0.0427	0.0386	0.0367	0.0356	0.0352	0.0350
$U_*^2 c_{90}$	0.0831	0.0678	0.0613	0.0583	0.0565	0.0559	0.0556
U_* (m/sec)	0.288	0.260	0.248	0.241	0.238	0.216	0.236
h (m)	0.0848	0.138	0.250	0.476	1.15	2.28	5.67
$U_*^2 c_{90} / g dm$	0.149	0.121	0.110	0.104	0.101	0.100	0.0994
dm / h	0.672	0.413	0.228	0.120	0.0496	0.0250	0.0101
f	0.30	0.19	0.10	0.057	0.041	0.032	0.025
U_o / U_*	5.16	6.49	8.94	11.8	14.0	15.7	18.0
U_o (m/sec)	1.49	1.69	2.22	2.84	3.33	3.71	4.25
$q = hU_o$	0.126	0.233	0.555	1.35	3.83	8.49	24.1
B(m) $\frac{12.3q}{49q}$	1.55	2.87	6.83	16.6	47.1	104.4	296.4
	6.17	11.4	27.2	66.2	187.7	416.0	1180.9
Q (m^3/sec)	0.195	0.669	3.79	22.4	180.4	886.4	7143.2
	0.777	2.66	15.1	89.4	718.9	3531.8	28460
Q (B=10m)	—	—	5.55	13.5	38.3	84.9	241.0
Q (B=15m)	—	—	8.33	20.3	57.5	127.4	361.5

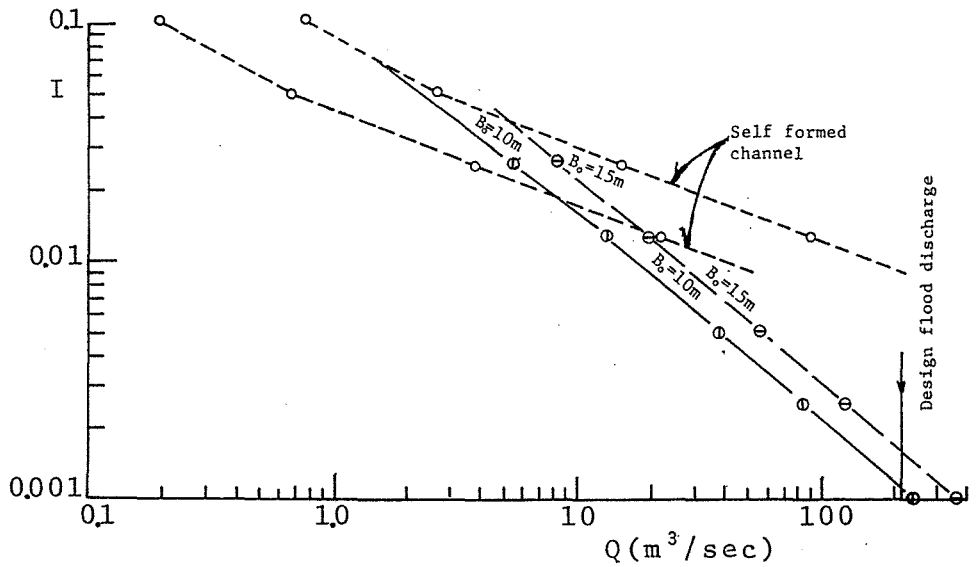

Fig. 5.3 The Relationship between Flow Discharge and Equilibrium Slope

Also Fig. 5.3 indicates that for a channel works width of 15 m, the flow will meander until the flow discharge reaches 6 - 17 m^3/sec. Here the channel works design width of 10 m corresponds well with the cross sectional width of the present channel, and one can say the flow discharge of 2 - 8 m^3/sec corresponding to that channel is the dominant discharge with respect to the lateral morphology. Also, following the previous line of reasoning, this can be regarded as corresponding to the 1.5-year probability flood discharge.

(3) Artificially roughened riverbed

One can find the static equilibrium slope I for a channel of overall head H and channel works reach length L by methods related above. The difference H-LL between overall head H and the head due to the static equilibrium slope must be dealt with by a falling works. However, as this difference increases, the channel length needed for an energy dissipator increases, and the gravel bed distance is shortened. Since that is the case, it is more economical to put aside the falling works and coat the bed surface with concrete. In general, in a channel plastered on three sides the flow velocity tends to be quick, and there are cases when it is necessary to consider management of confluence sections. Thus, one can consider roughening the rigid bed surface to reduce the flow velocity. Since characteristics of the resistance coefficient for roughness due to frame type roughness elements disposed transversally on a bed surface have been elucidated by many experiments already,[5] here the case of artificial roughness due to natural rock buried in the riverbed is considered.

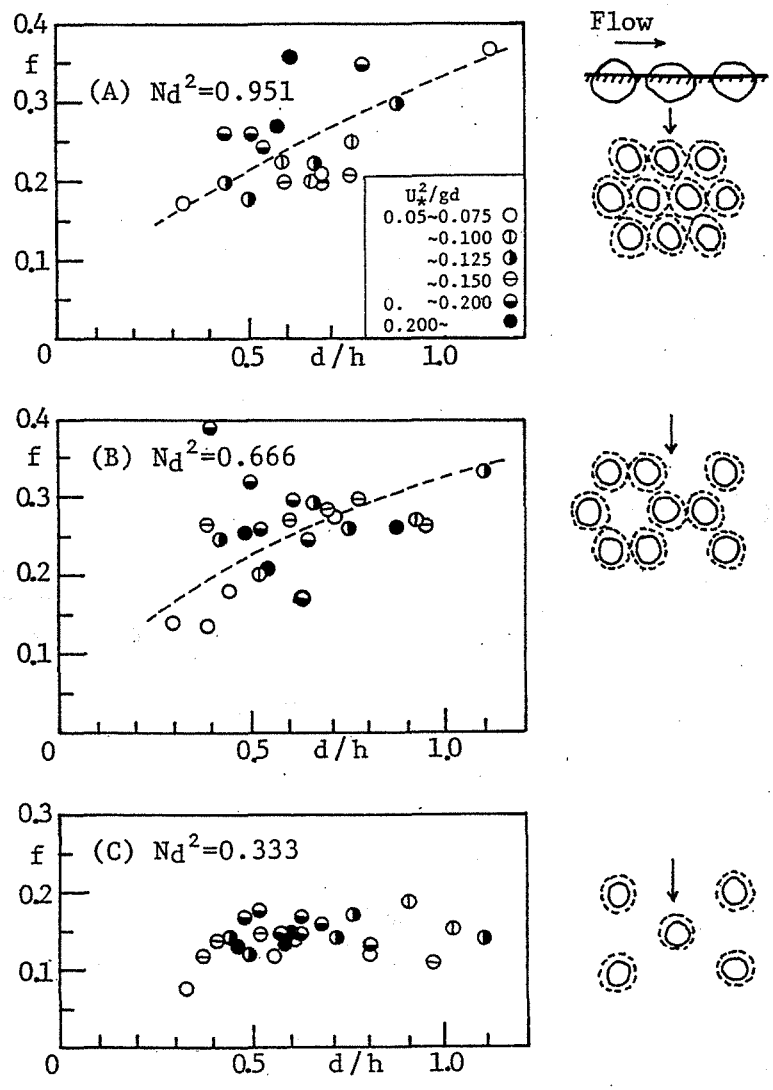

Fig. 5.4 The Change of Resistance Coefficient Due To Different Arrangements of Roughness Elements

Experiments were carried out for the case where 2/3 of the diameter was burried for three roughness densities: Nd^2 = 0.951, 0.666, and 0.333. The results are shown in Fig. 5.4.

In this case we see that U_*^2/gd is not an important factor. Further, the arrangements of the roughness elements are shown to the right of each graph. In the case of these experiments, the arrangement designated as B gave the largest resistance coefficient.

Consider again the Iwatsubodani Channel Works Plans mentioned above. From the results of the equilibrium slope analysis it was understood that nearly the whole head must be accommodated by falling works. However, if a large

number of small falling works are strung together, the gravel bed section will disappear. Thus, one can consider concentrating the head in one place by establishing a large falling works. However, in order that the falling water makes a stable hydraulic jump in times of design flood discharge, an extremely large auxiliary dam or front apron is necessary. Next, since the surroundings is a hot springs area, there is a possibility of creating noise pollution by the falling water, which recently has become an issue. In the final analysis it is more economical to cover it on three sides, rather than to build a large scale project. In this instance, the stream flows quickly due to the steep slope, so scouring at the confluence point with the main stream, impulse waves at the curved sections, and rising of the water level at the outer curves are problems. Thus, it would be advisable to incorporate some artificial roughness elements such as those described above.

Section 3: Conclusion

This Chapter discussed possibilities of applying the results of this thesis for erosion control planning. It discussed especially applications to channel works planning, and methods for finding equilibrium slope and channel works width. Channel Works Plans for Iwatsubodani in the Jintsu River Drainage System was taken as a concrete example, and the actual equilibrium slope was calculated. Finally experiments on resistance for artificial roughness elements made from natural rock were carried out, and the results presented.

The results of this thesis may also be valuable for predictions of the amount of slope erosion, calculation of riverbed deformation in mountain streams, and especially for discussion of regulating effects of erosion control dams.

REFERENCES

1) Kazuo Ashida, Tamotsu Takahashi, and Takahisa Mizuyama:
"A Hydraulic Study for Channel Works Planning", the SHIN-SABO 97, Nov. 1975, pp. 9-16.
2) Shigekiyo Tabata, and Souhei Abe:
"A Study on Channel Works (1)", the PWRI, Technical Memorandom No. 822, March 1973.
3) Shigekiyo Tabata:
"A Study on Channel Works (III)", the PWRI, Technical Memorandom No. 944, March 1974.
4) Pickup, G.:
"Adjustment of Stream-Channel Shape to Hydrologic Regime", Jour. of Hydrology, 30, 1976, pp. 365-375.
5) Ed. by Tojiro Ishihara:
"Water Engineering Hydraulics", Maruzen Co., 1972, p. 245.
6) Yoshiro Yoshioka et al:
"Model Experiments for Reduction of Noise generated by Water Falling from a Sediment Control Dam", Proc. of 1976 Erosion Control Meeting, pp. 72-73.

AFTERWORD

This thesis has advanced, the understanding of sediment transport phenomena which are treated mainly in the field of erosion control engineeering. Specifically the phenomena herein treated are flow resistance, bed load transport rate, critical tractive force, and channel pattern for a stream on a steeply sloped bed, having a small relative water depth and a wide grain size distribution. It has elucidated the influence of slope on these phenomena which was not very clear previously, and has obtained a number of results applicable to mountain rivers. There follows a summary of the results.

Chapter 1 presents the results of a number of experiments on channel pattern and sediment transport forms as it occurs in steeply sloped flumes of slope 1/100 to 1/4. The area was divided by slope and flow discharge and the characteristics of each region were clarified. Next, the physical quantities which determine the boundaries of those regions were considered, and general methods were indicated. The following results are particularly of note. The channel width for the threshold of meandering formation is proportional to the 1/2 power of the flow discharge within a range frame 10^{-6} to 10^{5} m^3 sec discharge, independent of bed material or slope. It is expressed in m/sec units as $B = 3.5 \sim 7.0\ Q^{1/2}$. Also, the sediment discharge for mud flow is close to that of a meandering stream.

From investigations of longitudinal line of sediment on rigid beds, it was understood that the width of a possible longitudinal eddy equals the water depth. Also, the flow velocity distribution is almost unaffected by the presence of sediment. On steep slopes, medium forms of sediment between bed load and mud flow appear and one sees also formation of dunes. These results are very useful in dealing with sediment transport phenomena in mountain rivers.

Chapter 2 concerns the resistance law for a flow. It showed that the important parameters dominating the phenomena, for a steram on a sleep slope, are relative water depth, slope, Froude Number, and U_*^2/gd. First, the velocity distribution was observed for a stream having large roughness elements. Since it tends to become uniform near a bed surface, the velocity distribution was divided into upper and lower regions. Application of different logarithmic velocity distribution equations for each region was proposed, and coefficients were determined. Next, values of the resistance coefficient were found experimentally, and it become clear that with an increase in U_*^2/gd and relative roughness the resistance coefficient increases sharply. This result was explained theoretically by an step-down model.

The resistance coefficient for a movable bed, especially a flat one, tends to be the same as for a fixed bed.

From experiments on gravel mixture bed characteristics, it become clear that the degree of roughness depends on the mean grain diameter, and that particles of each diameter are present on the average at a height proportional to the diameter. In the final analysis the resistance coefficient of a flow over a gravel mixture bed is the same as for uniform gravel when the mean grain diameter is used as representative of roughness.

Chapter 3 concerns critical tractive force for initiating the transport of gravel. First an overview of the conventional research was presented.

The functional relation of critical tractive force and Reynolds Number for sand grain was well understood. What was made clear was the influence of relative depth when relative depth is small.

First, from research on uniform gravel, it was clear that shieldes parameter τ_*sc, modified for the effect of slope, is a function of relative roughness d/h in regions of a perfectly rough turbulent flow. Also, experimental results showed τ_*sc increases abruptly with an increase in d/h. One can explain characteristics of the variation of critical tractive force theoretically by a resistance law and a gravel equilibrium equation.

Next was the case of gravel mixture. The critical tractive force for gravel mixture of the mean diameter is greater than that for uniform gravel due to the effect of being hidden by particles larger than the mean diameter. The percentage increases with an increase in $\sqrt{d_{84}/d_{16}}$, and the relation was elucidated experimentally for values of $\sqrt{d_{84}/d_{16}}$ up to 2.8. Next, the ratio of critical tractive force for each individual diameter and that for the mean diameter is a function of d/h and di/dm. When d/h is small the ratio can be expressed approximately by Egiazaroff equation. When d/h is large it is close to the one of uniform gravel. One can find the critical tractive force for each diameter from the above results, and by assuming a hiding coefficient for each diameter, one can explain its relationship theoretically.

Chapter 4 concerns the bed load transport rate. First a number of conventional bed load equations were explained. Next, a bed load equation for a flat river bed was derived from Bagnold's model. This equation was found to give good agreement by checking it with the data of Gilbert and others. Next, applying a modification of slope and comparing it with the author's data, the tendency for bed load transport rate to decrease with increase of slope was explained.

Also for gravel mixture, it was confirmed experimentally that the critical tractive force for ceasing the transport is nearly a constant independent of grain diameter. Next, for sediment in equilibrium, the critical tractive force used in the bed load equation should be a constant value independent of grain diameter.

Reasoning that this value ought to be closer to the ceasing critical tractive force rather than the initiating critical force, the critical tractive force is taken to be a constant of 0.85 times the initiating critical tractive force for gravel mixture.

Using this, a new bed load equation for gravel mixture is proposed.

This equation explains conventional experimental values extremely well.

By making modifications similar to those for uniform gravel, one can obtain almost completely satisfying results even for steeply sloped channels. However, a further detailed examination reveals on a gravel mixture bed with a wide grain size distribution, when the largest particles begin to move the smaller particles are hidden by the larger ones.

For this reason, sediment discharge and grain size distribution vary with time. Chapter 5 indicates methods of applying the knowledge obtained in the first four chapters to erosion control planning, for which there have been many experimental investigations, and especially to channel works planning. Also, as a practical example, the equilibrium slope was found for the Iwatsubodani channel works.

New knowledges concerning the influence of relative roughness and experimental consideration for channel pattern and bed load were proposed for uniform gravel and gravel mixture. The author believes that these results would have a significant contribution to the development of sediment hydraulics and especially to that of erosion control engineering.

Finally the author wants to express his deep appreciation to Professor Aritsune Takei of Kyoto University whose guidance I received throughout the competion of this thesis, Professor Kazuo Ashida of the Kyoto University Disaster Prevention Research Institute, and Assistant Professor Tamotsu Takahashi. The author also wants to express his gratitude Professor Mutsumi Kadoya of the Kyoto University Disaster Prevention Research Institute whose warm encouragement and consideration he received, and to Kyoto University Professor emiritas Ryuichi Endo.

The author also wants to thank, for advice and help with experiments and other things, Mr. Yoshinori Yoshida, technical official at the above Institute, and all those in the Erosion Control Section of the Institute and in the Ujigawa Hydraulics Laboratory.